INVESTIGATIONS OF ENERGY TRANSFER PROCESSES IN COORDINATION CHEMISTRY

ABSTRACT

Intermolecular energy transfer from excited Tb^{3+} ($^5D_4$ level) in the form $Tb(AA)_3.3H_2O$ to lanthanide and transition metal acetylacetonates in solution has been established. The behaviour is markedly solvent dependent, and the bimolecular rate constants for the quenching mechanism in all cases were significantly lower than the diffusion rate of the particular solvent. The rate of energy transfer to lanthanide acetylacetonates is temperature dependent, and its mechanism is interpreted as being dependent on the formation of mixed metal dimers in solution, energy transfer only being observed if the monomer exchange rate is significantly faster than the rate of decay of the Tb^{3+} $^5D_4$ emitting level. This mechanism of energy transfer is also proposed to occur in the case of certain transition acetylacetonates which tend to oligomerise. A second, temperature independent mechanism of energy transfer to some transition metal acetylacetonates was observed. This mechanism is proposed to be of a collisional type, with the requirement that the donor and acceptor ions being in a specific orientation to each other in the collisional complex, before transfer of energy takes place. This orientation effect could explain why the observed bimolecular energy transfer rates are significantly lower than the diffusion rates.

The existence of oligomeric acetylacetonate species containing Tb^{3+} and Co^{++} or Ni^{++} ions has been established in solution and in the solid state.

The absence of Eu^{3+} ion phosphorescence in $Eu(AA)_3 . 3H_2O$ is attributed to the occurrence of a charge transfer band in this complex.

Temperature dependence of the Tb^{3+} $^5D_4$ phosphorescence lifetime in $Tb(AA)_3 . 3H_2O$ in solution is investigated, and is found to be highly solvent-dependent.

Investigations of Energy Transfer Processes in Coordination Compounds

A Thesis

presented for the degree of

DOCTOR OF PHILOSOPHY

in the Faculty of Science of the

University of St. Andrews

by

G.D. Ross Napier, B.Sc.

October 1976

University of St. Andrews

DECLARATION

I declare that this thesis is my own composition, that the work of which it is a record has been carried out by me, and that it has not been submitted in any previous application for a Higher Degree.

This thesis describes results of research carried out at the Department of Chemistry, University of St. Andrews, under the supervision of Dr. T.M. Shepherd since October 1st 1973.

G.D. Ross Napier

CERTIFICATE

I hereby certify that G.D. Ross Napier has spent eleven terms of research work under my supervision, has fulfilled the conditions of Ordinance No. 12 (St. Andrews) and Resolution of the University Court, 1967, No. 1, and is qualified to submit the accompanying thesis in application for the degree of Doctor of Philosophy.

T.M. Shepherd
Director of Research

ACKNOWLEDGEMENTS

I would like to express my gratitude to Dr. T.M. Shepherd for his interest, help and encouragement during the course of this work. Thanks are also due to my friends and colleagues, Duncan Neilson, Laurence Rudkin to name but two of the many.

I am indebted to the Science Research Council for a grant to finance this work, and to Professor Lord Tedder and Professor P.A.H. Wyatt for providing research facilities.

Finally, I wish to thank Mrs W. Pogorzelec for patiently and skilfully typing this thesis.

CONTENTS

Page

Summary

Intermolecular energy transfer from excited Tb^{3+} ($^5D_4$ level) in the form $Tb(AA)_3.{}^3H_2O$ to lanthanide and transition metal acetylacetonates in solution has been established. The behaviour is markedly solvent dependent, and the bimolecular rate constants for the quenching mechanism in all cases were significantly lower than the diffusion rate of the particular solvent. The rate of energy transfer to lanthanide acetylacetonates is temperature dependent, and its mechanism is interpreted as being dependent on the formation of mixed metal dimers in solution, energy transfer only being observed if the monomer exchange rate is significantly faster than the rate of decay of the Tb^{3+} $^5D_4$ emitting level. This mechanism of energy transfer is also proposed to occur in the case of certain transition acetylacetonates which tend to oligomerise. A second, temperature independent mechanism of energy transfer to some transition metal acetylacetonates was observed. This mechanism is proposed to be of a collisional type, with the requirement that the donor and acceptor ions being in a specific orientation to each other in the collisional complex, before transfer of energy takes place. This orientation effect could explain why the observed bimolecular energy transfer rates are significantly lower than the diffusion rates.

The existence of oligomeric acetylacetonate species containing Tb^{3+} and Co^{++} or Ni^{++} ions has been established in solution and in the solid state.

The absence of Eu^{3+} ion phosphorescence in $Eu(AA)_3 . 3H_2O$ is attributed to the occurrence of a charge transfer band in this complex.

Temperature dependence of the Tb^{3+} $^5D_4$ phosphorescence lifetime in $Tb(AA)_3 . 3H_2O$ in solution is investigated, and is found to be highly solvent-dependent.

Chapter 1

Introduction

(i) General Photochemistry

Photochemistry may be defined as the area of scientific investigation concerned with the making and breaking of bonds in chemical compounds by the absorption of a photon, or photons, usually in or near the visible region of the electromagnetic spectrum. The term "photochemistry" has however also been used to describe investigations of systems where the absorption of a photon occurs, and the system ultimately returns to its initial state. Since no lasting chemical change occurs this area of excited state chemistry is perhaps better described by the general term "photophysics", as used by Birks[1]. Most of the work described in this thesis falls into this "photophysical" category.

Energy states of molecules where there is no net spin, are designated "singlet"[2,3,4] states, the ground state being conventionally termed S_0, and the lowest energy excited singlets S_1, S_2, etc. For every excited singlet state, there is a corresponding state where the spins of one pair of electrons are parallel, ie. the spin multiplicity, $2s+1 = 3$. These are termed triplet states, and according to Hund's first rule, these states are lower in energy than the corresponding singlets. A molecular orbital representation of excited states is shown in figure 1,1.

Figure 1, 1. Molecular orbital representation of excited states

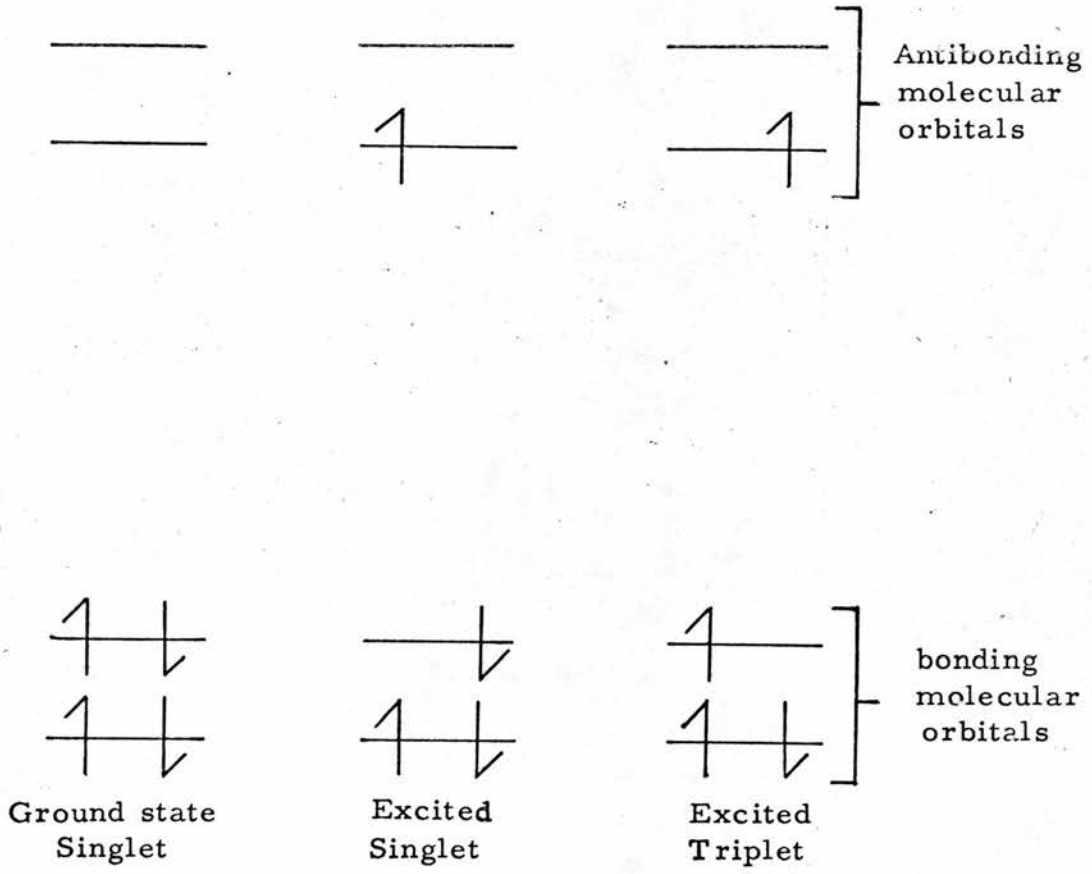

On absorption of a photon to give one of the excited singlet states, a variety of processes may occur, and they are illustrated in figure 1, 2. In comparison with the S_0 and S_1 states, the energy separation between the other excited singlets is relatively small, and results in considerable overlap of their vibrational levels. Consequently, excitation to a singlet state higher than S_1 will rapidly result in the loss of excess energy and the return to the S_1 state. This process is called internal conversion. A molecule

Figure 1, 2. Representation of photophysical processes which may occur on absorption of a photon by a molecule[i]

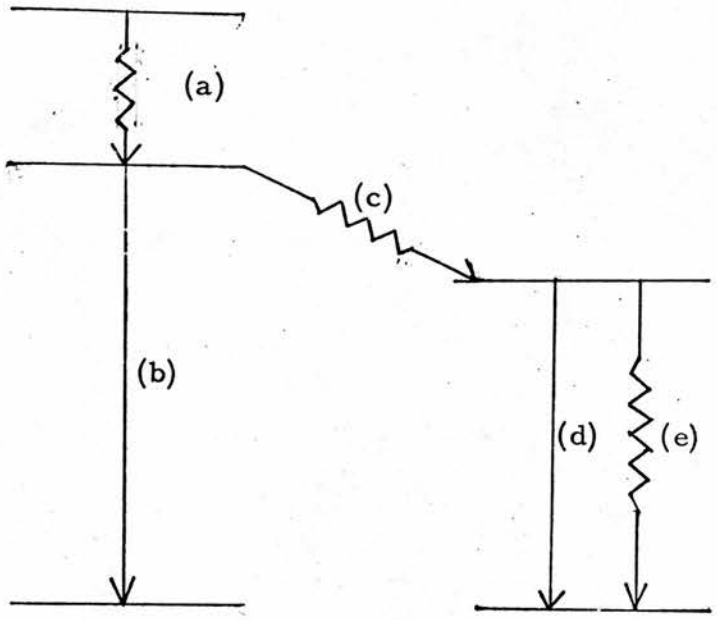

(a) Internal conversion

(b) Fluorescence

(c) Intersystem crossing

(d) Phosphorescence

(e) Vibrational relaxation

(i) Radiative transitions are denoted by $\longrightarrow$

Non-Radiative transitions are denoted by $\rightsquigarrow$

in the S_1 state can lose its energy radiatively, ie. $S_1 \longrightarrow S_0$ this process being termed fluorescence, since it involves no spin change.

Direct population of the triplet level from the ground state

singlet is a very inefficient process, since radiative transitions between states of different multiplicities in a molecule are theoretically forbidden. The triplet level, T_1, can in many cases be populated by intersystem crossing from the S_1 level. Since the radiative or non-radiative transitions from the T_1 level to the S_0 level are spin-forbidden, the T_1 lifetime is relatively long compared with that of the S_1 level, and is therefore more susceptible to environmental quenching. Vibrational levels of the S_0 often overlap those of the T_1, and the T_1 can lose its energy via a cascade process through these vibrational levels to the S_0. This is termed vibrational relaxation. The T_1 can in certain cases lose its energy radiatively to the S_0. This step involves a change in spin multiplicity, and is defined as phosphorescence. The various photophysical processes which have been discussed are summarised in table 1, 1.

(ii) Chemistry of the Lanthanides

The lanthanides are a group of fourteen metallic elements, beginning with cerium (atomic number, Z = 58), and ending with lutetium (Z = 71), and are characterised by the filling of the 4f shell. The general configuration for any lanthanide element is $[Xe]4f^n 5d^1 6s^2$ [5]. The elements are highly electropositive [6], and their chemistry is predominantly that of the tripositive state. Lanthanide tripositive, Ln^{3+}, ions, because of their relatively large size (Ce^{3+} ionic radius is 0.103 nm, cf. Cr^{3+} whose ionic radius is 0.063 nm) tend to form complexes which have high

Table 1,1. Summary of Photophysical Processes

Term	Definition	Approximate Rate (S^{-1})	Typical Process
Absorption	Promotion of an electron to an energetically higher level	10^{15}	$S_1 \leftarrow S_0$
Internal Conversion	Non-radiative transfer of energy between two states of the same multiplicity	10^{11}-10^{15}	$S_i \rightsquigarrow S_1$
Fluorescence	Radiative energy transfer between two states of the same multiplicity	10^{7}-10^{9}	$S_1 \rightarrow S_0$
Intersystem Crossing	Non-radiative transition from a state of given multiplicity to a state of different multiplicity	10^{8}	$S_1 \rightsquigarrow T_1$
Quenching	Kinetic interaction with the adjacent environment	10^{5}-10^{7}	$S_1 \rightsquigarrow S_0$
Phosphorescence	Radiation transition from a state of given multiplicity to a state of different multiplicity	10-10^{3}	$T_1 \rightarrow S_0$
Vibrational Relaxation	Loss of energy from an excited level to the ground state via a cascade process through overlapping vibrational levels of different electronic states	10^{12}	$T_1 \rightsquigarrow S_0$

$\longrightarrow$ = Radiative transition

$\rightsquigarrow$ = Non-radiative transition

coordination numbers. Compounds with coordination numbers of 6, 7, 8, 9 and 12[7] have been reported, though the most common are 8, 9 and 10.

Lanthanide ions have predominantly "class A" character and show some reluctance to coordinate to donor atoms other than oxygen and nitrogen. Simple lanthanide salt solutions exhibit very sharp absorption peaks arising from transitions involving the 4f electrons. On complexing, the Ln absorptions are invariably very similar to the simple salt[8]. This indicates that the 4f electrons are extremely well shielded, and do not take any very significant part in bond formation on complexing.

Stable Ln ion complexes, relative to the hydrated cations, are only obtained when chelating ligands are employed, particularly if these ligands contain a highly electronegative donor, eg. oxygen or nitrogen. Some examples of chelating ligands are shown in figure 1, 3. These compounds are all bidentate ligands, and numerous lanthanide[8-14] complexes with such ligands have been isolated.

The investigations reported in this thesis are mainly concerned with lanthanide β-diketoenolates, the ligand having the general formula:

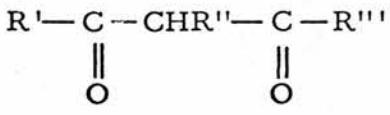

where R', R'' and R''' are generally alkyl or aryl substituents. To form complexes, the hydrogen on the central carbon atom is lost, and the β-diketoenolate anion bonds to the metal ion as a bidentate chelating agent via the two oxygen atoms to form a

six-membered ring. In the case of the lanthanides, there are two main classes of β-diketoenolate complexes:-

(i) tris complexes ($Ln(\beta\text{-diketoenolate})_3$)

(ii) tetrakis complexes $(Ln(\beta\text{-diketoenolate})_4)^-$.

Because of the tendency of lanthanide ions to form complexes which have high coordination numbers, the tris complexes are usually isolated as solvates, the degree of solvation depending on the

Figure 1, 3.

(a) NITROGEN DONORS

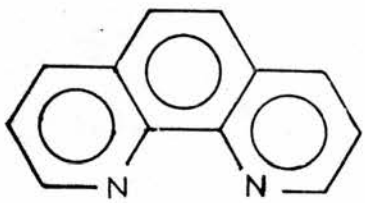

1, 10-phenanthroline

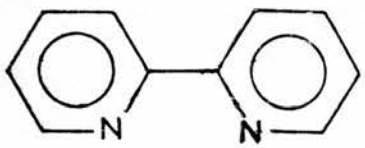

2, 2'-dipyridyl

(b) OXYGEN DONORS

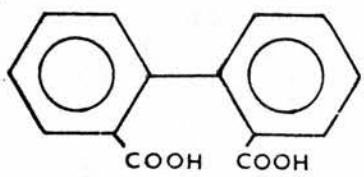

2, 2'-biphenyldicarboxylic acid

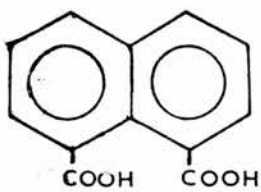

1, 8-naphthalic acid

reaction conditions. The tetrakis compounds are anionic, and consequently are isolated in the presence of a cation.

General methods of synthesis for tris and tetrakis complexes of the lanthanides are described in Chapter 2.

(iii) Spectroscopic Properties of Lanthanide Ions and Chelates

Spectral properties, in or near the visible region of lanthanide ions in the complexed form are in general very similar to those exhibited by the simple ions[15], due to the shielding of the 4f electrons. Absorption spectra of these ions show weak bands, corresponding to Laporte-forbidden transitions within the 4f shell. The absorption spectral profiles of the d-transition metals show a much greater dependence on the chemical environment of the metal ion than the lanthanides. This is because, in the case of d-transition metal ions, the order of perturbation of the d-electrons is spin-orbit coupling $<$ crystal field effects $<$ interelectronic repulsion, whereas in lanthanide ions, the order for the perturbation of the 4f electrons is crystal field effects $<$ spin orbital coupling $<$ interelectronic repulsion[16].

The transitions observed in emission and absorption spectra of lanthanide ions can be assigned to transitions between energy levels predicted by the Russell-Saunders coupling approximation. This scheme can be used successfully in the case of the lanthanides, because crystal field perturbations are at least an order of magnitude lower than those due to spin-orbit coupling. The spin orbital coupling constants are of the order of several thousand cm^{-1}

hence the lowest energy level, $^{2s+1}_{J}L$ will be ca. 1000 cm^{-1} below the next energy level. At room temperature, this value is much larger than kT, hence in all the lanthanide tripositive ions with the exceptions of Eu^{3+} and Sm^{3+}, virtually no population of any energy level other than the ground state occurs.

(iv) Phosphorescence of Lanthanide Chelates

Weissman[17] first reported that excitation of the organic ligands in certain lanthanide chelates resulted in phosphorescence characteristic of the lanthanide ion. This indirect population of the lanthanide ion levels has been a subject of great interest, and the phenomenon has been widely studied. The mechanism of intramolecular energy transfer from the organic part to the lanthanide ion is generally understood to involve the lowest ligand triplet[18-23], and is schematically reported in figure 1,4.

The quantum efficiency of intersystem crossing to the triplet Φ_T, is

$$\Phi_T = \frac{k_3}{k_1+k_2+k_3} \qquad \text{(see fig. 1,4),}$$

that of intramolecular energy transfer, $\Phi_{I.M.}$, is

$$\Phi_{I.M.} = \frac{k_6}{k_4+k_5+k_6}$$

and that of lanthanide ion phosphorescence, Φ_{Ln}, is

$$\Phi_{Ln} = \frac{k_7}{k_7+k_8} \quad .$$

The overall quantum efficiency for the lanthanide ion phosphorescence

is $\Phi_T \Phi_{I.M.} \Phi_{Ln}$. For the intramolecular energy transfer step to occur efficiently, the lanthanide ion must have at least one acceptor energy level below the ligand triplet. The intramolecular energy

Figure 1,4. Processes which may occur in a lanthanide chelate on absorption of a photon of light

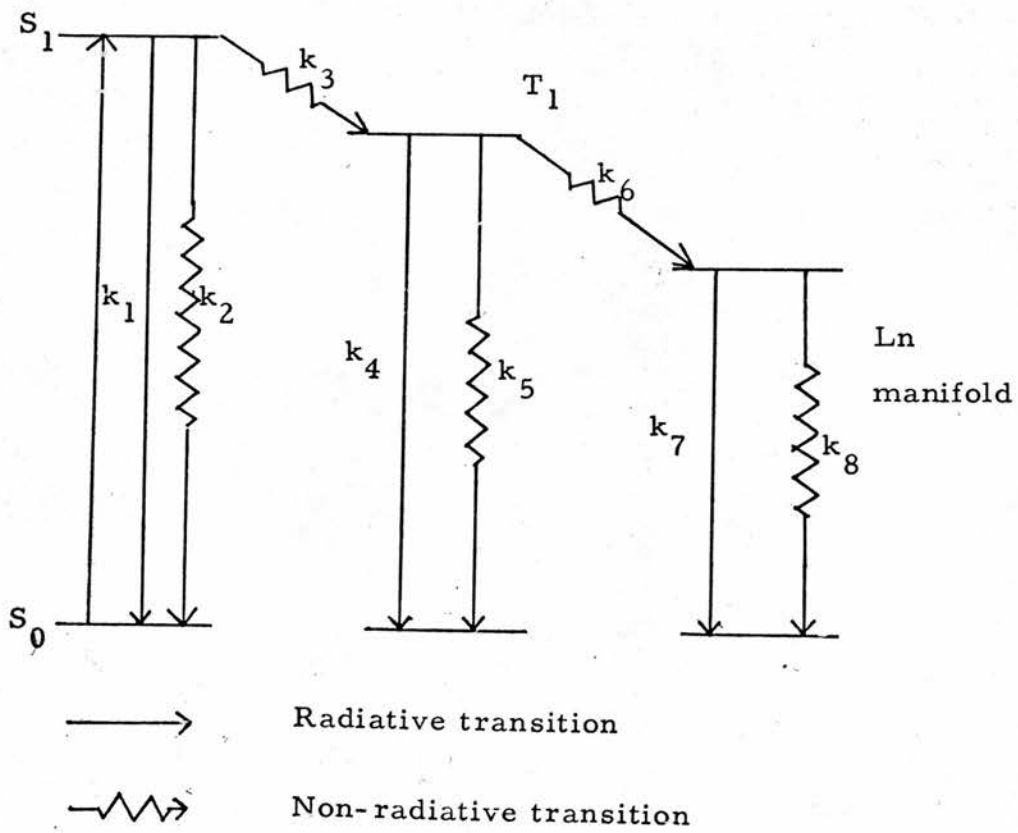

k_1 = fluorescence rate from ligand singlet

k_2 = non-radiative deactivation rate of singlet

k_3 = intersystem crossing rate

k_4 = rate of ligand phosphorescence

k_5 = non-radiative deactivation rate of triplet

k_6 = intramolecular energy transfer rate

k_7 = lanthanide ion phosphorescence rate

k_8 = rate of non-radiative deactivation of the Ln ion

transfer rate compares favourably with the rate of radiative transition from the triplet, and therefore the rate probably exceeds $10^{10} s^{-1}$.

Kleinerman[24], however, has suggested that in certain lanthanide chelates, mainly where the ligands are atomatic aldehydes, carboxylic acids, or alcohols, intramolecular energy transfer can proceed without the participation of the lowest ligand triplet. This occurs in chelates where the lowest triplet is below the lanthanide ion emissive level, and Kleinerman proposed that any phosphorescence observed was the result of energy transfer from the lowest excited singlet of the ligand to the lanthanide ion manifold. Whatever the exact mechanism of intramolecular energy transfer, the process is very efficient, and in all chelates used in this work where lanthanide ion phosphorescence is observed, the Ln emissive levels are situated below the lowest ligand triplet. Intramolecular energy transfer in these complexes may then reasonably be expected to proceed via the lowest ligand triplet.

In the literature, emission from the lanthanide ion in luminescent chelates is often termed lanthanide ion fluorescence, possibly to distinguish it from possible phosphorescence from the ligand triplet. In this thesis, it will be referred to by the more correct term, phosphorescence, since it almost invariably involves a spin change.

Freeman and Crosby[25] observed that the emission from the lanthanide ion follows a first order decay law. The decay can be described,

$$I_t = I_o \exp(-kt)$$

where I_o = phosphorescence intensity at time zero

I_t = phosphorescence intensity at time t

k = rate constant for the decay process (S^{-1})

t = time in seconds.

The exponential lifetime, ($\tau = {}^{1}/_{k}$), is a useful way to describe the rate of the decay process. Phosphorescent exponential lifetimes of lanthanide ions are typically of the order of ca. 1-2 ms. Wave[26] has reviewed methods for measuring lifetimes of phosphorescent samples, and Peterson[27] has described the techniques best suited for the study of lanthanide ion phosphorescence. Phosphorescence lifetimes were measured in this work, using the technique of pulse fluorimetry, where the sample is excited by short duration light pulses, and the luminescent decay observed after the excitation. The length of pulse should preferably be considerably shorter than the luminescent lifetime. The experimental arrangement is described in Chapter 2.

(v) Intermolecular Energy Transfer

Intermolecular energy transfer, where the energy of excitation of a donor molecule is lost to an acceptor molecule has been known for many years. A trivial process may occur radiatively, where a photon is emitted by the donor, and subsequently absorbed by the acceptor. It may, however, also take place by a non-radiative process due to the interaction between the donor and acceptor during the excited state lifetime of the donor.

Terenin et al[28] first observed triplet-triplet intermolecular energy transfer in rigid media at 77K. They studied the quenching of the phosphorescence of aromatic aldehydes and ketones by naphthalene, and naphthalene-like derivatives. Triplet-triplet intermolecular energy transfer in fluid solution was first investigated by Bäckström[29] et al, who used diacetyl as the donor in benzene solution at room temperature. Numerous subsequent investigations into energy transfer between organic molecules have been made[1].

Lanthanide ions and chelates in solution can undergo various types of intermolecular energy transfer. Bhaumik and El Sayed[30, 31] reported sensitised lanthanide ion phosphorescence in europium chelates in EPA solution, as a result of energy transfer from the triplet level of excited ketones, eg. benzophenone, to the triplet of the ligand of the chelate, followed by intermolecular transfer to the europium ion manifold, with subsequent europium ion emission. Filipescu et al[32-35] have demonstrated that ketones in the excited triplet state in various solvents and rigid glasses can transfer their excitation energy to lanthanide ions efficiently, with subsequent lanthanide ion emission. Gallagher et al showed that, in acetic acid solution, excited 4,4'-dimethoxybenzophenone (DMB) can transfer its energy of excitation to Eu^{3+} ions only in the presence of Tb^{3+} ions. They concluded that a two-step energy transfer process occurs, with the Tb^{3+} ion acting as an intermediate which accepts energy from DMB, and then transfers it to the Eu^{3+} ion, followed by the characteristic red phosphorescence of the Eu^{3+} ion.

Chrysochoos and Evers[37] studied the transfer of energy from excited Tb^{3+} ions to Eu^{3+} ions using the lanthanide chlorides in dimethylsulphoxide, and observed a decrease in the Tb^{3+} ion phosphorescence intensity as the Eu^{3+} ion concentration increased, and also the appearance of a weak Eu^{3+} emission band. Atipenko, Ermolaev et al[38-42], in a series of papers have reported the mechanism of energy transfer from Tb^{3+} and Eu^{3+} ions to other lanthanide tripositive ions in various solvents. The transfer process involves a dynamic energy transfer step where some form of collisional interaction between the donor and acceptor ions occurs.

Studies of the quenching of phosphorescence in the presence of an acceptor are especially useful in obtaining knowledge concerning the excited state of the emitting species.

These investigations are normally made by measuring either the phosphorescence yield or lifetime of an emitting species in the presence of varying concentrations of an acceptor. If a single dynamic quenching process occurs, the so-called "Stern-Volmer" relation[43] is obeyed, viz:-

$$\frac{\phi_o}{\phi} - 1 = k_{SV}[Q]$$

where ϕ_o is the quantum yield in the absence of quencher, Q,

ϕ is the quantum yield in the presence of quencher, [Q],

[Q] is the quencher concentration (mol dm^{-3})

k_{SV} is the Stern-Volmer gradient.

A similar relationship may be derived if lifetimes are monitored, viz:-

$$\frac{\tau_o}{\tau} - 1 = k_{SV}[Q]^{43}$$

where τ_o = lifetime of the donor in the absence of quencher,

τ = lifetime of the donor in the presence of quencher, [Q].

A schematic representation of a dynamic quenching process is shown in figure 1,5. The Stern-Volmer expression may be derived from consideration of the radiative and non-radiative rate constants shown in figure 1,5 as follows.

The quantum yield for the phosphorescence of D^* in the absence of quencher, ϕ_o, is

$$\phi_o = \frac{k_1}{k_1+k_2}, \qquad \text{——— 1}$$

and the quantum yield in the presence of quencher, ϕ, is

$$\phi = \frac{k_1}{k_1+k_2+k_3[Q]} \qquad \text{——— 2}$$

By dividing 2 by 1 ,

$$\frac{\phi_o}{\phi} = \frac{k_1+k_2+k_3[Q]}{k_1+k_2} = 1 + \frac{k_3}{k_1+k_2}[Q] \qquad \text{——— 3}$$

The value $\frac{1}{k_1+k_2}$ is equal to the exponential lifetime of D^*, τ_0, in the absence of quencher. The Stern-Volmer relation can thus be written as

$$\frac{\phi_o}{\phi} = 1 + k_3 \tau_o [Q] \qquad \text{——— 4}$$

Experimentally, plots of $(\phi_o/\phi - 1)$ versus quencher concentration yield the Stern-Volmer gradient, and if τ_o can be determined, k_3, the bimolecular rate constant for the quenching process can be

Figure 1,5. Schematic representation of a dynamic quenching process

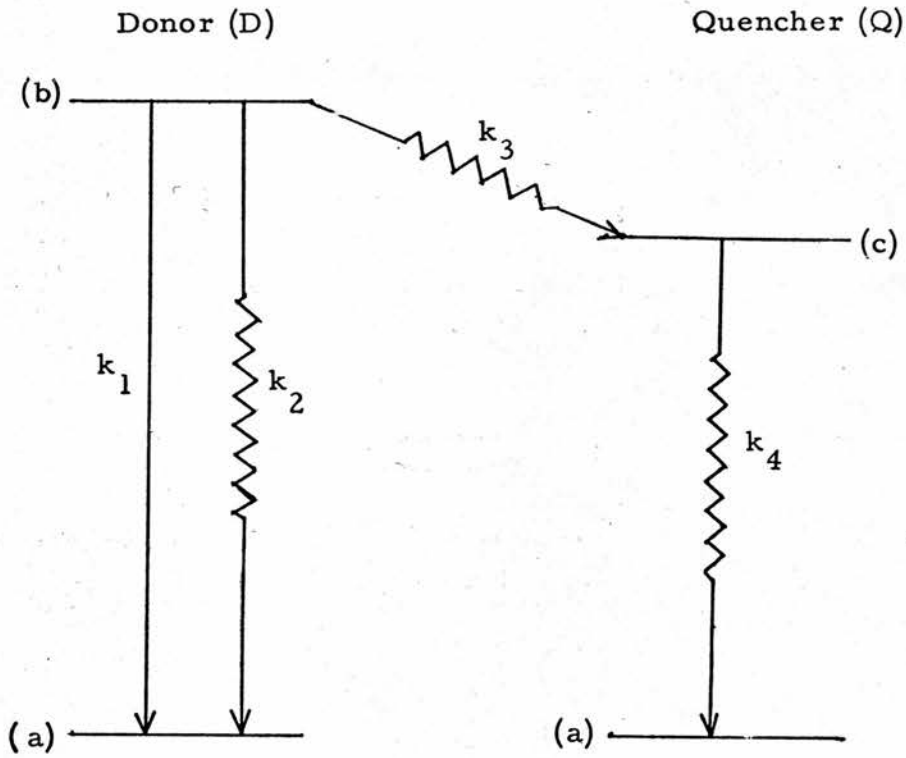

(a) Ground state energy levels of donor and acceptor

(b) Excited, emissive level of donor, D^*

(c) Excited energy level of acceptor

k_1 = radiative deactivation rate of (b)

k_2 = non-radiative deactivation rate of (b)

k_3 = bimolecular intermolecular energy transfer rate constant

k_4 = non-radiative deactivation rate of (c)

calculated. If lifetimes are considered rather than quantum yields, and τ, the lifetime of D^* in the presence of quencher in concentration $[Q]$ is,

$$\tau = \frac{1}{k_1+k_2+k_3[Q]} \qquad \text{——— 5}$$

Dividing 5 into $\tau_o = 1/k_1+k_2$, the relation

$$\frac{\tau_o}{\tau} = 1 + \frac{k_3[Q]}{k_1+k_2} \qquad \text{——— 6}$$

is derived. The Stern-Volmer gradients for a single quenching process will therefore be identical, whether lifetimes of quantum yields are considered. In the absence of absorption by the quencher, the phosphorescence intensity, I, is proportional to the quantum yield, and hence plots of I_o/I versus $[Q]$ will yield the Stern-Volmer gradient.

Dynamic quenching in solution depends on the donor and acceptor species coming into close enough proximity for energy transfer to occur. The bimolecular rate constant for energy transfer which is derived from Stern-Volmer plots, in many systems is close to the diffusion rate constant, k_d, of the solvent. k_d may be derived from the Debye equation,

$$k_d = \frac{8NkT}{3000\eta} b(e^b-1)^{-1} \quad ^{44}$$

where η is the viscosity of the solution in poise, and

$$b = \frac{Z_D Z_Q E^2}{r\,kT}$$

where Z_D and Z_Q are the charges on the donor and acceptor respectively

E = the charge on the electron,

r = the encounter distance between donor and acceptor,

η = the dielectric constant of the solution, and

k = Boltzmann's constant.

The intermolecular energy step can proceed by one of two mechanisms:-

a) a Coulombic or Förster-type[45] interaction,

b) an electron transfer or Dexter-type[46] interaction.

For the Förster-type interaction to occur, the rate of transfer depends on the overlap of the donor emission, and the acceptor absorption spectra. Energy transfer via this mechanism occurs at encounter distances of up to ca 2-6 nm, and can exceed the diffusion rate[47].

The electron exchange mechanism is governed by the less restrictive Wigner's spin rule, where spin must only be conserved in the interaction. This process takes place at a much shorter encounter distance than the Förster-type mechanism, less than ca 0.06-0.15 nm. An example of long-range Förster-type energy transfer is that from the anthracene[47] excited singlet to the perylene excited singlet, while triplet-triplet energy transfer from phenanthrene.d_{10} to naphthalene.d_8 in viscous solution at 87K proceeds via the electron exchange mechanism[48].

Chapter 2

Experimental Techniques

(i) Preparation of Compounds

β-Dicarbonyl compounds with at least one proton on the central carbon atom may undergo a keto-enol tautomerism, shown in figure 2, 1.

Figure 2, 1

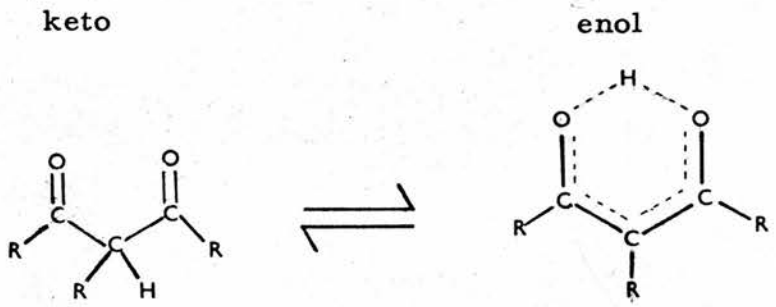

Under suitable conditions, the enolic proton can be replaced by a metal ion. Complexes with β-diketoenols have been reported for all metals, with the exceptions of some of the radioactive elements. This type of complex has been known for over one hundred years, and the subject of metal β-diketoenolate chemistry was reviewed as long ago as 1914 by Morgan and Moss[49].

β-Diketoenols with a wide variety of substituents at R_1, R_2, and R_3 (see figure 2, 1) have been complexed with metal ions, and Table 2, 1 shows abbreviations which will be used in the text for the anionic ligands of particular interest.

Table 2, 1:- Abbreviations

Abbrev	Anion	Structural formula
AA*	acetylacetonate	$[(CH_3CO)_2CH]^-$
BTFA	beneoyltrifluoroacetylacetonate	$(C_6H_5COCHCOCF_3)^-$
HFAA	hexafluoroacetylacetonate	$[(CF_3CO)_2CH)]^-$

* - HAA = acetylacetone

Fernelius and Bryant[50] have reviewed the general methods of preparation of metal β-diketoenolates. One of the most common methods of synthesis is the direct reaction of a β-diketoenol compound with a metal ion in solution, and subsequent precipitation of the metal β-diketoenolate complex. Two equilibria take place which are of importance in this synthetic method,

(i) $H(\beta\text{-diketoenolate}) \rightleftharpoons H^+ + (\beta\text{-diketoenolate})^-$

(ii) $M^{n+} + y(\beta\text{-diketoenolate})^- \rightleftharpoons [M(\beta\text{-diketoenolate})_y]^{(n-y)+}$.

To improve the yield of the complex, the equilibrium (i) may be pushed to the right by buffering. This has been successfully carried out in certain cases by using metal acetates[51]. Another method is to slowly add a weak base[52], eg. ammonia, thereby producing more of the β-diketoenolate anion. Care must be taken when using this method to ensure that the pH is kept below the value where the metal hydroxide precipitates, thereby contaminating the product[53]. Many syntheses for the preparation of specific metal complexes have recently been developed.

(a) Preparation of Lanthanide trisacetylacetonates

The reaction of acetylacetone with lanthanide ions has been widely studied, although much of the early literature on the subject gives conflicting information, largely due to poor analytical data. The yields of lanthanide acetylacetonates are generally rather low. Stites, et al[52], in reacting $LnCl_3$ salts with ammonium acetylacetonate in water, showed that control of the pH of solution could greatly improve the yield, and Pope et al[54], found that by recrystallising the crude product from the Stites preparative method in 60% alcohol solution (by volume), the lanthanide tris-acetylacetonate trihydrate was produced and confirmed this by C and H analyses. Richardson et al[55], reported that mono and dihydrates of the lanthanide tris-acetylacetonates can be prepared from the crude Stites product by recrystallisation from 95% cold ethanol and acetylacetone respectively.

In the experimental investigations detailed in chapters 3, 4 and 5 various lanthanide tris-acetylacetonate trihydrates were used. These were synthesised using the method of Stites et al[52], followed by the purification method suggested by Pope[54]. The synthetic method employed is detailed as follows.

Preparation of $LnCl_3.nH_2O$

Lanthanide oxides (Koch-Light 99.9%) were converted to the hydrated chlorides, $LnCl_3.nH_2O$, by refluxing in hydrochloric acid until dissolution was complete. In many cases, the dissolution was found to be more rapid when 70% acid rather than the concentrated was used. The solid lanthanide chlorides were obtained by removal

of excess HCl and water on a rotary evaporator. The chlorides obtained were not further washed, in case any insoluble compound, probably oxy-chloride, was produced.

Preparation of $Ln(AA)_3.3H_2O$ complexes

Ammonium acetylacetonate was prepared by adding redistilled acetylacetone dropwise to an equivalent molar amount of ammonium hydroxide in a stirred aqueous solution. The resulting $NH_4(AA)$ solution (4.5 mole equivalents) was then added dropwise to a stirred aqueous solution of the lanthanide chloride (1 mole equivalent). The pH of the stirred solution was monitored throughout, and was brought to within 0.1-0.2 pH units of the pH values where precipitation of the lanthanide hydroxide occurs by addition of very dilute ammonia. The pH's where precipitation of lanthanide hydroxides occur[54] are shown in Table 2,2.

Table 2,2:- pH of solution where precipitation of lanthanide hydroxide occurs

pH	Lanthanide
6.9	Cerium
6.6	Praesodymium, Neodymium
6.5	Samarium, Europium, Gadolinium
6.4	Terbium, Dysprosium, Holmium
6.3	Erbium
6.1	Ytterbium

The crude product was filtered off, washed with water, air dried, and dissolved in 95% hot ethanol. On dissolution, a few drops

of acetylacetone were added to minimise hydrolysis and sufficient water was added to produce a 60% ethanol solution. The solution was allowed to cool slowly, and the crystals which separated were washed once with 50% ethanol, once with water, air dried and stored in tightly-stoppered bottles. The resulting $Ln(AA)_3.3H_2O$ complexes were analysed for C and H, and in all cases were within 0.3% of the theoretical elemental percentages. The analytical data for the $Ln(AA)_3.3H_2O$ complexes are shown in Table 2,3.

Table 2,3:- Analytical data for $Ln(AA)_3.3H_2O$ complexes

	ANALYSES			
	Calculated		Found	
Lanthanide	C	H	C	H
Ce	36.44	5.29	36.59	5.54
Pr	36.59	5.49	36.66	5.57
Nd	36.34	5.45	36.38	5.66
Sm	35.96	5.43	35.39	5.42
Eu	35.79	5.37	35.65	5.33
Gd	35.47	5.36	35.26	5.28
Tb	35.33	5.34	35.20	5.36
Dy	35.06	5.26	35.03	5.04
Ho	34.89	5.25	35.16	5.33
Er	34.74	5.21	34.72	5.20
Yb	34.35	5.15	34.10	5.17

(b) Preparation of Other Metal Acetylacetonates

Various metal acetylacetonates were used in experimental investigations described in Chapters 4 and 5. These were prepared by methods similar to those described earlier in this chapter, and

the specific synthetic pathways used are given in the references shown in Table 2, 4, as well as their C and H analyses.

Table 2, 4:- Analytical data and preparative methods for non-lanthanide metal acetylacetonates

Compound	Analysis				Reference for Synthesis
	Calculated %C	%H	Found %C	%H	
$Al(AA)_3$	55.57	6.53	55.59	6.29	56
$VO(AA)_2$	45.28	5.28	45.09	5.33	57
$Cr(AA)_3$	51.57	6.06	51.70	6.08	58
$Mn(AA)_3$	51.13	6.01	51.24	6.28	59
$Mn(AA)_2.2H_2O$	41.53	6.23	40.33	6.36	60(a)
$Co(AA)_3$	50.57	5.95	50.84	6.04	61
$Co(AA)_2.2H_2O$	40.97	6.18	40.88	6.20	62(b)
$Ni(AA)_2.2H_2O$	41.00	6.15	41.12	6.45	63(c)
$Cu(AA)_2$	45.89	5.39	45.93	5.36	64
$Zn(AA)_2.H_2O$	42.70	6.11	42.69	5.93	65(d)
$Pd(AA)_2.2H_2O$	39.65	4.62	39.80	4.71	66

Notes:-

(a) Anhydrous $Mn(AA)_2$ was prepared from $Mn(AA)_2.2H_20$ by heating for two hours at 393K in a vacuum oven at a pressure of a few mm Hg[67].

(b) Anhydrous $Co(AA)_2$ was prepared by heating $Co(AA)_2.2H_2O$ at 330K for 6 hours at a few mm Hg[68].

(c) Anhydrous $Ni(AA)_2$ was prepared by subliming $Ni(AA)_2.2H_2O$ at 465-500K at 0.2-0.4 mm Hg[63].

(d) Anhydrous $Zn(AA)_2$ was prepared by subliming $Zn(AA)_2.H_2O$ at *ca.* 400K at 0.1 mm Hg[65].

(c) Preparation of $Ln(BTFA)_4.pipH$ Chelates

An aqueous solution of the lanthanide salt (1 mole equivalent) was added dropwise to a stirred 95% ethanol solution of

benzoyltrifluoroacetone (HBTFA) (4.5 mole equivalents), and piperidine (pip) (4.5 mole equivalents). The product precipitated on standing, and the yield could be increased by the addition of a few drops of water. The precipitate was filtered off, and air dried. Each complex was analysed for C and H, and the analytical data are given in Table 2,5.

Table 2,5:- Analytical data for $Ln(BTFA)_4.pipH$ complexes

Complex	Analysis			
	Calculated		Found	
	%C	%H	%C	%H
$Tb(BTFA)_4.pipH$	48.88	3.28	48.69	3.40
$Eu(BTFA)_4.pipH$	49.18	3.27	49.32	3.57
$Nd(BTFA)_4.pipH$	49.63	3.24	49.58	3.42

(d) Purification of Solvents

Benzene

Solvent benzene was distilled, stored over sodium metal wire, and redistilled before use[69].

n-Butanol

Solvent n-butanol was dried by treatment with sodium metal followed by refluxing with an appropriate amount of di-n-butylphthallate. Dry n-butanol was then obtained by fractional distillation, the first fractions being discarded[69].

n-Propanol

Dry n-propanol was prepared using a similar method to that used for n-butanol, and refluxing with di-n-propylphthallate[69].

Pyridine

Solvent pyridine was refluxed over solid KOH, and purified pyridine obtained by fractional distillation[69].

(ii) Ground State Absorption Spectroscopy

Absorption spectra in the ultraviolet and visible regions were obtained using a Perkin-Elmer model 402 Ultraviolet Spectrophotometer. This instrument has a wavelength range of 190 to 850 nm, and an optical density range of 0 to 1.5. All measurements were carried out at room temperature using 1 cm path length (unless otherwise stated) optically matched quartz cells with PTFE stoppers. The pure solvent was used as the reference. Extinction coefficients are quoted in units of $cm^{-1} mol^{-1} dm^{-3}$.

(iii) Emission Spectroscopy

(a) The Perkin-Elmer Hitachi MPF-2A Spectrofluorimeter

This instrument can be used to determine the excitation and emission spectra of luminescent solids or solutions. Use of different cell compartments permits spectra to be obtained at temperatures ranging from 77K to room temperature and above.

The excitation light source is a 150 watt Xenon lamp, giving a near continuum from ca. 270 nm to above 850 nm. The excitation monochromator allows irradiation of samples in the range 200-700 nm with monochromated light. The emission monochromator selectively

monitors the intensity of radiation emitted by the sample between 200 and 800 nm. Both monochromators are of the Czerny-Turner grating variety (600 lines mm^{-1}). The gratings can be manually scanned, or motor driven.

Excitation spectra were obtained by setting the emission monochromator at, or near the emission maximum, and the intensity of emission was monitored as the excitation wavelength was scanned through the desired range. Emission spectra were measured by setting the excitation wavelength at, or near, the absorption maximum of the sample, and the emission wavelength scanned. Resolution of spectra depended on the excitation and emission slit widths, which can both be altered within the range 1 to 40 nm.

Two modes of operation are possible with this instrument,

(i) Manual mode,

(ii) Reference mode.

In the manual mode, no correction is made for any short or long term fluctuations which may occur in the intensity of the Xenon lamp, and which may be caused, for example, by changes in the lamp supply voltage.

In the reference mode, the excitation light passes through a beam splitter, and a small fraction of the light is focussed on to a reference photomultiplier, the output of which inversely controls the gain of the main photomultiplier. In this system, there is some compensation for fluctuations in excitation light intensity. This mode was used for all measurements reported in this thesis.

(b) Sampling Techniques

Emission spectral profiles were recorded using the right-angled viewing technique, where the exciting light passes through the sample in a direction at right angles to that along which the fluorescence or phosphorescence is viewed. In using this technique, dilute solutions must be used (optical density < 0.02) to avoid the possibility of distortion of the spectral profile due to self absorption. This occurs if the emission and absorption bands of the sample overlap, and is known as the inner filter effect[70]. If dilute solutions are not used, corrections to the observed spectra may have to be made. Lanthanide ion emission in chelates is however usually considerably red-shifted, with respect to the ligand absorption bands and therefore no inner filter restrictions are imposed on the concentration of the sample.

In the investigations into intermolecular energy transfer between lanthanide chelates in solution, described in Chapter 3, front face illumination was used. This arrangement has the advantage that the phosphorescent yield of strongly absorbing solutions (with no inner filter effects) can be more accurately measured than is possible with right-angled viewing techniques. The experimental apparatus was the MPF-2A solid sampler, carrying an adapter to hold a 1 mm quartz cell. The cell was held at 30^{o} to the incident beam. A defocussing lens was placed in front of the cell, thereby illuminating the whole of the front face of the sample cell, rather than illuminating by the fine line of the unaltered incident light beam. This reduced errors

which could have arisen due to alterations in the precise positioning of the sample relative to the emission photomultiplier, and consequent errors in the observed emission intensity.

(c) Correction of Excitation Spectra

Excitation spectra, obtained by the method described in section 3(a) of this chapter are uncorrected spectra. These are plots of emission photomultiplier voltage against excitation wavelength[70], and depend on the molar extinction coefficient of the sample at wavelength λ, ($\varepsilon(\lambda)$), the quantum efficiency of the emitting sample ϕ_f, and the radiative output, $I(\lambda)$, of the excitation source. $I(\lambda)$ is dependent on the nature of the source and the characteristics of the monochromator. To obtain the true excitation spectrum, the variation of $I(\lambda)$ with wavelength must be determined. This was carried out by Dr. J.F. Ireland[71], and the method used was that described by Argauer and White[72]. This method employs a compound which has identical absorption and excitation spectra. A comparison between the uncorrected excitation spectrum and the absorption leads to a measure of the relative intensity of the excitation source at different wavelengths. Correction factors for relative intensity at different wavelengths are thus determined, and uncorrected spectra for other samples can be corrected using these factors. The compound used to calibrate the instrument was the aluminium chelate of 2,2'-dihydroxy-1,1'-aso-naphthalene-4-sulphonic acid sodium salt, which allowed calibration in the region 220 to 600 nm.

(d) Correction of Emission Spectra

Absolute emission spectra relate the quantum intensity of emission to wavelength. The observed photomultiplier output on the MPF-2A is dependent on the photomultiplier sensitivity at different emission wavelengths, the dispersions of the emission monochromator and light losses, and therefore must be corrected to obtain the true emission spectrum. This was carried out by Dr. J.F. Ireland[71] using a series of reference fluorescent solutions, the absolute fluorescence spectra of which have been previously determined. The series is chosen to give as wide a range of calibration as is required. Comparison of the observed emission spectra with the true spectra of these compounds yields conversion factors which, as in the case of excitation spectra correction, may be used to convert other sample spectra to their true profiles. The compounds used for calibration are detailed in Table 2, 6.

Table 2, 6:- Compounds used to obtain spectral sensitivity curve

Compound	Emission Range (nm)
2-aminopyridine	330-450
Quinine sulphate	400-550
3-aminophthalimide N, N-Dimethyl m-nitroaniline	450-630
Aluminium (PBBR) chelate[(a)]	580-700
4-dimethylamine-4'-nitrostilbene	600-750

(a) Compound used in correction of excitation spectra

(e) Automatic Digitalisation and Correction of Excitation and Emission Spectra

Manual correction of excitation and emission spectra is a very slow process, and it is therefore advantageous to transfer data from the spectrofluorimeter automatically to paper tape which can then be processed by computer[73]. This was achieved by correcting the output of the MPF-2A to a Solartron LM 1604 digital voltmeter with an EX 3054 positive fan-out unit. The voltmeter was interlinked with a Solartron 3230 data transfer unit, using a Facit 4070 paper tape punch as an output device. The uncorrected detector voltage was thus stored in computer-readable form. True spectral profiles were obtained by processing the uncorrected data on paper tape with the programme SPECTRUM, written by Dr. C.R.S. Dean and Dr. T.M. Shepherd[74].

(iv) Excited State Lifetime Measurements

(a) Apparatus

A locally designed spectrofluorimeter was used to obtain lifetimes of phosphorescent solids and solutions over the temperature range 77K to ca 330K. A schematic diagram of the apparatus is shown in Figure 2,2.

The sample cell was placed in a four-quartz-windowed Dewar, thereby allowing the sample to be held at various temperatures. Emitted light was viewed at right angles to the excitation source. The decay curves of the samples were obtained using a signal

averaging technique, where the measurement cycle was initiated by the signal averager (Data Laboratories Ltd, 200 point averager DL102), providing a pulse which was used to trigger the E.G. and G., type FX-6A flash tube. Different intensities of flash could be obtained by varying the voltage across a 16μF capacitor. The maximum voltage available was 800V. Emission, as previously described, was viewed at right angles to the flash, and was focussed into the 1200 line per mm monochromator incorporated in a Hilger Watts Monospec 1000 and thence to the EMI 9526 photomultiplier. After a predetermined delay, to eliminate any trace of the flash, the phosphorescence decay curve was stored in the signal averager. The decay of emitted light was monitored over a pre-determined period, known as the "sweep-time". This sweep-time was adjustable, and it was found that the most accurate results were obtained when the sweep-time was approximately equal to the phosphorescent lifetime of the sample. The decay curve was displayed on the oscilloscope, and the measurement cycle was repeated 2^n times, where n=0 to 8, until a satisfactory signal to noise ratio resulted. The data in the signal averager memory were then fed on to paper tape using the data transfer unit described[73] in section 3(e) of this chapter, and were computer processed using a least squares method to check exponentiality, and to determine the exponential lifetime of the sample. The data were processed by an IBM 360/44 computer.

Note

The high resolution $Tb(AA)_3.3H_2O$ emission spectrum shown in Chapter 3 was obtained using a modification of the Monospek 1000, which has been described by T.D. Brown[74].

Figure 2, 2:- Schematic diagram of lifetime apparatus

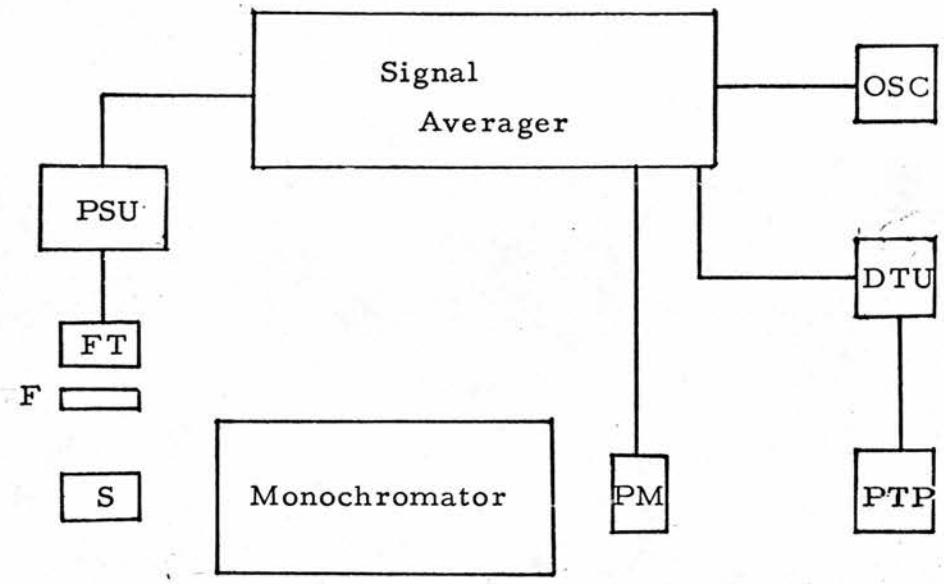

S = sample compartment

F = ultraviolet pass filter

FT = flash tube

PSU = power supply unit for FT

OSC = oscilloscope

DTU = data transfer unit

PTP = paper tape punch

PM = photomultiplier

(b) Programme LIFETIME

This programme was written by Dr. C.R.S. Dean and Dr. T.M. Shepherd, and uses the data stored on paper tape to perform a least squares regression to obtain the best straight line between the natural logarithm of the phosphorescence intensity against time. Since all phosphorescent samples used in this work exhibit first order decay curves, the gradient of this line is equal to the exponential lifetime of the excited sample. The programme

also calculates the deviation from true exponentiality. Lifetimes obtained using this technique were reproducible to better than ±3%.

(v) Molecular Weight Determinations

Molecular weight determinations in solution were made using a Mechrolab Vapour Pressure Osmometer Model 301A. This instrument consists of two principal units; the sample chamber, and the control unit. Measurements are made by placing one drop of pure solvent on one thermistor bead, and one drop of sample solution on the other bead. These thermistor beads are placed side by side in the sample chamber which is saturated with solvent vapour. The heat of vapourisation is a colligative property, and is therefore dependent on the concentration of solute, hence a temperature difference is created between the two drops. The temperature difference between the two thermistor beads is determined by using a control unit employing a Wheatstone Bridge. Since the temperature shift is a colligative property, the instrument may be calibrated with a known concentration range of known solute. Unknown concentrations of sample solutions may then be directly determined from the calibration curve. The instrument was calibrated using benzil in dry benzene at 310K, and the accuracy was determined using 1, 3, 5-trinitrobenzene, and was found to be better than ±10%.

Chapter 3

Intermolecular Energy Transfer between Lanthanide tris-acetyl acetonates in Solution

If $Tb(AA)_3.3H_2O$ is irradiated in the ligand absorption band, intramolecular energy transfer occurs from the excited ligand triplet to the Tb^{3+} excited levels, with subsequent emission from the Tb^{3+} $^5D_4$ level[75]. The reported quantum yield is 0.19 in ethanol solution[75]. Intermolecular energy transfer from the Tb^{3+} $^5D_4$ level to other lanthanide tripositive ions in the form $Ln(AA)_3.3H_2O$ has been studied in solution. Phosphorescent lifetimes were measured using the apparatus described in Chapter 2, and phosphorescent yield measurements were made using the front face viewing technique[70] with 1 mm quart cells.

(a) Intermolecular Energy Transfer in n-Butanol Solution

(i) Lifetime Measurements

$Tb(AA)_3.3H_2O$ is susceptible to hydrolysis in solution. In wet ethanol the hydrolysis can be followed by observing a gradual blue shift in the ligand absorption band. This shift is probably due to hydrolysis reactions with the slow production of free acetylacetone, and ultimately $Ln(OH)_3$. The initial and limiting spectra of $Tb(AA)_3.3H_2O$ in ethanol are shown in Figure 3,1. The following equilibria describe the proposed hydrolysis.

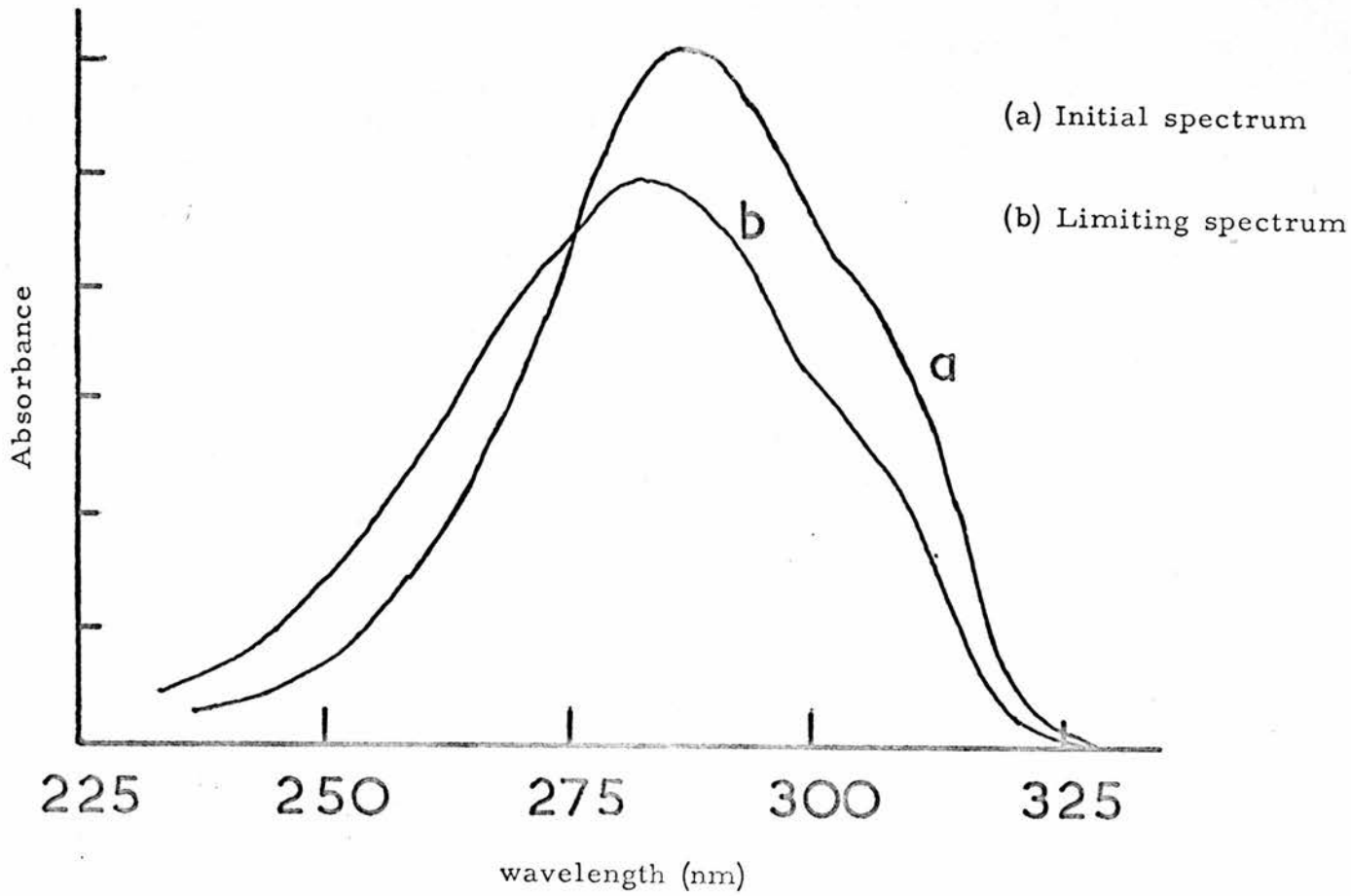

Fig. 3, 1: absorption spectrum of $Tb(AA)_3.3H_2O$ in ethanol

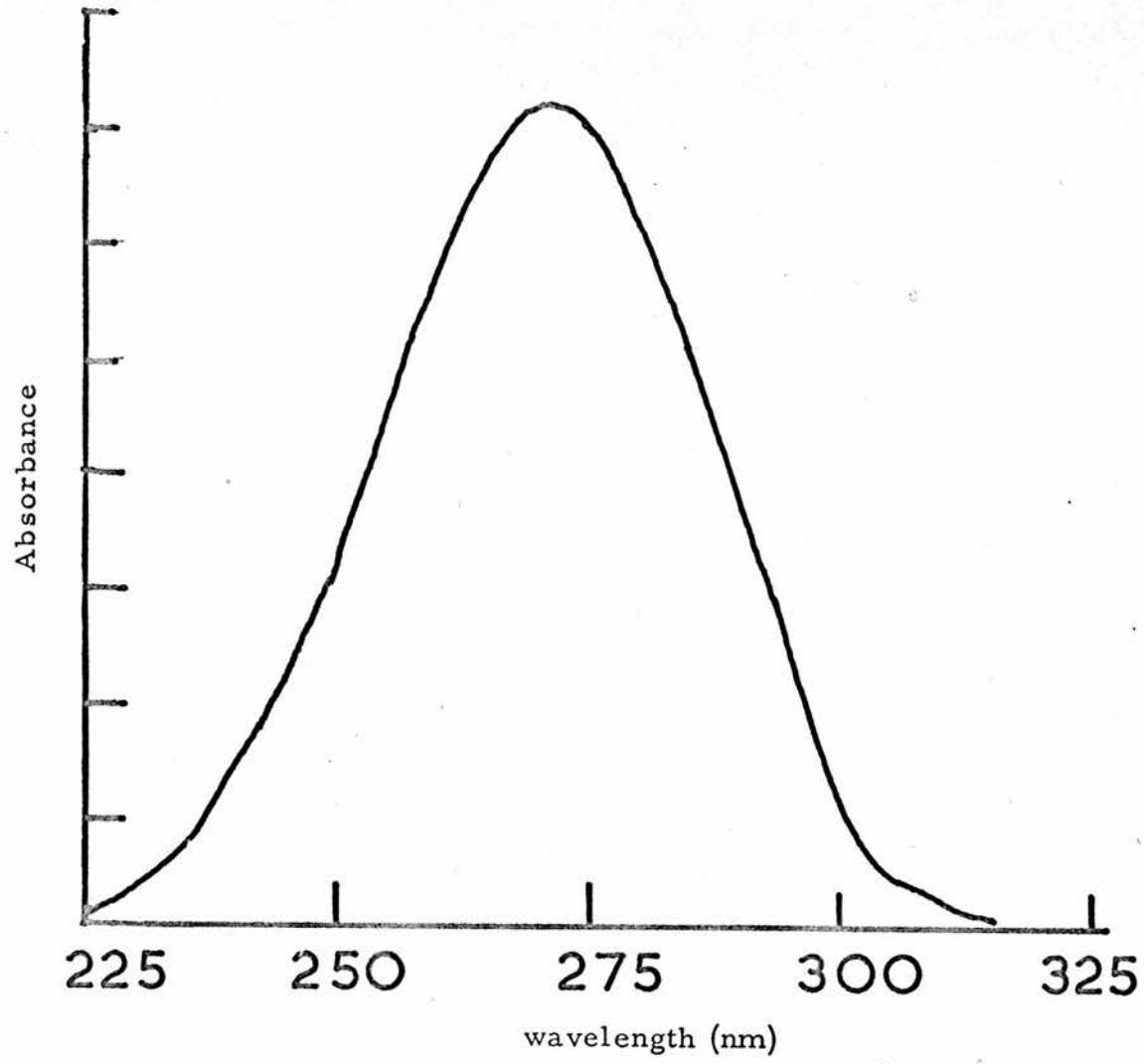

Fig. 3, 2: Absorption Spectrum of acetylacetone in ethanol

$$H_2O + Tb(AA)_3 \rightleftharpoons Tb(AA)_2.OH + CH_3COCH_2COCH_3$$

$$Tb(AA)_2\text{-}OH + H_2O \rightleftharpoons Tb(AA)(OH)_2 + CH_3COCH_2COCH_3$$

$$Tb(AA)(OH)_2 + H_2O \rightleftharpoons Tb(OH)_3 + CH_3COCH_2COCH_3 \ .$$

The limiting spectrum will thus be that of acetylacetone if this reaction scheme goes to completion. The spectrum of acetylacetone in ethanol is shown in Figure 3,2.

Dry ethanol is very hygroscopic and initial studies of $Tb(AA)_3.3H_2O$ in this solvent did not give reliable results. It was therefore decided to use dry n-butanol as a solvent. In solutions of $Tb(AA)_3.3H_2O$ in dry n-butanol, no significant blue shift in the ligand spectrum over a time period of ca $1\frac{1}{2}$ hours was observed. The absence of blue shift indicated that no significant hydrolysis of $Ln(AA)_3.3H_2O$ complexes would take place in dry n-butanol solution, during the time taken to carry out experiments on these solutions. The use of $Tb(AA)_3.3H_2O$ as the donor species has the advantages of

(i) the high quantum efficiency of Tb^{3+} phosphorescence on irradiation of the ligand absorption band[75],

(ii) the position of the Tb^{3+} $^5D_4$ emitting level (ca 20,200 cm^{-1}), which lies above many potential acceptor levels, and

(iii) the large energy difference between the Tb^{3+} $^5D_4$ level and the ligand triplet, at ca 25,000 cm^{-1} [76,77], which minimises any significant thermal depopulation of the Tb^{3+} $^5D_4$ level to the triplet at room temperature[78].

The corrected emission spectrum of $Tb(AA)_3.3H_2O$ in n-butanol is shown in Figure 3,3. The bands correspond to emission from the Tb^{3+} $^5D_4$ level to the ^7F multiplet. The maximum intensity of

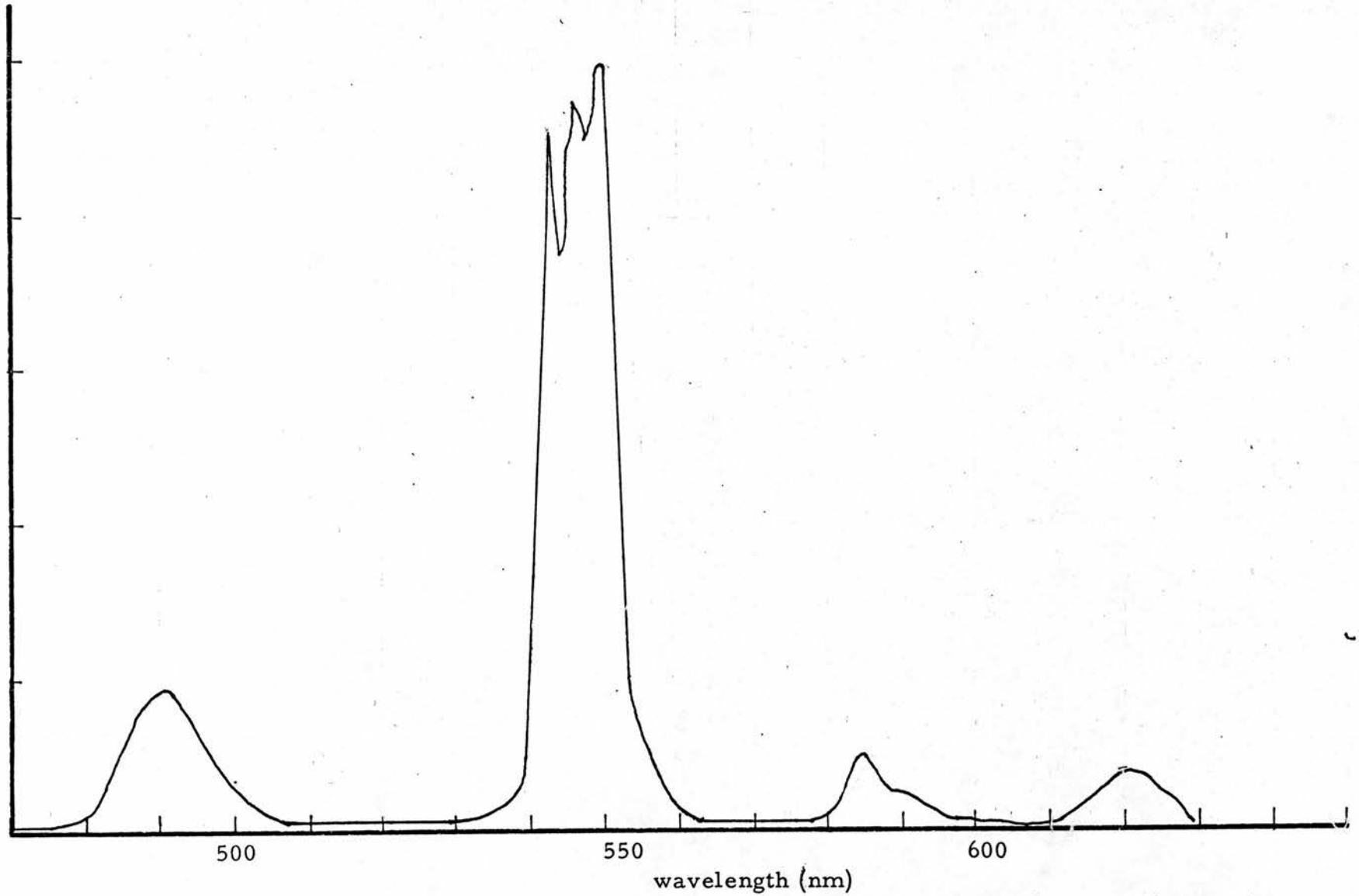

Fig. 3, 3: The corrected emission spectrum of $Tb(AA)_3 . 3H_2O$ in n-butanol (10^{-2} mol dm^3) at 293K

emission occurs at 547.5 nm, which is the $^5D_4 \longrightarrow {}^7F_5$ transition, and this band was monitored during the work. The lifetime of this band over the concentration range 10^{-4} to 10^{-2} mol dm^{-3} is constant within experimental error at 790 ± 15 μs, in n-butanol solution at 293K. Solutions of terbium and added lanthanide complex in n-butanol were made up with the total concentration kept constant at either 0.005 mol dm^{-3} or 0.01 mol dm^{-3} in each series of measurements. This minimised variations in the geometry of the excited region of the sample, and any possible concentration dependent dissociation of the complexes.

The lifetime, τ, of the Tb^{3+} $^5D_4$ level in these solutions was monitored, and in all cases examined, except where the acceptor complex was that of Gd^{3+} or Yb^{3+}, τ decreased with increasing concentration of the added quencher. The decrease in τ indicates that the Tb^{3+} $^5D_4$ level is undergoing energy transfer to the added complexes. The Tb^{3+} $^5D_4$ level lies ca 5000 cm^{-1} below the lowest ligand triplet, and therefore transfer of energy to the excited ligand levels of $Ln(AA)_3.3H_2O$ is improbable. The results suggest that the energy transfer occurs to the excited levels of the Ln^{3+} ions. This is supported by the Gd and Yb results, since the Gd^{3+} ion has no energy levels below ca 32000 cm^{-1} [8], precluding Tb^{3+} $^5D_4 \rightsquigarrow Gd^{3+}$ energy transfer, and the Yb^{3+} ion with its $4f^{13}$ configuration, has only one Laporte forbidden excited state, the $^7F_{5/2}$ level which lies at about 10000 cm^{-1}. Energy transfer over an energy difference of ca 10000 cm^{-1} is not likely to be efficient. Energy levels of some Ln^{3+} ions are shown in Figure 3,4. The negative results with Gd^{3+}

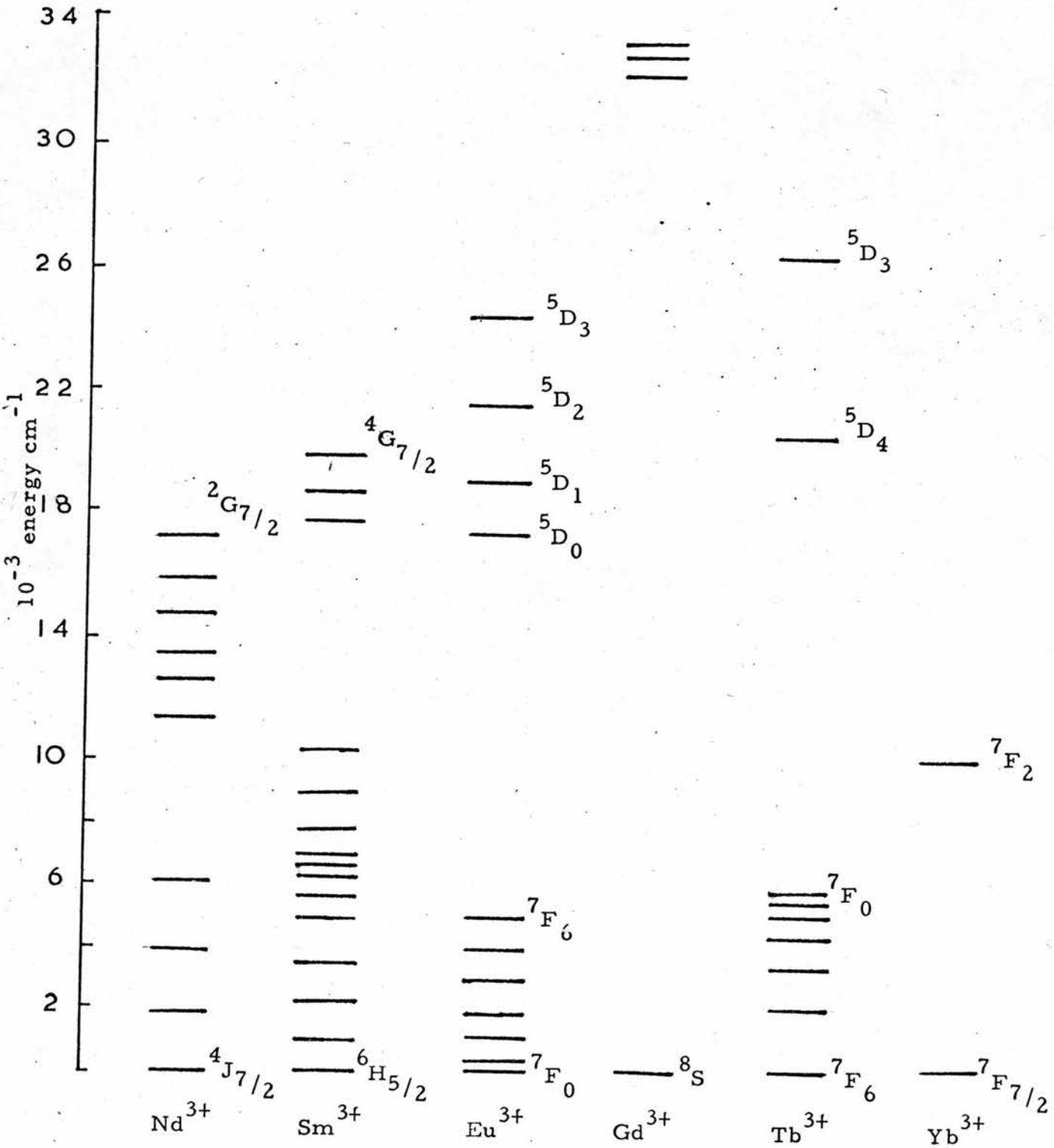

Fig. 3,4: Energy levels of some Ln^{3+} ions

Fig. 3,5: Typical plots of $(\tau_o/\tau_{[Ln]}-1)$ against [Ln] at 0.005 mol dm^{-3} total complex concentration in n-butanol at 293K

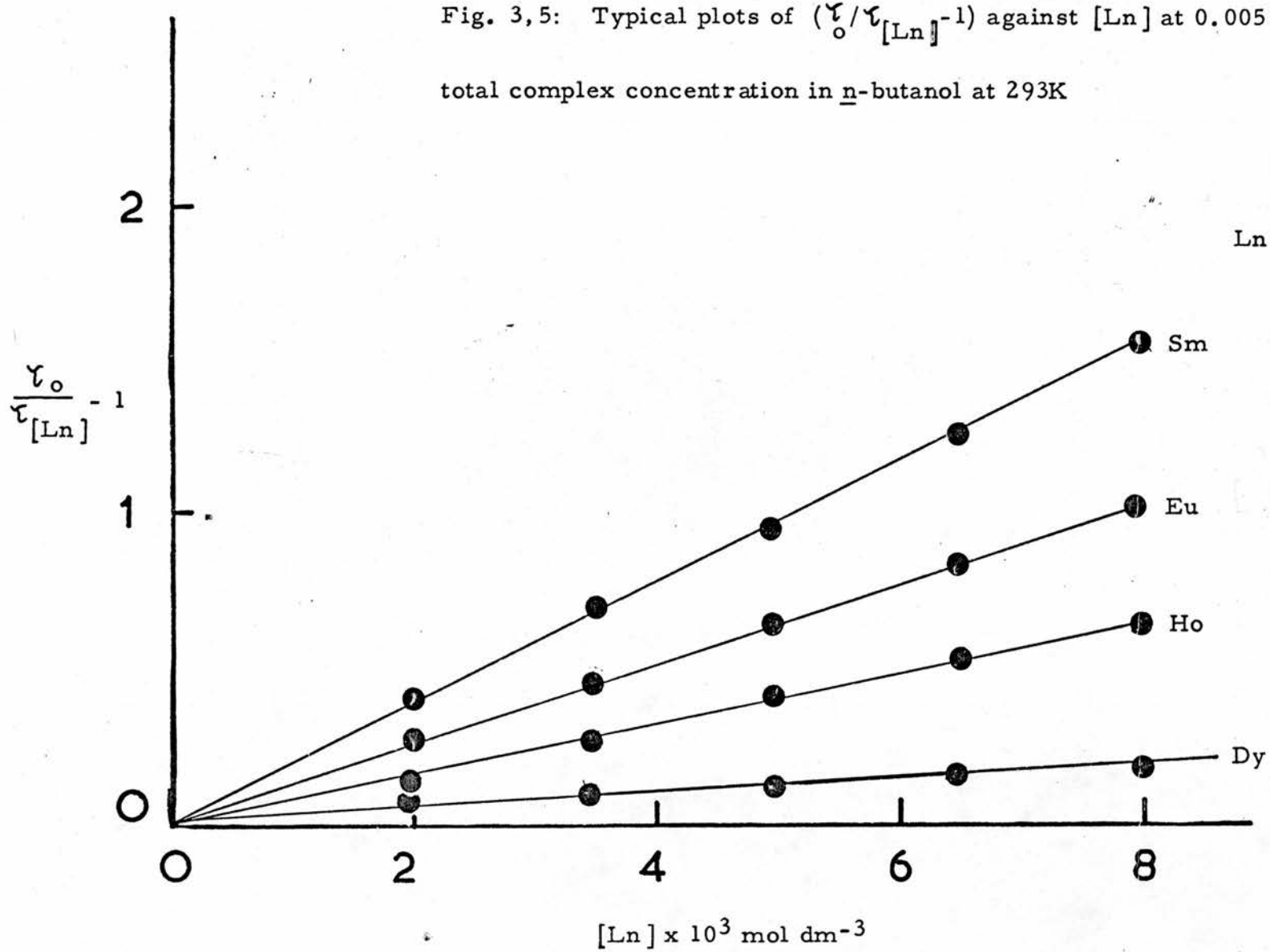

and Yb^{3+} complexes confirm that ligand excited levels are not involved in the energy transfer step, since they should, to a good approximation, be independent of the Ln^{3+} ion.

In all cases where a decrease in the Tb^{3+} $^5D_4$ lifetime with added quencher was observed, the Stern-Volmer relation was obeyed, ie.

$$\frac{\tau_o}{\tau} - 1 = k_{SV}[Q] \qquad \text{——— 1}$$

where τ_o = exponential lifetime of the Tb^{3+} $^5D_4$ level in the absence of quencher,

τ = exponential lifetime of the Tb^{3+} $^5D_4$ level in the presence of added quencher,

$[Q]$ = concentration of quencher in mol dm^{-3},

k_{SV} = Stern-Volmer gradient.

Typical plots of $\frac{\tau_o}{\tau} - 1$ against [Ln] at 0.005 mol dm^{-3} total concentration are shown in Figure 3,5. Stern-Volmer gradients for various quenchers are shown in Table 3,1, along with the bimolecular rate constant, k, for the intermolecular energy transfer step, derived from $k = \frac{k_{SV}}{\tau_o}$ (see Chapter 1).

The measurements were repeated at a total molar concentration of 10^{-2} mol dm^{-3}, for Ln=Nd, Sm, Eu and Ho. The results again obeyed the Stern-Volmer relation, and the k_{SV} and k values are given in Table 3,2.

These values are lower than those obtained at 5×10^{-3} mol dm^{-3} total concentration, indicating that the energy transfer rate is lower in the more concentrated solutions. Further runs at 0.0025 and 0.00125 mol dm^{-3} showed no significant change in the k values from those

Table 3, 1:- Stern-Volmer gradients, k_{SV} and bimolecular rate constants, k, for quenching of the Tb^{3+} $^5D_4$ level in $Tb(AA)_3.3H_2O$ [(a)] by $Ln(AA)_3.3H_2O$ complexes in n-butanol at 293K, at total concentration of 0.005 mol dm^{-3}

Ln	k_{SV} ($mol^{-1} dm^3$)	$k \times 10^{-5}$ ($mol^{-1} dm^3 s^{-1}$)
Pr	370	4.7
Nd	390	4.9
Sm	390	4.9
Eu	260	3.3
Gd	-	- [(b)]
Dy	40	0.5
Ho	160	2.0
Er	120	1.5
Yb	-	- [(b)]

(a) $\tau_o = 790 \mu s$

(b) $k < 2 \times 10^{-2} mol^{-1} dm^3 s^{-1}$

Table 3, 2:- k_{SV} and k values for quenching of the Tb^{3+} $^5D_4$ level in $Tb(AA)_3.3H_2O$ [(a)] by $Ln(AA)_3.3H_2O$ in n-butanol solution at 293K, at a total concentration of 1×10^{-2} mol dm^{-3}

Ln	k_{SV} ($dm^3 mol^{-1}$)	$k \times 10^{-5}$ ($mol\ dm^{-3} s^{-1}$)
Nd	290	3.67
Sm	320	4.1
Eu	210	2.7
Ho	140	1.8

(a) $\tau_o = 790 \mu s$

obtained at 0.005 mol dm^{-3}. The lower rate in the case of the 0.01 mol dm^{-3} runs may be concerned with the fact that this concentration is close to the stability limit of tris acetylacetonate complexes of the lanthanides in n-butanol.

The values of k, the bimolecular rate constant, are considerably lower than the diffusion rate constant, k_D, of n-butanol at 293K, where $k_D = 3.3 \times 10^9$ $dm^3 mol^{-1} s^{-1}$. This value is derived from the Debye equation[44], detailed in Chapter 1. Chrysochoos and Evers[37] obtained an average rate constant for energy transfer between Tb^{3+} and Eu^{3+} in dimethylsulphoxide (DMSO) solution, of $(2.2 \pm 0.4) \times 10^3$ $dm^3 mol^{-1} s^{-1}$. Ermolaev et al[38] have reported values of 2.7×10^3 $dm^3 mol^{-1} s^{-1}$ and 1×10^4 $dm^3 mol^{-1} s^{-1}$ for $Tb^{3+} \rightsquigarrow Ho^{3+}$ and $Tb^{3+} \rightsquigarrow Nd^{3+}$ respectively in DMSO at 293K. These reported values are significantly lower than those obtained for the $Tb(AA)_3 . 3H_2O \rightsquigarrow Ln(AA)_3 . 3H_2O$ system in n-butanol.

The radiationless transfer step may occur by (a) a Coulombic (Förster type)[45] mechanism involving multipole-multipole interactions and/or by (b) an electron exchange (Dexter type)[46] mechanism. Both the donor (Tb^{3+}) and the acceptor (Ln^{3+}) transitions involved in the transfer process arise from changes in the 4f configuration alone, and hence are Laporte forbidden. The donor transition, $^5D_4 \rightarrow {}^7F_n$ in common with many, if not all of the acceptor transitions, is also spin forbidden, for example the Eu^{3+} acceptor transitions may be $^5D_n \rightarrow {}^7F_0$ where n=0 or 1. In addition, the lanthanide ion absorption bands are very narrow. The forbidden nature of the transitions results in the absorption bands having molar extinction coefficients

which seldom exceed 5 $mol^{-1} cm^2$. The Förster equation may be written in the form,

$$k_D(r_A)_D = \text{constant} \times r^{-6} \times \int_0^{\infty} f_D(\bar{\nu}) \sum_A (\bar{\nu}) \, d\frac{\bar{\nu}}{4} , \qquad \text{—— 2}$$

where $k_D(r_A)$ = transfer rate constant at distance, r, between donor and acceptor, τ_D = donor lifetime, $f_D(\bar{\nu})$ = donor phosphorescence yield and $\sum_A (\bar{\nu})$ = acceptor molar extinction coefficient.

The transfer rate constant, k, for singlet-singlet spin allowed energy transfer can exceed 10^{11} $dm^3 mol^{-1} s^{-1}$ [47], the donor lifetime usually being of the order of 10^{-8} s, leading to typical values of k_{SV}, the Stern-Volmer gradient of ca 10^3 $dm^3 mol^{-1}$. In view of the low absorption coefficients of lanthanide ions, and the possible restrictions of overlap due to the narrow bandwidths, the value of the integral term in equation 1 is likely to be several orders of magnitude lower for lanthanide-lanthanide ion energy transfer occurring between discrete complexes than for singlet-singlet transfer.

It is therefore very unlikely that a Coulombic process is responsible for the observed behaviour. The electron exchange mechanism is governed by the less restrictive Wigner's spin selection rule, and is spin allowed for $Tb^{3+} \rightsquigarrow Ln^{3+}$ transfer. For example $Tb(^5D_4) + Eu(^7F_0) \longrightarrow Tb(^7F_6) + Eu(^5D_1)$ his spin conservation. Also, the absorption coefficient of the acceptor is not a rate determining factor, and thus energy transfer may occur if the lanthanide ions are brought into close proximity, and there is some degree of overlap between the donor emission and the acceptor absorption spectra. There is no a priori reason to preclude the operation of such a mechanism.

A simple model of the energy transfer process in solution may therefore involve a simple collision between the donor and acceptor complexes with electron exchange energy transfer. The closest approach of the two Ln^{3+} ions in the undissociated complexes is estimated to be 0.7 nm. To obtain further information on the energy transfer step, studies were carried out on the lifetime of mixed crystals of the form $Ln_xTb_{1-x}(AA)_3.3H_2O$. This is possible since the lanthanide complexes are isomorphous. If the mechanism is an electron exchange energy transfer step in solution, with the low rate constants being a consequence of the well shielded f-orbitals, the transfer rate in mixed crystals should be equal to or greater than that observed in solution, since adjacent Ln^{3+} and Tb^{3+} ions in the solid state have a separation of ca 0.7 nm. The lifetimes of the Tb^{3+} $^5D_4$ level in mixed crystals of $Eu_xTb_{(1-x)}(AA)_3.3H_2O$ were determined for x=0, 0.1, 0.3 and 0.5. The Stern-Volmer type plot of these lifetimes is shown in Figure 3,6. Assuming that the density of the mixed crystals is 1.5, a value of k_{SV}=0.3 $dm^3 mol^{-1}$ as x tends to zero is obtained. This value is three orders of magnitude lower than the corresponding k_{SV} in n-butanol solution. The proposed model thus appears to be inadequate, and the results suggest that the Ln^{3+} and Tb^{3+} ions in solution are required to come into closer proximity than 0.7 nm in order to be consistent with the observed value of k_{SV}.

From the collected data, the following conclusions may be drawn.

(a) The excited Tb^{3+} ion transfers its energy to the Ln^{3+} ions,

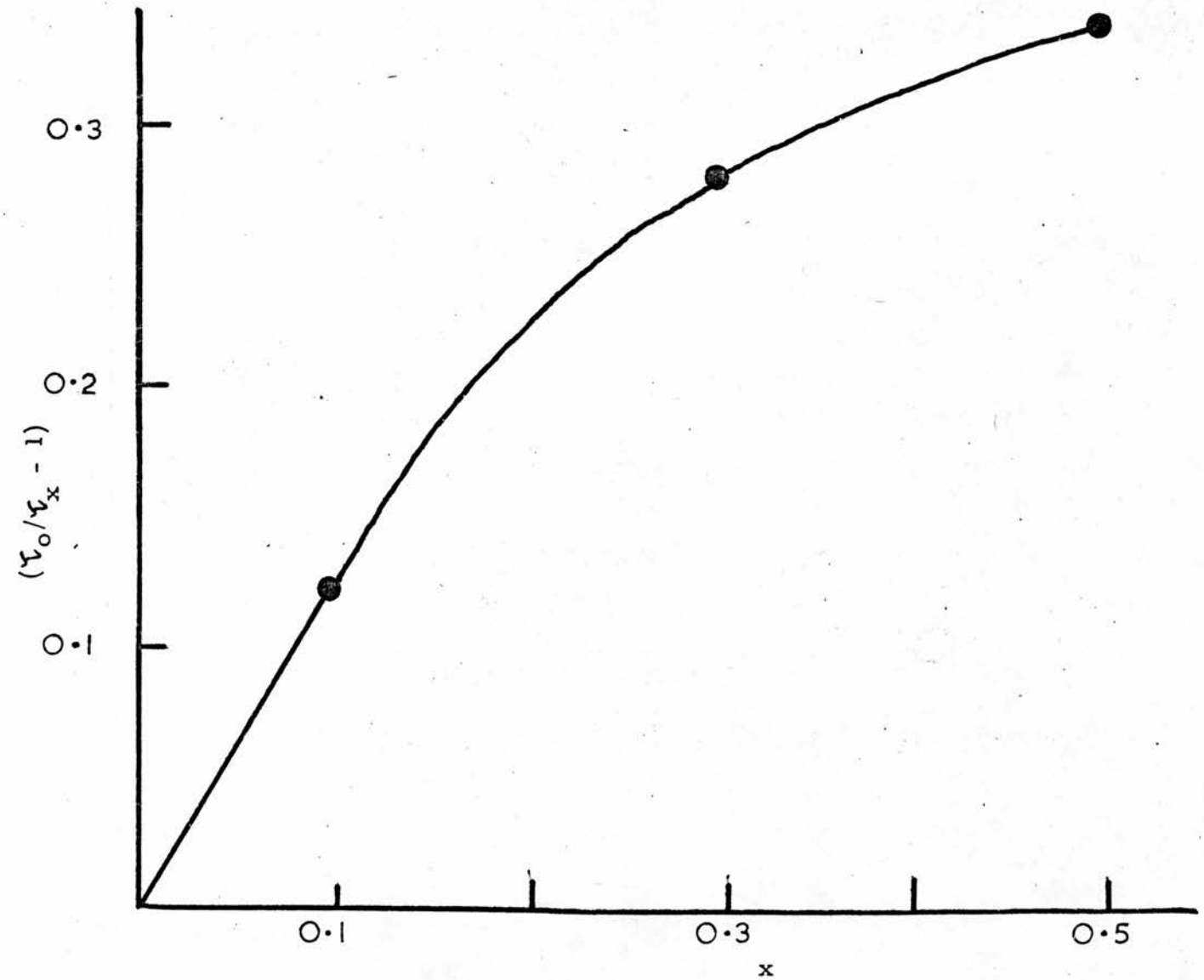

Fig. 3,6: Plot of $(\tau_o/\tau_x - 1)$ against x in the mixed crystals, $Eu_xTb_{(1-x)}(AA)_3 \cdot 3H_2O$
Temperature 293K

where the Ln^{3+} has suitable acceptors levels, and not to the ligand.

(b) The rate of energy transfer ($10^5 dm^3 mol^{-1} s^{-1}$) is some 10^4 times lower than that expected of a diffusion controlled process.

(c) A Coulombic-type energy transfer mechanism is not likely to be sufficiently rapid to explain the observed rates.

(d) An electron exchange transfer mechanism is possible.

(e) Efficient energy transfer between Tb^{3+} and Ln^{3+} acceptor ions only occurs at encounter distances significantly less than 0.7 nm.

It is also significant that the previous investigations of Chrysochoos[37] and Evers which were carried out in DMSO solution gave intermolecular energy transfer rates between Tb^{3+} and Eu^{3+} "bare" ions of 2.2×10^3 $dm^3 mol^{-1} s^{-1}$, ie. ca 10^2 times lower than the results obtained for the acetylacetonate complexes in n-butanol. This suggests that the nature of the solvent and/or complexing the ions may play an important role in the energy transfer process. Also, conclusion (e), above, precludes any readily conceivable energy transfer process which involves discrete donor and acceptor complexes and raises the possibility of processes involving non-monomeric species in solution.

This work was extended by investigating the energy transfer processes between $Tb(AA)_3 . 3H_2O$ and $Ln(AA)_3 . 3H_2O$ in several solvents other than n-butanol. J.D. Neilson and Dr. T.M. Shepherd were largely responsible for this part of the work, and it is summarised in part (b) of this chapter, as it is relevant to the studies on the transfer rate of energy from $Tb(AA)_3 . 3H_2O$ to

transition metal acetylacetonates, which is described in Chapter 4.

(ii) Phosphorescence Yield Measurements

The results described in the previous section have been concerned with energy transfer from the Tb^{3+} $^5D_4$ level alone. It is also possible that other intermolecular energy transfer processes occur in solution, for example between the ligand excited states and a lanthanide ion level. If a process of this type leads to an alteration in the population of the excited ligand or Tb^{3+} levels (other than the $^5D_4$), the Tb^{3+} phosphorescence yield will be affected. In the absence of any intermolecular population of the higher excited states, equation 3 should be obeyed,

$$\frac{\phi_o}{\phi_{Ln}} = \frac{\tau_o}{\tau_{Ln}} = R_{Ln} \qquad \text{——— 3}$$

where ϕ_o is the Tb^{3+} $^5D_4$ phosphorescence yield in the absence of quencher and ϕ_{Ln} is the phosphorescence yield in the presence of [Ln]. With solutions of constant lanthanide complex concentration, the ratio R_{Ln} may be experimentally determined by making allowance for the mole fraction of Tb^{3+} complex present, x, and the relative absorbances of the Ln^{3+} and Tb^{3+} complexes at the excitation wavelength, λ, (see equation 4),

$$R_{Ln} = \frac{I_o \quad x}{I_{Ln}[x+r(1-x)]} \qquad \text{——— 4}$$

where I_o and I_x are the measured phosphorescence outputs in the absence and presence of lanthanide complex respectively, and r is

the ratio of Ln^{3+} complex absobance to that of the Tb^{3+} complex at the excitation wavelength, λ. The phosphorescence ratio, R_{Ln} has been measured in n-butanol solutions of total concentration 0.005 mol dm^{-3} at 293K, on addition of $Ln(AA)_3.3H_2O$ where Ln=Pr, Nd, Sm, Eu, Gd, Dy, Ho, Er and Yb. The Tb^{3+} $^5D_4$ emission at 547.5 nm was monitored on excitation at 290 nm. The ratios, r, between $Ln(AA)_3.3H_2O$ and $Tb(AA)_3.3H_2O$ absorbance at 290 nm have been determined, and are given in table 3, 3. With the exception of Ln=Pr, and perhaps Eu, all the R_{Ln} values were identical, within experimental error to the previously obtained values of $\frac{\tau_o}{\tau_{Ln}}$.

Table 3, 3:- Ratios, r, between $Ln(AA)_3.3H_2O$ and $Tb(AA)_3.3H_2O$ absorbances at 290 nm in n-butanol at 293K

Complex	r
Pr	0.954
Nd	1.070
Sm	1.096
Eu	1.048
Gd	1.048
Dy	1.175
Ho	1.096
Er	1.231
Yb	1.023

It may therefore be concluded that in this concentration region the data can be satisfactorily explained in terms of only one energy transfer step taking place, namely $Tb^{3+} \rightsquigarrow Ln^{3+}$.

For the praesodymium complex, the R_{Ln} values were consistently higher than the corresponding $\frac{\tau_o}{\tau}$ values. This suggests that a further intermolecular energy transfer step from the Tb^{3+} complex, other than that from the $^5D_4$ level to the Pr^{3+} complex occurs. If this is a single addition process, the equation,

$$R_{Ln} \frac{\tau_{Ln}}{\tau_o} = 1 + K'[Ln] \qquad \text{——— 5}$$

should be obeyed, where K' is the Stern-Volmer quenching constant for the second process. The plot shown in Figure 3,7, shows that the Tb^{3+} complex does undergo an additional single energy transfer process, with a K' value of 110 $dm^3 mol^{-1}$.

R_{Ln} has also been measured in solutions of total concentration 0.01 mol dm^{-3}, with Ln=Nd, Sm, Eu or Ho. At this higher concentration, deviations between R_{Ln} and $\frac{\tau_o}{\tau_{Ln}}$ values were observed in all cases, each one obeying equation 3. The K values are given in Table 3,4.

Table 3,4:- Stern-Volmer quenching constants, K', of the additional energy transfer process from $Tb(AA)_3.3H_2O$ to other $Ln(AA)_3.3H_2O$ complexes in n-butanol solution at 293K

Ln	K' ($dm^3 mol^{-1}$)
Pr[a]	110
Nd	22
Sm	11
Eu	52
Ho	11

(a) Obtained with total lanthanide complex concentration of 0.005 mol dm^{-3}, other values obtained at 0.01 mol dm^{-3}

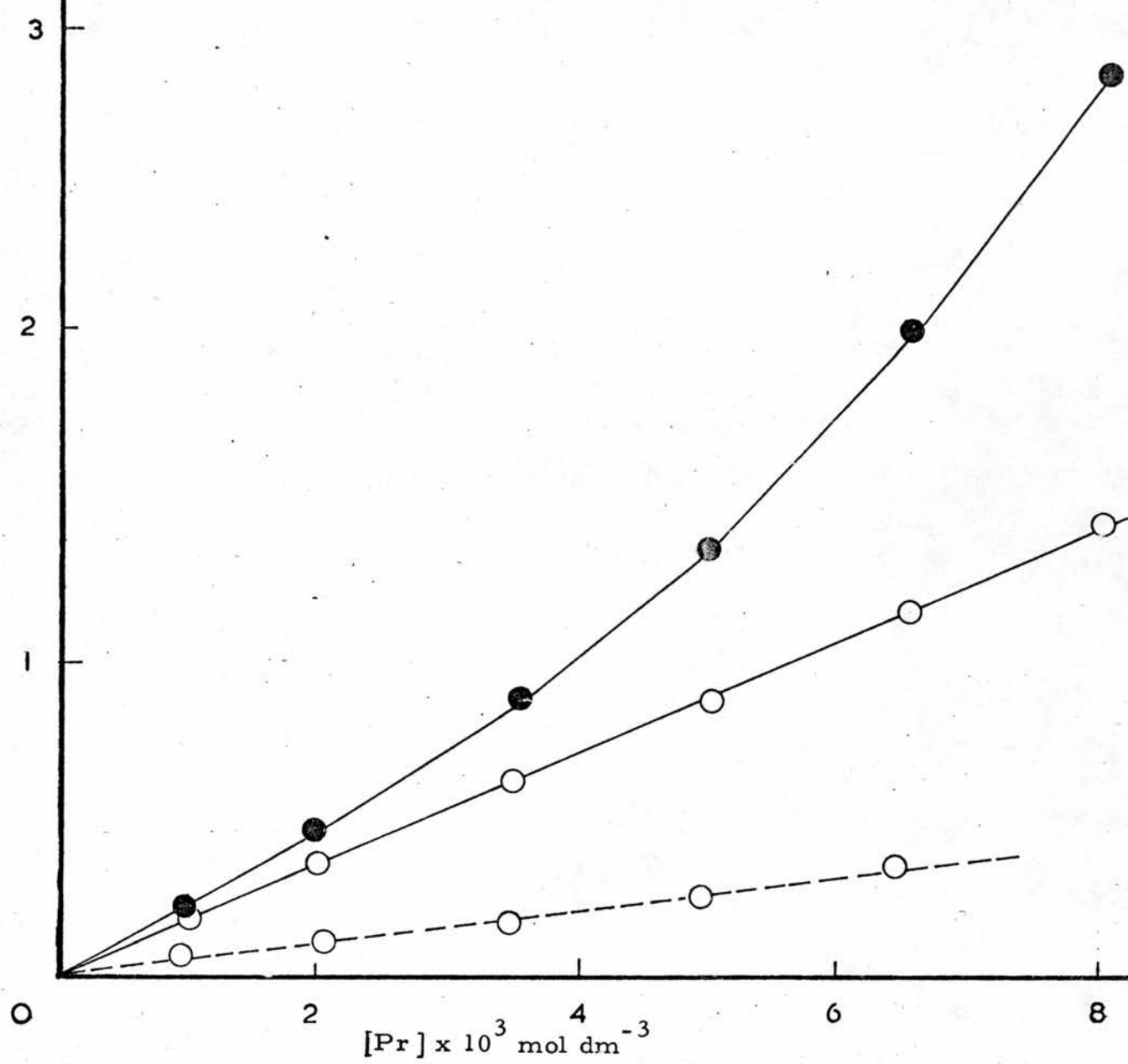

Fig. 3,7: Plots of $(\phi_o/\phi_{[Pr]}-1)$ (—●—●—●—), $(\tau_o/\tau_{[Pr]}-1)$ (—O—O—O—), and $(R_{[Pr]}\,\tau_{[Pr]}/\tau_o-1)$ (--O--O--O--) against [Pr] in n-butanol solution at 293K

Total complex concentration 0.0005 mol dm^{-3}

The variations in K' with difference acceptor complexes indicate that the transfer step is dependent on the acceptor ion levels, and not on the ligands. The donor excited state in the Tb^{3+} complex must lie above the Tb^{3+} $^5D_4$ level, and since the energy transfer process leads to a decrease in Tb^{3+} phosphorescence at 547.5 nm, this level must be involved in intramolecular energy transfer in the Tb^{3+} complex. Several Tb^{3+} levels, including the $^5D_2$ and $^5D_3$ lie between the acetylacetonate lowest excited singlet, S' and the lowest triplet, T_1 (see Figure 3,8). The intramolecular energy transfer[20,18] mechanism leading to lanthanide ion phosphorescence in β-diketoenolates is generally accepted to involve transfer of energy from the lowest ligand triplet to the lanthanide ion manifold, with subsequent emission. In this mechanism, only the T_1 and S_1 levels are potential donors, since the Tb^{3+} $^5D_3$ level does not form part of the intramolecular energy transfer route. Both the S_1 and T_1 levels should have very short lifetimes, being of the order of $< 10^{-9}$ sec. The values of K' in Table 3,4 would thus imply that the values for k', the bimolecular rate constant, are greater than 10^{10} dm mol^{-1} s^{-1}. For transfer from either the T_1 or S_1 levels to the Ln^{3+} levels, rate constants exceeding the diffusion rate would not be expected, since Coulombic transfer is spin forbidden. The alternative explanation is that a higher Tb^{3+} level, eg the $^5D_3$, is the donor. This would require an $S_1 \rightsquigarrow Tb^{3+}$ intramolecular energy transfer step, previously proposed by Kleinerman[24]. If the lifetime of the excited Tb^{3+} level is 10^{-7} s, then a diffusion controlled electron exchange transfer step could account for the observed values of K'.

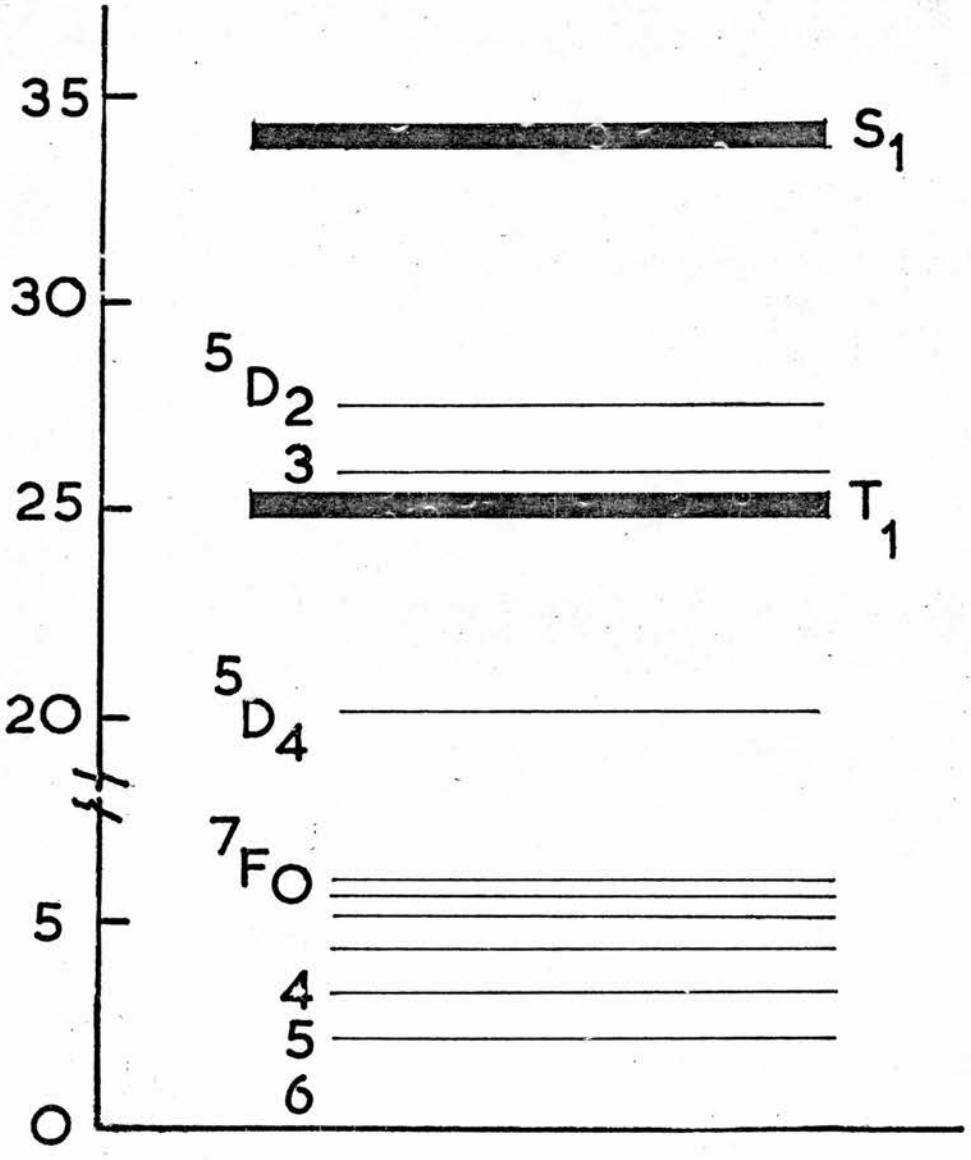

Fig. 3, 8: Schematic diagram of energy levels of $Tb(AA)_3 . 3H_2O$ in n-butanol solution. Not all the higher Tb^{3+} levels are included.

Two energy transfer steps from $Tb(AA)_3.3H_2O$ to other $Ln(AA)_3.3H_2O$ complexes have thus been observed in n-butanol, but the precise mechanism has not been elucidated. In the case of the lifetime studies, concerning transfer from the Tb^{3+} $^5D_4$ level, observed transfer rates were much lower than the diffusion rate in n-butanol. To examine the effect of the solvents, quenching of the Tb^{3+} $^5D_4$ level in $Tb(AA)_3.3H_2O$ by $Eu(AA)_3.3H_2O$ in dry benzene was attempted, and no significant energy transfer was observed. Dimerisation or oligomerisation of $Ln(AA)_3.3H_2O$ complexes is favoured in non-polar solvents[79], eg. benzene. This type of behaviour may explain the lack of transfer in benzene. Further studies into the mechanism of energy transfer have been made, and are reported in section (b) of this chapter.

(b) Intermolecular Energy Transfer in Other Solvents

Neilson and Shepherd[80] have pursued investigations of energy transfer between $Tb(AA)_3.3H_2O$ and other $Ln(AA)_3.3H_2O$ in a variety of solvents, and have concluded that dimerisation is indeed crucial to the transfer process. In molecular weight measurements, they found that in non-polar solvents, eg. benzene, the lanthanide acetylacetonates exist almost exclusively as dimers. In solvents with more coordinating power, eg. acetone and acetonitrile, the complexes probably exist in a monomer-dimer equilibrium.

In mixed solutions of $Tb(AA)_3.3H_2O$ and $Ln(AA)_3.3H_2O$, an equilibrium of mixed dimer formation has been shown to occur, viz:

$$Tb_2(AA)_6.6H_2O + Ln_2(AA)_6.6H_2O \rightleftharpoons 2TbLn(AA)_3.3H_2O.$$

Quenching of the Tb^{3+} $^5D_4$ level is neither observed in non-polar solvents, nor in highly polar solvents. In the case of non-polar solvents, it has been proposed that the rate of exchange of monomer between dimers is very slow compared with the Tb^{3+} $^5D_4$ lifetime of ca 900 μs in the Tb^{3+} dimer, and that the phosphorescence yield of the mixed dimer is almost zero. No decrease of will therefore be observed as the $Ln(AA)_3.3H_2O$ complex is added. The bimolecular transfer rates observed in n-butanol are therefore not direct spectroscopic terms, but a function of the Tb^{3+} $^5D_4$ lifetime being longer than the rate of monomer exchange to form mixed dimers. They conclude that the principal deactivation step is a monomer-dimer interaction, viz:

$$(Tb)_2^* + Ln \rightleftharpoons TbLn + Tb.$$

In the case of pyridine, the lanthanide complexes are monomeric, the coordinating power of the solvent being sufficient to inhibit their formation. The results therefore strongly suggest that energy transfer from the Tb^{3+} $^5D_4$ level in $Tb(AA)_3.3H_2O$ to $Ln(AA)_3.3H_2O$ in solution is dependent on the formation of a mixed dimer, in which the excited Tb^{3+} ion is very rapidly deactivated, and that a bimolecular energy transfer rate is only observed if the exchange rate of monomer between dimers is comparable to the lifetime of the Tb^{3+} $^5D_4$ level.

The work of Neilson and Shepherd therefore explains the transfer from the Tb^{3+} $^5D_4$ level. The observed extra energy transfer stage (see section (i)b of this chapter), however is not explained by their

results. A possible explanation might be that in n-butanol, there is a relatively high proportion of both terbium and lanthanide complex in monomer form. The simple quenching mechanism,

$$Ln + Tb^{*} \rightleftharpoons TbLn$$

might well be expected to take place. Two quenching mechanisms may therefore operate:-

1. $Ln + Tb_2^{*} \rightleftharpoons LnTb + Tb$
2. $Ln + Tb^{*} \rightleftharpoons LnTb.$

The second may deactivate the Tb^{3+} $^5D_3$ level alone, therefore leaving lifetime measurements on the Tb^{3+} $^5D_4$ level unaffected.

Chapter 4

Intermolecular Energy Transfer from $Tb(AA)_3.3H_2O$ to Various Metal Acetylacetonates in Solution

(i) Introduction

Intermolecular energy transfer between excited state $Tb(AA)_3.3H_2O$ and other $Ln(AA)_3.3H_2O$ complexes in solution has been discussed in Chapter 3. Equivalent studies in the transfer of energy to other metal acetylacetonates in solution have been carried out and are reported in this chapter. $Tb(AA)_3.3H_2O$ was again chosen as the donor complex for the same reasons as described in Chapter 3. All the metal acetylacetonate complexes were irradiated in the ligand absorption band, and the $Tb^{3+}\ ^5D_4$ emission at 547.5 nm was monitored. Only the relationship between the lifetime, τ, of the emitting level with the concentration of quencher was followed, since the d-d absorption of the quencher metal ions in the visible region interfered with phosphorescence yield measurements. The $Tb(AA)_3.3H_2O$ concentration was maintained at 5×10^{-3} mol dm^{-3} and the quencher concentration was varied between the limits 2×10^{-4} to 1×10^{-3} mol dm^{-3}. In each case where a significant decrease in the $Tb^{3+}\ ^5D_4$ lifetime in the presence of added metal complex was observed, the Stern-Volmer relation was obeyed (see Chapter 1). Since the mechanism of the quenching processes was found to be dependent on both the nature of the acceptor complex and the solvent, the data are discussed in groups of acceptor complexes with similar behaviour.

(ii) $\underline{Zn(AA)_2}$ and $\underline{Al(AA)_3}$

Hydrated zinc acetylacetonate is known only in the monohydrate form with a 5-coordinate zinc ion[81]. Recent molecular weight determinations, including our own, have suggested that the corresponding anhydrous complex, $Zn(AA)_2$[65], is probably trimeric in non-donor solvents such as benzene. This is in conflict with the results of Graddon[82], who may have examined an impure sample, since the method used to dehydrate the monohydrate could have been sufficiently drastic to partially convert the acetylacetonate ligand to the acetate[65]. Thus, in non-polar solvents the monohydrate is monomeric, and the anhydrous complex is probably trimeric.

The aluminium $\underline{tris}$ acetylacetonate complex is octahedral and monomeric in the solid state[83]. Since it reacts only very slowly with $FeCl_3$ in ethanol[56] to give the characteristic red colouration[84] of β-diketoenolate complexes of iron(III), it has been suggested that $Al(AA)_3$ is monomeric and kinetically stable in solution.

$Al(AA)_3$, $Zn(AA)_2.2H_2O$ and $Zn(AA)_2$ did not significantly affect the Tb^{3+} $^5D_4$ lifetime in $Tb(AA)_3.3H_2O$ in mixed solutions in any of $\underline{n}$-butanol, pyridine and benzene. The maximum concentration of added metal complex was 1×10^{-3} mol dm^{-3}, which allowed a limiting value of the bimolecular rate constant, k, to be estimated at 5×10^{-2} $mol^{-1} dm^3 s^{-1}$. Zn(II) and Al(III) have d^{10} and p^6 outer electronic configurations respectively and hence have no Laporte forbidden absorption bands. The lowest energy excited

levels of both these metal ions are much higher than the Tb^{3+} $^5D_4$ emitting level at 20,200 cm^{-1}. The negative results in all three solvents indicate that energy transfer is dependent on the added metal ion present having excited levels below the emitting level. Any significant degree of energy transfer from the Tb^{3+} $^5D_4$ emitting level to any of the excited ligand levels is also precluded by these results. The behaviour is therefore analogous to that previously found with the $4f^7$ Gd^{3+} complex (see Chapter 3). where in that case, the lowest excited state although Laporte forbidden, also lies above the Tb^{3+} $^5D_4$ level.

(iii) $\underline{CrAA_3}$, $\underline{Mn(AA)_3}$ and $\underline{Co(AA)_3}$

The Cr^{3+} ion has a d^3 configuration, and its complexes are almost always hexacoordinate, and are both thermodynamically stable and kinetically inert. Ligand exchange reactions in solution may have half-lives of up to several hours. The $Cr(AA)_3$ complex is octahedral and monomeric in the solid form[85]. The visible spectrum shows a band at 17500 cm^{-1} and this has been assigned as the $^4T_2 \leftarrow {}^4A_2$ d-d transition[86].

Complexes of Mn(III) (d^4) tend to disproportionate in solution to yield compounds of Mn(II) and Mn(IV). Despite the expected Jahn Teller distortion of a high spin d^4 electronic configuration, $Mn(AA)_3$ has been found to be an almost perfect octahedron in the solid state with a maximum difference in the Mn-O bond lengths of 0.03 Å[87]. The visible spectrum of $Mn(AA)_3$ shows bands at $\underline{ca}$ 9500 cm^{-1} and $\underline{ca}$ 18000 cm^{-1} with extinction coefficients, $\Sigma \rangle$ 100 mol $dm^{-3}cm^{-1}$.

All known complexes of Co(III) (d^6) are octahedral. These complexes exhibit slow ligand exchange in solution. The half lives are shorter than those of similar Cr(III) complexes, and the isomerisation reactions of optically active Co(III) complexes have been widely studied. The $Co(AA)_3$ complex is octahedral and shows four bands in its visible spectrum. The two stronger bands, at ca 17700 cm^{-1} and 24800 cm^{-1} have been assigned as the d-d transitions from the singlet ground state $^1A_{1g}$ to the upper $^1T_{1g}$ and $^1T_{2g}$ states respectively.

The addition of $Cr(AA)_3$, $Mn(AA)_3$ and $Co(AA)_3$ to solutions of $Tb(AA)_3.3H_2O$ in benzene, n-butanol and pyridine has been found in all cases to lower the lifetime of the Tb^{3+} $^5D_4$ level, and to obey the Stern-Volmer relationship. The results are summarised in Table 4,1.

From Table 4,1, it is clear that the rates of energy transfer do not decrease with solvent viscosity. It is also apparent from Table 4,1, that in all three solvents, the $Mn(AA)_3$ shows a faster energy transfer rate than does $Co(AA)_3$, which in turn is slightly faster than $Cr(AA)_3$. The k values are at least three orders of magnitude lower than the relevant estimated diffusion rates at 293K.

Ratios of the bimolecular quenching rates, k at 293K for each quencher in the various solvents are shown in Table 4,2. The quenching rate ratios are identical within experimental error for any given solvent pair and are independent of the quenching metal ion. This suggests that a similar quenching mechanism operates for all quenching ions.

Table 4, 1:- Bimolecular rate constants, k (10^{-6} mol^{-1} dm^3 s^{-1}), for intermolecular energy transfer from the Tb^{3+} $^5D_4$ level in $Tb(AA)_3.3H_2O$ to other metal acetylacetonates in various solvents at 293K. Viscosities and estimated diffusion rates of the solvents at 293K and τ_o, the Tb^{3+} $^5D_4$ lifetime in the absence of quencher.

Quencher	Solvent		
	Benzene	n-Butanol	Pyridine
$Cr(AA)_3$	0.29	1.11	0.69
$Mn(AA)_3$	0.98	3.59	2.19
$Co(AA)_3$	0.45	1.63	0.97
Viscosity of solvent (poise)	0.00652	0.02948	0.0974
Diffusion rate[a] of solvent (kd mol dm^3 s^{-1})	1.0×10^{10}	2.20×10^9	6.6×10^9
τ_o (μs)	900	790	610

(a) Calculated from the formula shown in Chapter 1, (v).

Table 4, 2:- Ratios of bimolecular intermolecular energy transfer rates in various solvents for different quenchers at 293K

Quencher	$k_{n\text{-but}}/k_{benzene}$	$k_{n\text{-but}}/k_{pyridine}$	$k_{pyridine}/k_{benzene}$
$Cr(AA)_3$	3.82	1.61	2.38
$Mn(AA)_3$	3.66	1.64	2.23
$Co(AA)_3$	3.62	1.68	2.16

The ratio k_{pyr}/k_{benz} is ca 2.2 ± 0.1. Since it is known that $Tb(AA)_3.3H_2O$ is dimeric in benzene and monomeric in pyridine, the

proximity of the ratio to 2.0 may be simply a reflection of the concentration of donor species ie. monomers in pyridine and dimers in benzene.

Solutions of 1×10^{-3} mol dm^{-3} of $Tb(AA)_3.3H_2O$ and 1×10^{-3} mol dm^{-3} of each of the quenchers in n-butanol and benzene were mixed, irradiated at 290 nm, in the ligand absorption band, and the Tb^{3+} $^5D_4$ phosphorescence at 547.5 nm monitored against time. The Tb^{3+} phosphorescence decreased immediately (ie. experimentally 0.5s), and did not show the slow decrease observed with benzene solutions of mixed Tb^{3+} and Ln^{3+} acetylacetonate complexes observed by Neilson and Shepherd[80]. The lifetimes of mixed frozen solutions of $Tb(AA)_3.3H_2O$ (5×10^{-3} mol dm^{-3}) and $Cr(AA)_3$ in n-butanol were measured, and are given in Table 4,3.

Table 4,3:- Lifetimes (τ) of the Tb^{3+} $^5D_4$ level in mixed frozen solutions of $Tb(AA)_3.3H_2O$ (5×10^{-3} mol dm^{-3}) and $Cr(AA)_3$ in n-butanol at 77K

Conc. $Cr(AA)_3$ (mol dm^{-3})	τ (μs)
0	1003
2×10^{-4}	1010
4×10^{-4}	999
8×10^{-4}	1005
10×10^{-4}	995

No significant deactivation of the Tb^{3+} $^5D_4$ level therefore takes place in frozen solution. This, coupled with the absence of any observable static quenching in fluid solution suggests that the intermolecular energy transfer mechanism depends on the quenching

species encountering the Tb^{3+} emitting ion.

Experiments using $Cr.Cl_3.6H_2O$ as the quencher rather than the $Cr(AA)_3$ complex were carried out in the polar solvents pyridine and n-butanol, and the results are given in Table 4,4.

Table 4,4:- Bimolecular rate constants, k (10^{-6} mol^{-1} dm^3 s^{-1}) for energy transfer from $Tb(AA)_3.3H_2O$ to $Cr(AA)_3$ and $CrCl_3.6H_2O$ in n-butanol and pyridine solutions at 293K

Solvent	$CrCl_3.6H_2O$, k values	$Cr(AA)_3$, k values
n-butanol	1.10	1.11
pyridine	0.69	0.67

Analogous experiments with the Mn^{3+} and Co^{3+} ions are not possible. The solvated ion k values in these solvents are, within experimental error, identical to those for the $Cr(AA)_3$ complex. This indicates that the quenching process is not specifically dependent on the presence of acetylacetonate ligands, and that the quenching rate depends only on the presence of the quencher metal ion in either the complexed state, or in the solvated state, or as is likely in these circumstances, some intermediate state. The results do not however support the view that energy transfer occurs via a dimer intermediate such as has been suggested for lanthanide-lanthanide transfer.

The possible mechanism of energy transfer from $Tb(AA)_3.3H_2O$ to other $Ln(AA)_3.3H_2O$ has been discussed in Chapter 3. In those cases, energy transfer was proposed to be dependent on the formation

of mixed dimers, and dynamic quenching was only observed in relatively weakly coordinating solvents such as n-butanol, where the rate of monomer exchange is faster than the rate of decay of the Tb^{3+} $^5D_4$ level. Energy transfer to lanthanide complexes was not observed in either the strongly coordinating pyridine or non-coordinating benzene solutions. The observation that $Cr(AA)_3$, $Mn(AA)_3$ and $Co(AA)_3$ accept energy from $Tb(AA)_3.3H_2O$ in pyridine and benzene as well as in n-butanol solutions again suggests that a different energy transfer mechanism from that operating in the case of the lanthanide complexes is taking place.

All three of the quencher complexes are likely to be monomeric in each of the solvents used, and a possible model for the deactivation of the terbium complex by these transition metal trisacetylacetonates is through a collisional process,

$$Tb^* + Q \longrightarrow (TbQ)^* \longrightarrow Tb + Q^* ,$$

where the energy transfer occurs in a collisional complex, $(TbQ)^*$. If energy transfer occurred on every "collision" then the observed bimolecular rate constant, k, for each quenching metal complex should approximate to the diffusion rate. As shown in Table 4,1, the k values are at least three orders of magnitude lower than the estimated diffusion rate at 293K. This behaviour could be the result of a substantial activation energy requirement for the formation of the $(TbQ)^*$ species. Under these circumstances the energy transfer rate constant, k, should be temperature dependent and should, at least to a good approximation, follow the relationship

$$k = A \exp(-E/RT) \qquad \text{——— 1}$$

where k = bimolecular quenching rate constant ($mol^{-1} dm^3 s^{-1}$)
A = preexponential term ($mol^{-1} dm^3 s^{-1}$)
E = activation energy ($J\ mol^{-1}$)
R = gas constant ($J\ mol^{-1} K^{-1}$)
T = temperature (K)

The dependence of τ on the concentration of added quencher was therefore determined at two additional temperatures, 273K and 323K for the $Cr(AA)_3$, $Mn(AA)_3$ and $Co(AA)_3$ systems in n-butanol. In all cases linear Stern-Volmer plots were obtained and the resulting values for the bimolecular quenching rate constants are given in Table 4,5. The values of τ_o on the basis of which the Stern-Volmer plots were drawn are also given. A fuller description of the temperature dependence of τ_o is given in Chapter 7.

Table 4,5:- Bimolecular rate constants, k (10^{-6} $mol^{-1} dm^3 s^{-1}$) for intermolecular energy transfer from the Tb^{3+} $^5D_4$ level in $Tb(AA)_3.3H_2O$ to transition metal tris-acetylacetonates in n-butanol at 273K, 293K and 323K

Quencher	Temperature		
	273K	293K	323K
$Cr(AA)_3$	1.10	1.11	1.40
$Mn(AA)_3$	2.61	3.59	3.61
$Co(AA)_3$	1.41	1.63	1.40
τ_o (μs)	870	790	680

The results in Table 4,5 show that there is no regular temperature dependence in the values of k with any of these three quenchers, and do not therefore support the view that the rate of energy transfer is

controlled directly by an activation energy of the type discussed above. If, in equation 1, it is assumed that A is equal to the diffusion rate (ie. 2.2×10^9 mol $dm^3 s^{-1}$ for n-butanol at 293K) then it may be calculated that in order to explain the k values, activation energies of 18.5, 15.6 and 17.6 kJ mol^{-1} for $Cr(AA)_3$, $Mn(AA)_3$ and $Co(AA)_3$ respectively would be required for the formation of $(TbQ)^*$. These values, ignoring any temperature dependence of A would result in an increase in bimolecular quenching rate constant by a factor of greater than three over the range 273-323K. This clearly does not occur, and suggests that the activation energy for the formation of $(TbQ)^*$ is zero or at most a few kJ mol^{-1} which would be within the limits of experimental accuracy.

A possible explanation is that the collison complex is readily formed in solution, and that the energy transfer process requires particular orientation of the donor and acceptor ions. The proposal that the observed bimolecular rate constants for the energy transfer process are the result of an orientation controlled mechanism in the case of $Cr(AA)_3$, $Mn(AA)_3$ and $Co(AA)_3$ being the quenchings is inconsistent with the experimental observations:-

(a) the values of k are considerably lower than the diffusion rates and bear no direct relationship to them;

(b) no energy transfer is observed in solid solution;

(c) the energy transfer rates are identical irrespective of whether $CrCl_3.6H_2O$ or $Cr(AA)_3$ was used as the acceptor species;

(d) no significant temperature dependence of k was observed.

(iv) $\underline{Cu(AA)_2}$ and $\underline{Pd(AA)_2}$

Cu^{2+} and Pd^{2+} have $3d^9$ and $4d^8$ configurations respectively. Complexes of these ions are usually 4-coordinate and in the case of Pd^{2+} are almost invariably square planar. Cu^{2+} also forms square planar complexes in addition to distorted tetrahedral complexes when it is 4-coordinate, although in solution the vacant octahedral sites may be occupied by loosely bound solvent molecules. $Pd(AA)_2$ is typical of square planar Pd(II) complexes[88], and is monomeric in solution. $Cu(AA)_2$ has been known for many years, and is also monomeric in solution[89], and has been reported to be square planar in the solid[90]. It is also sufficiently stable to be sublimed at atmospheric pressure without decomposition. In strong donor solvents, such as pyridine, one of the vacant octahedral positions may be occupied by a solvent molecule to give a square pyramidal configuration[64]. The Pd(II) complex, however, can accept two solvent molecules to give a pseudo-octahedral arrangement[89].

The Pd(II) and Cu(II) acetylacetonates are therefore similar in that they are square planar and monomeric in non-donor solvents and form adducts with pyridine. The effect of both of these complexes on the Tb^{3+} $^5D_4$ emitting level lifetime in $Tb(AA)_3.3H_2O$ has been studied in benzene, n-butanol and in pyridine solutions, and the results are summarised in Table 4, 6.

As in the case of $Mn(AA)_3$, $Cr(AA)_3$ and $Co(AA)_3$, no consistent trend of the k values against viscosity is observed (see Table 4, 1). Energy transfer to both $Cu(AA)_2$ and $Pd(AA)_2$ occurs in each of benzene, n-butanol and pyridine. In each solvent, k values are of

Table 4, 6:- Bimolecular rate constants, k (10^{-6} mol^{-1} dm^3 s^{-1}) for $Tb(AA)_3.3H_2O$ being quenched by $Pd(AA)_2$ and $Cu(AA)_2$ in various solvents

	n-butanol			benzene	pyridine
Quencher	273K	293K	323K	293K	293K
$Cu(AA)_2$	0.89	1.87	1.60	0.31	0.21
$Pd(AA)_2$	0.85	0.89	1.01	0.05	3.62

the order of those observed for the tris-complexes described in section (iii) of this chapter. Since the complexes are monomeric in solution, it may not be unreasonable to postulate a mechanism of energy transfer from $Tb(AA)_3.3H_2O$ to $Cu(AA)_2$ and $Pd(AA)_2$ which is not unlike that proposed for the transition metal tris-acetylacetonates. Again no regular variation of k with temperature in n-butanol solution is observed, lending further support to the proposed mechanism. $CuCl_2.2H_2O$ also accepts energy from the $Tb^{3+}\ ^5D_4$ level in n-butanol solution, giving a bimolecular rate constant for energy transfer of 1.81×10^6 mol^{-1}dm^{3}s^{-1}, compared with the 1.87×10^6 mol^{-1}dm^{3}s^{-1} value for the $Cu(AA)_2$ complex. Again complexing appears to have no significant effect on the bimolecular rate constant.

The k values in pyridine are anomalous, that for $Cu(AA)_2$ being low, and for $Pd(AA)_2$, very high. This may be a function of these complexes forming adducts with the solvent molecules, the Cu(II) complex accepting one solvent donor to form a square planar arrangement, and the Pd(II) loosely bonding to two solvent molecules to form a distorted octahedron. If the same type of deactivation mechanism operates for these two complexes as for the transition metal acetylacetonates, the orientation of the donor and acceptor ions, after the formation of the $(TbQ)^*$ complex will again be crucial. It may be that in pyridine solution, the $Cu(AA)_2.py$ adduct may be inhibited from attaining the optimum geometrical arrangement of the metal ions for transfer to proceed, thereby accounting for the anomalously low k value. The distorted octahedral $Pd(AA)_2.py_2$

adduct, however, may facilitate the rearrangement of the $(TbQ)^*$ collisional complex to enable energy transfer to take place.

(v) $\underline{Ni(AA)_2}$

$Ni(AA)_2$ is paramagnetic, and for a long time this was interpreted as evidence for a tetrahedral stereochemistry. The visible spectrum was interpreted by Jørgensen[91] as characteristic of an octahedral stereochemistry. Some form of oligomerisation is necessary if the nickel ion is in an octahedral environment and this has been confirmed by X-ray structure determinations[92, 93, 94]. These showed that the $Ni(AA)_2$ complex exists as a trimer in the solid state, with the structure[94] shown in Figure 4, 1.

Molecular weight measurements have been made on the $Ni(AA)_2$ complex in various solvents[95, 96]. These studies indicate that, in non-coordinating solvents, such as benzene and triphenylmethane, the trimer is preserved intact at room temperature. The trimer has been observed to depolymerise only at elevated temperatures (150^o in diphenylmethane)[97], and it has also been shown to break down to monomeric units by coordination with bases such as pyridine. The $Ni(AA)_2$ complex therefore exists as a stable trimer in weakly-coordinating solvents, and as a monomer in strongly coordinating solvents.

The lifetime of the Tb^{3+} $^5D_4$ level in $Tb(AA)_3.3H_2O$ has been determined in n-butanol, benzene and pyridine solutions containing up to 10^{-3} mol dm^{-3} $Ni(AA)_2$ at 293K. Measurements were also made in n-butanol at 273K and 323K. In no case was any significant

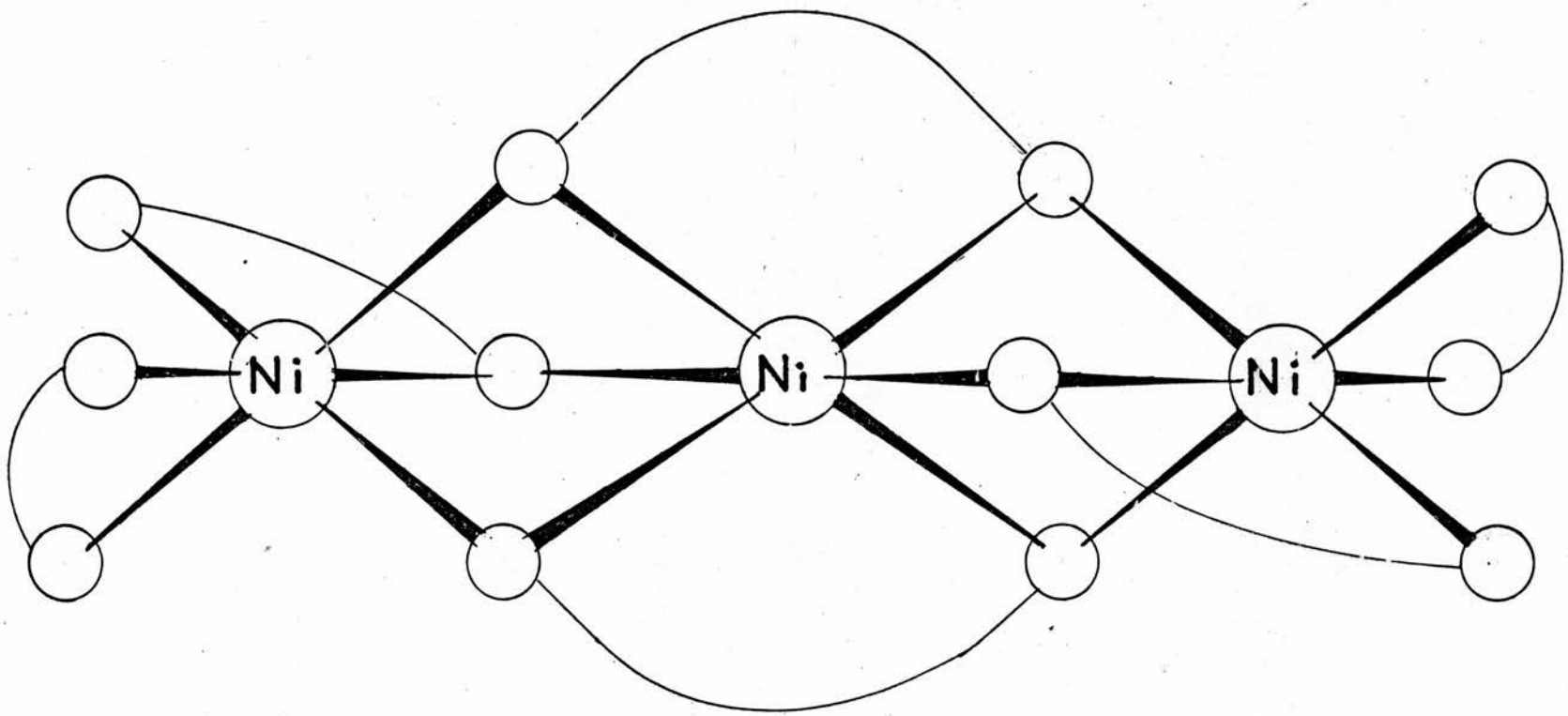

Figure 4, 1: The structure of $Ni(AA)_3$. The acetylacetonate ligands are depicted as 

decrease in lifetime from the appropriate τ_o. These results indicate that the upper limit for a dynamic bimolecular quenching rate constant is $< 5 \times 10^2$ mol^{-1}dm^{3}s^{-1}. This situation is in marked contrast to the behaviour described in sections (iii) and (iv) of this chapter, and indicates that any dynamic quenching by the Ni(II) complex is at least four orders of magnitude less rapid than those dynamic processes exhibited by the acetylacetonates of Cr(III), Mn(III), Co(III), Cu(II) and Pd(II).

It was observed, however, that after mixing individual benzene solutions of $Ni(AA)_2$ and $Tb(AA)_3.3H_2O$, a relatively slow decrease of the Tb^{3+} phosphorescence at 547.5 nm occurred, which eventually reached a limiting value (see Figure 4, 2). This change in phosphorescence yield was not accompanied by any change either in the emission spectral profile of the Tb^{3+}, or in the Tb^{3+} $^5D_4$ lifetime. Mixtures of the individual solutions of the two complexes in n-butanol gave a similar result (see Figure 4, 2), but in pyridine solution no time-dependent decrease in Tb^{3+} phosphorescence yield occurred. The behaviour in benzene solution is very similar to that previously observed for lanthanide tris-acetylacetonate quenchers[80], and it is likely that a static quenching process involving the formation of mixed metal oligomers is occurring. In n-butanol solution, it is again possible to reconcile the observed results with a similar static quenching process, although the degree of oligomerisation in this relatively polar solvent would be expected to be lower. This interpretation presupposes that the mean lifetime of the mixed oligomers is long in comparison with the Tb^{3+} $^5D_4$ lifetime, ie. much greater than ca 1 ms.

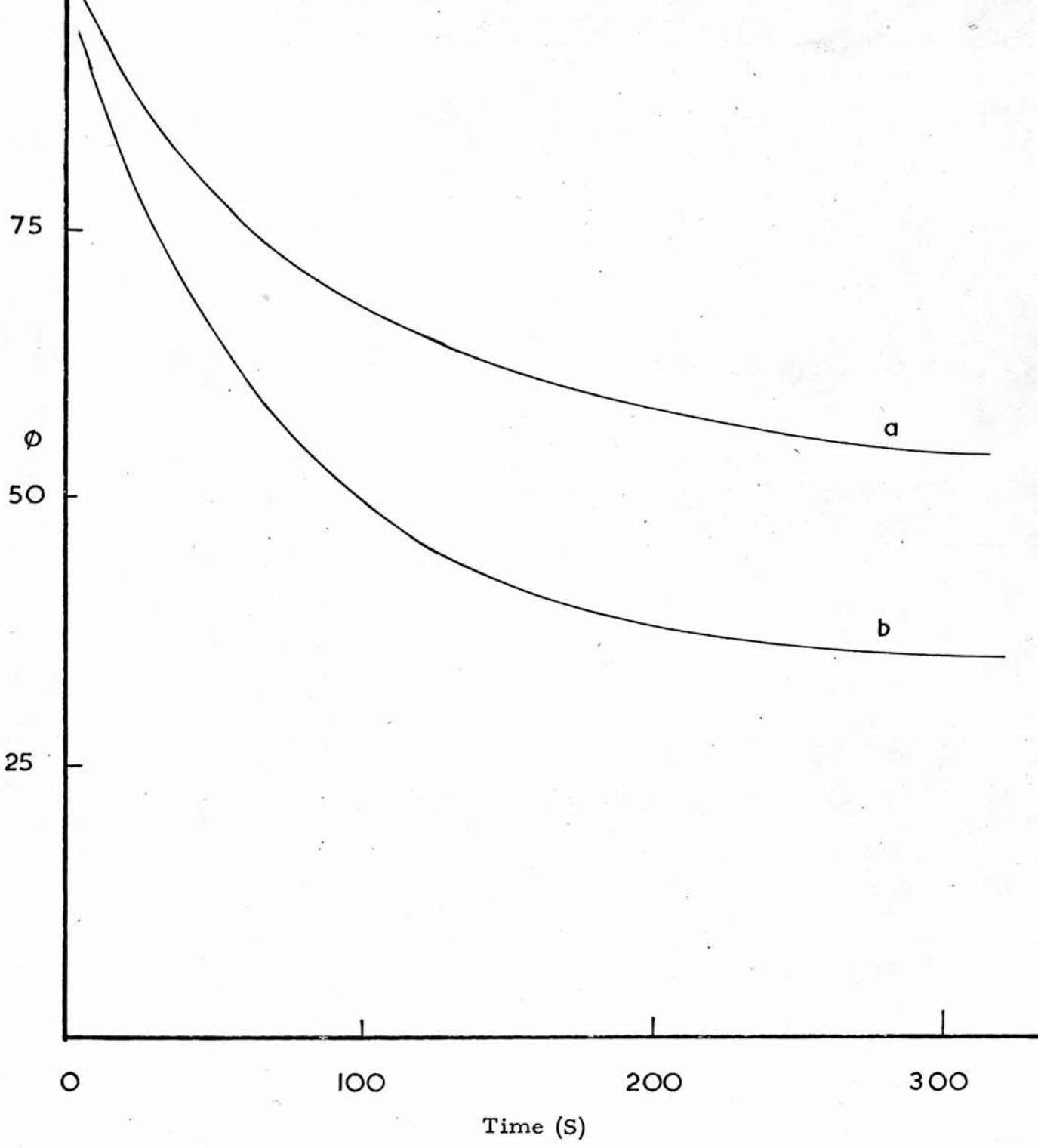

Figure 4, 2: The decreases in Tb^{3+} phosphorescence yield, Φ, (arbitrary units) after mixing equal volumes of 0.0025 mol dm^{-3} $Tb(AA)_3.3H_2O$ and 0.0025 mol dm^{-3} $Ni(AA)_2$ in (a) n-butanol and (b) benzene solutions at 293K

In pyridine solution, both the Ni and Tb complexes are monomeric, the Ni complex being largely in the form $Ni(AA)_2py_2$ [89]. The lack of any decrease in Tb^{3+} phosphorescence on mixing pyridine solutions of the two complexes is therefore consistent with the absence of long-lived oligomeric species in the solution, which would be necessary to give static quenching. It is surprising, however, that in this solvent there is no evidence of dynamic quenching (ie. no decrease in τ), similar to that found with the previously described metal ions. This suggests that energy transfer from Tb^{3+} to Ni^{2+} is inherently less likely than, for example, transfer from Tb^{3+} to Cr^{3+}.

Similar experiments were carried out in n-butanol and pyridine solutions using $NiCl_2.6H_2O$ as the quencher. No static quenching was evident in either solvent, but finite dynamic quenching rate constants were obtained (see Table 4,7).

Table 4,7:- Bimolecular rate constants, k (10^{-6} mol^{-1} dm^3 s^{-1}) for the quenching of the Tb^{3+} $^5D_4$ level in $Tb(AA)_3.3H_2O$ by $NiCl_2.6H_2O$ in n-butanol and pyridine solutions at 293K

Quencher	Pyridine	n-Butanol
$NiCl_2.6H_2O$	0.083	0.178

It is probably significant that these rate constants are at least an order of magnitude lower than those found with $CrCl_3.6H_2O$.

(vi) $\underline{Co(AA)_2}$, $\underline{Mn(AA)_2}$ and $\underline{VO(AA)_2}$

Prior to 1960, the paramagnetic complex $Co(AA)_2$ was thought to be tetrahedral in structure, but X-ray structural determinations have shown that the cobalt ion is in an octahedral environment, surrounded by six oxygen atoms[98]. The structure is depicted in Figure 4, 3. Molecular weight studies in solution[99, 100] have shown that oligomerisation also occurs; the degree of association being dependent on the concentration and the solvent. The oligomers are readily broken down on addition of strongly coordinating bases, for example pyridine[100], and in pyridine solution, the $Co(AA)_2$ is monomeric. The available evidence suggests that the $[Co(AA)_2]_4$ tetramer is less stable than the corresponding $[Ni(AA)_3]_3$ trimer, which may reflect the relatively higher crystal field stabilisation energy of octahedral to tetrahedral stereochemistry in the case of Ni^{2+}.

The structure of anhydrous $Mn(AA)_2$ has not been firmly established in the solid state, but molecular weight data[101] suggest that it may exist as a trimer in non-polar solvents. $Mn(AA)_2$ is reported to be monomeric in diphenylamine[101], unlike $Co(AA)_2$ and $Ni(AA)_2$ which oligomerise in this solvent. The oligomeric species formed by $Mn(AA)_2$ is therefore much less stable than those formed by $Ni(AA)_2$ and $Co(AA)_2$.

X-ray structural analysis has shown that solid $VO(AA)_2$[102], is monomeric and in the form of a square pyramid. The V atom is slightly above the plane of the basal oxygen atoms. In non-polar solvents, it is reported to form a dimer[103, 99]. The dimer will

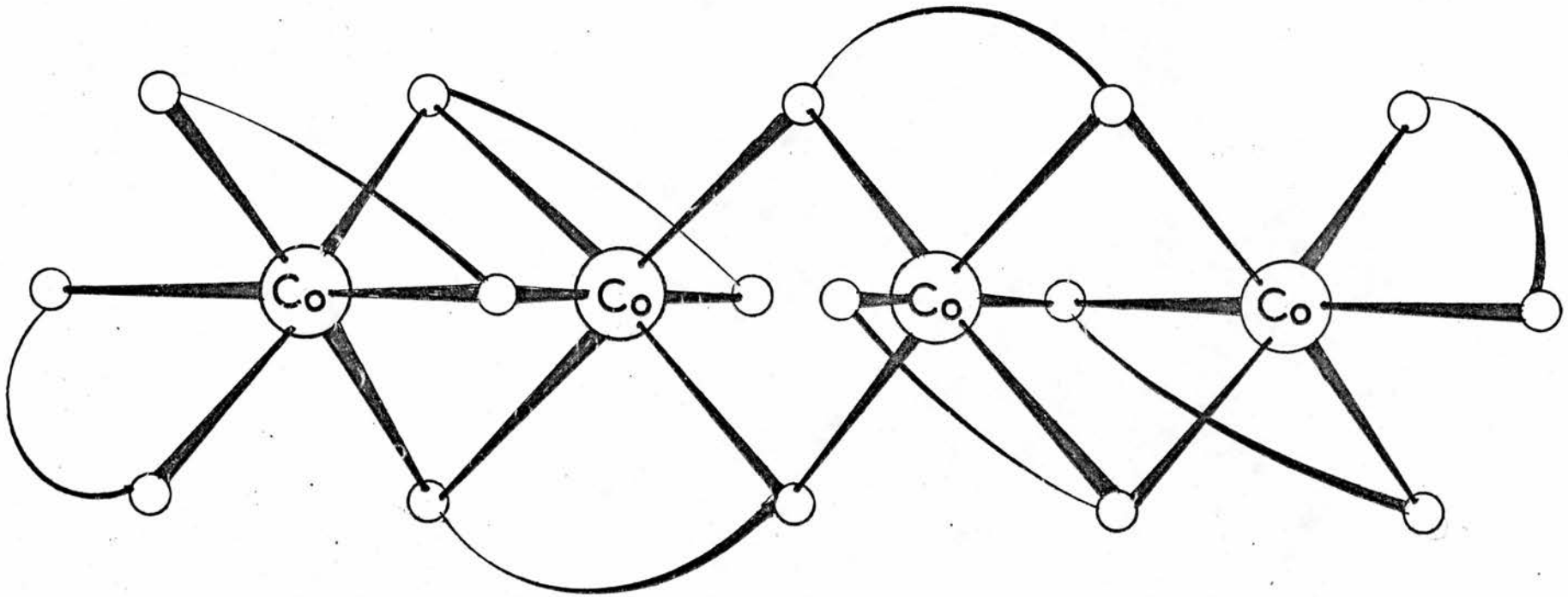

Figure 4, 3: The structure of $Co(AA)_4$. The acetylacetonate ligands are depicted as 

probably be very readily broken down.

The quenching of the Tb^{3+} $^5D_4$ level in $Tb(AA)_3.3H_2O$ by $VO(AA)_2$, $Co(AA)_2$ and $Mn(AA)_2$ has been studied in n-butanol, benzene and pyridine. In all cases where energy transfer was observed, the Stern-Volmer relation was obeyed. The bimolecular rate constants derived from the Stern-Volmer relation are shown in Table 4, 8.

Table 4, 8:- Bimolecular rate constants, k (10^{-6} mol^{-1} dm^3 s^{-1}) for intermolecular energy transfer from the Tb^{3+} $^5D_4$ level in $Tb(AA)_3.3H_2O$ to the quenching complexes listed, in various solvents and at different temperatures

Quencher	Solvent						
	n-butanol			benzene	pyridine		
	273K	293K	323K	293K	273K	293K	323K
$Co(AA)_2$	0.615	1.276	3.840	0.002	0.173	0.199	0.139
$Mn(AA)_2$	1.370	3.031	4.823	0.12	(a)	(a)	(a)
$VO(AA)_2$	0.939	1.632	3.213	0.29	0.267	0.281	0.356

(a) no significant quenching observed (limiting k value $< 5 \times 10^{-2}$ dm^3 mol^{-1} s^{-1})

In the case of n-butanol solutions, the k value for each of the quenchers increase with increasing temperatures. This indicates that the rate determining step in the energy transfer process is temperature dependent. The k value in n-butanol of each of the quenching complexes have been found to obey the relation

$$k = A \exp(-E/RT)$$ (see section (iii) of this chapter).

The plots of ln k versus $\frac{1}{T}$ for each quencher are shown in Figure 4,4, and the activation energies derived from the plots are 25.6 KJmol^{-1}, 18.1 KJ mol^{-1} and 18.8 KJ mol^{-1} for the quenching by $Co(AA)_2$, $VO(AA)_2$ and $Mn(AA)_2$ respectively. The quenching complexes all exhibit oligomerisation in non-polar solvents, and it is likely that they, like the $Tb(AA)_3.3H_2O$ complex, will be at least partly associated in n-butanol solution. The mechanism for energy transfer from $Tb(AA)_3.3H_2O$ to the $Co(AA)_2$, $Mn(AA)_2$ and $VO(AA)_2$ complexes in n-butanol solution is therefore probably very similar to the mechanism for transfer to $Ln(AA)_3.3H_2O$ complexes. The rate determining step probably involves a mixed dimer formation, ie.

$$Tb_2^* + (M)_n \rightleftharpoons TbM^* + M_{n-1} + Tb,$$

and the excitation energy of the Tb^{3+} is very rapidly transferred to the acceptor ion in the mixed dimer. That energy transfer is observed to $Co(AA)_2$, $VO(AA)_2$ and $Mn(AA)_2$ and not to $Ni(AA)_2$ in n-butanol and benzene solutions is probably due to the $Ni(AA)_2$ complex forming much more stable oligomers, which will be much larger liked than the lifetime of the Tb^{3+} $^5D_4$ level. The oligomers formed by the $Co(AA)_2$, $Mn(AA)_2$ and $VO(AA)_2$ complexes will be much less stable, and will probably have a rapid rate of monomer exchange. This rate is probably faster than the rate of decay of the Tb^{3+} $^5D_4$ lifetime, thus a dynamic quenching process is observed.

The energies of activation for the transition metal bis-acetylacetonate complexes, viz, 25.6 KJ mol^{-1}, 18.1 KJ mol^{-1} and 18.8 KJ mol^{-1} are very similar to the activation energies for energy transfer to $Sm(AA)_3.3H_2O$ and $Eu(AA)_3.3H_2O$ (23.0 and 23.2 KJ mol^{-1}

Figure 4,4: Plots of ln k vs $\frac{1}{T}$ for the quenching of $Tb(AA)_3 . 3H_2O$ by $Co(AA)_2$ (+ — + — +), $Mn(AA)_2$ (●— ● —●) and $VO(AA)_2$ (—⊙—⊙—) in n-butanol solution .

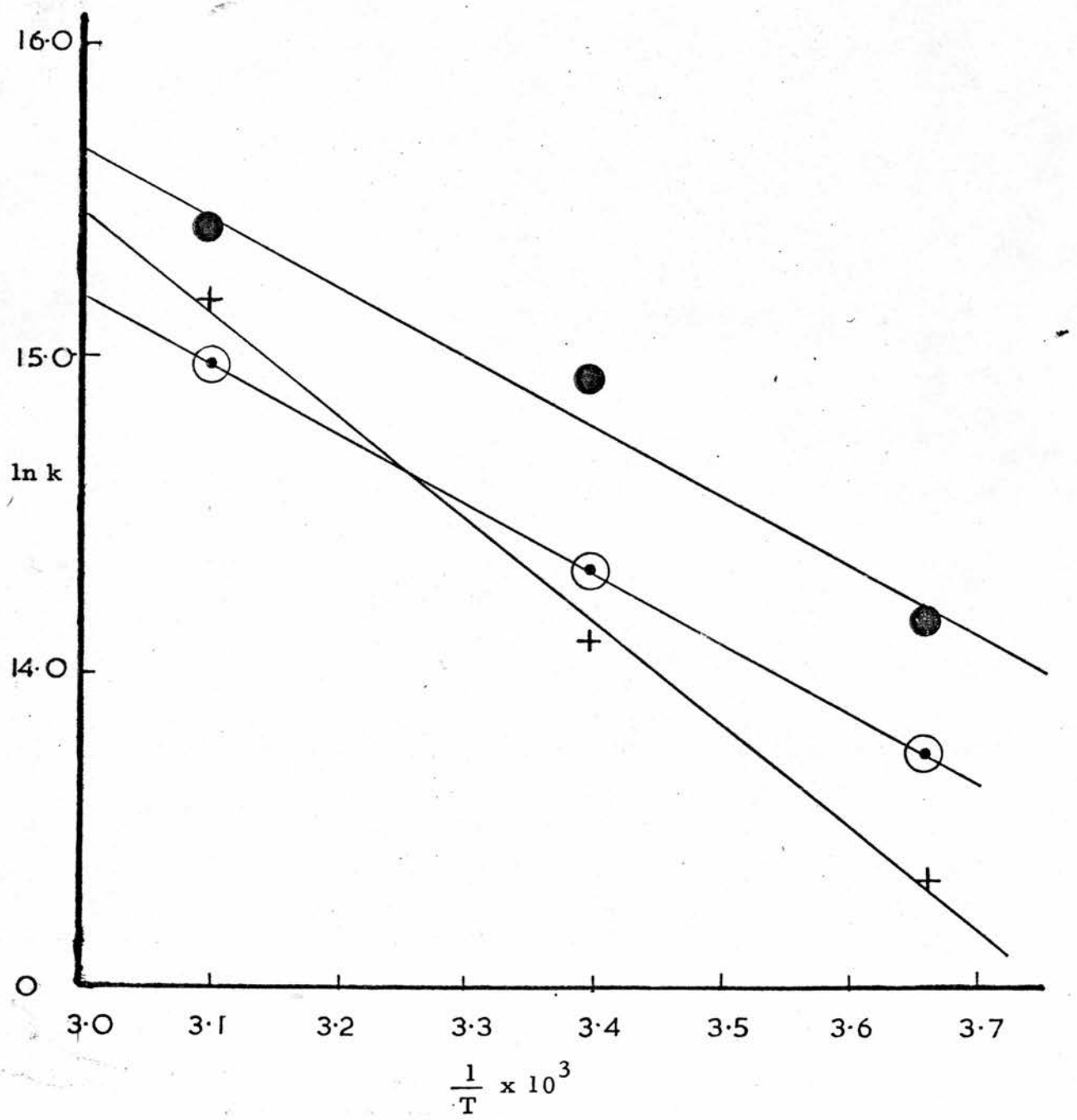

respectively[80]). These values are also close to the energy of activation for viscous flow of n-butanol (19.41 KJ mol^{-1}) [104]. To establish if the energy of activation was a function of mass transport in solution, quenching experiments were carried out in n-propanol with $Co(AA)_2$, $Mn(AA)_2$ and $VO(AA)_2$. Again the Stern-Volmer relation was obeyed for each set of data, and k values derived from these plots are summarised in Table 4,9.

Table 4,9:- Bimolecular rate constants, k (10^{-6} mol^{-1} dm^3 s^{-1}) for quenching of the Tb^{3+} $^5D_4$ level in $Tb(AA)_3.3H_2O$) in n-propanol solutions

Quencher	Temperature		
	273K	293K	323K
$Mn(AA)_2$	1.08	1.99	3.95
$Co(AA)_2$	0.55	1.28	4.56
$VO(AA)_2$	0.63	1.10	2.68
$Sm(AA)_3.3H_2O$	0.17	0.43	0.71
τ_o (μs)	870	800	730

Again temperature dependence of k is observed in all cases, as well as in that of $Sm(AA)_3.3H_2O$. The Stern-Volmer plots for $VO(AA)_2$ are shown in Figure 4,5. by way of example. The k values for each quencher were again found to fit equation 1 , viz. $k=Aexp(-E/RT)$. Energies of activation derived from plots of ln k versus $\frac{1}{T}$ are given in Table 4,10.

Figure 4,5: Stern-Volmer plots for the quenching of Tb^{3+} $^5D_4$ phosphorescence in $Tb(AA)_3 . 3H_2O$ by $VO(AA)_2$ in n-propanol solution at 273K (-●——●—), 293K (— + — +) and 323K (-⊙—— ⊙—).

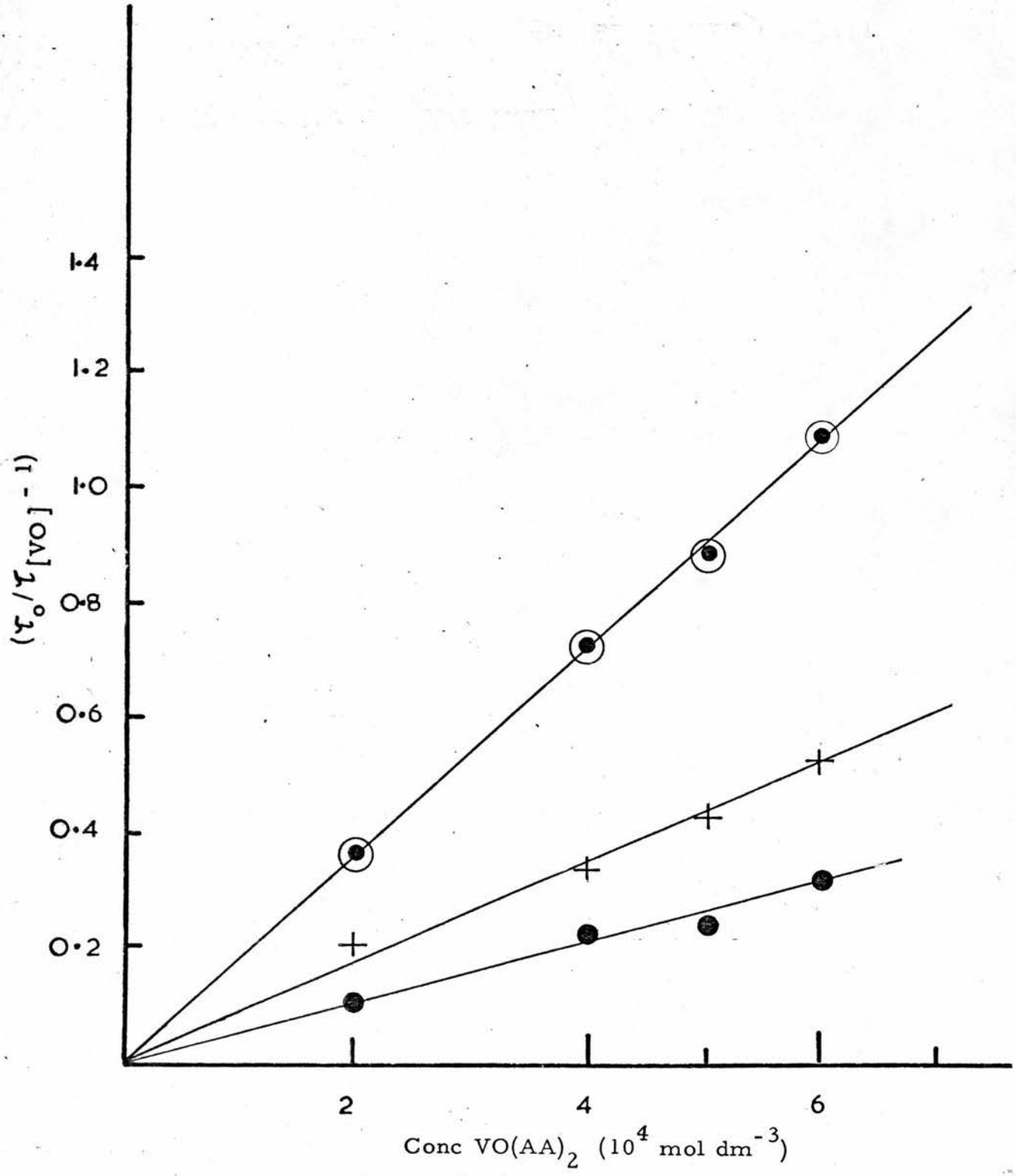

Figure 4, 6: Plots of ln k vs $\frac{1}{T}$ for the quenching of $Tb(AA)_3 . 3H_2O$ by $Co(AA)_2$ ($-\odot$ ——$\odot$—), $Mn(AA)_2$ (+ — + —), and $VO(AA)_2$ ($-\bullet$ ——$\bullet$ —) in n-propanol solution

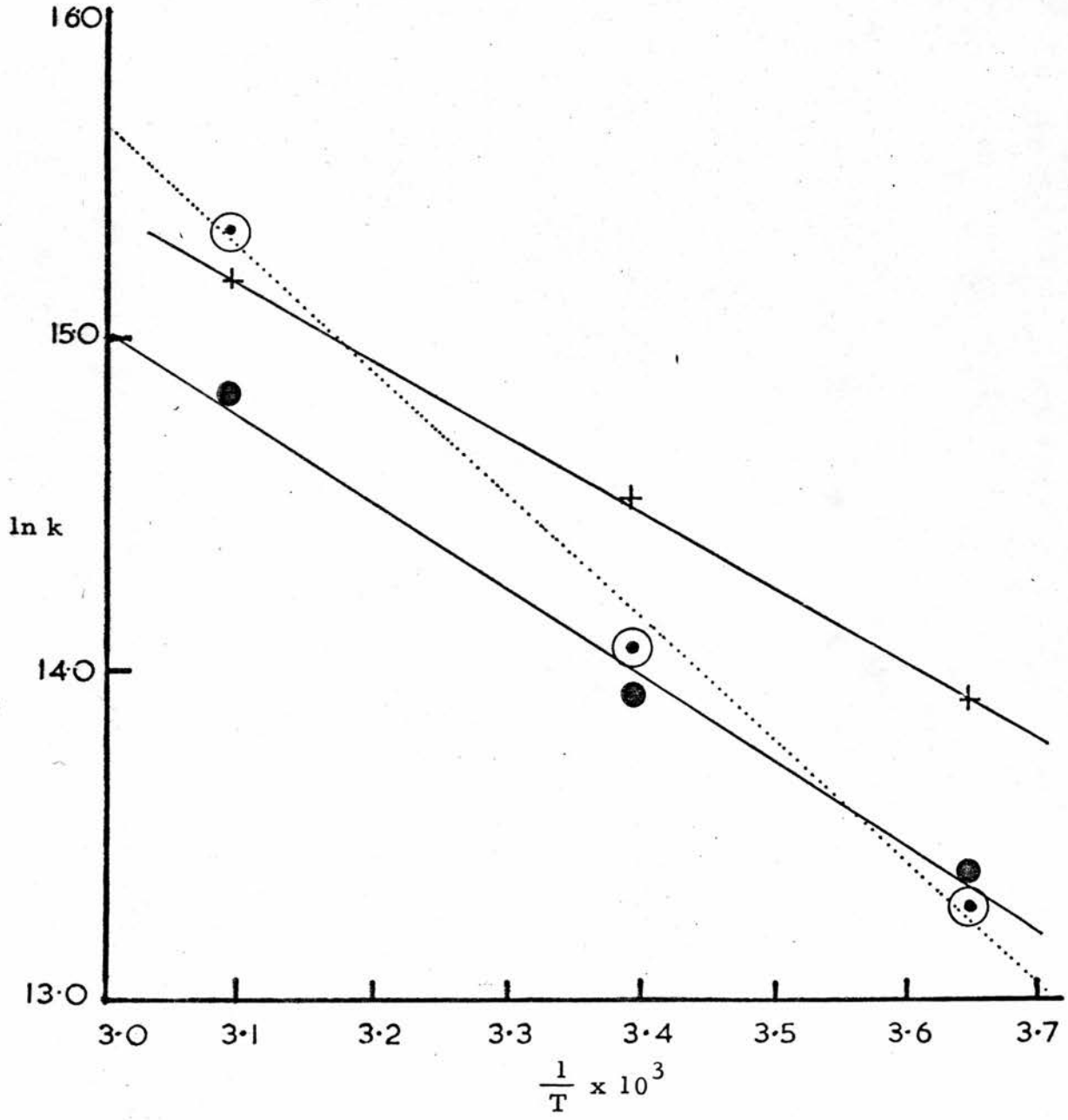

Table 4, 10:- Energies of activation, E, for the quenching of the $Tb^{3+}\ ^5D_4$ level in $Tb(AA)_3.3H_2O$ in n-propanol and n-butanol solutions

Quencher	E for n-butanol ($KJ\ mol^{-1}$)	E for n-propanol ($kJ\ mol^{-1}$)
$VO(AA)_2$	18.1	21.1
$Mn(AA)_2$	18.8	19.1
$Co(AA)_2$	25.6	30.5
$Sm(AA)_3.3H_2O$	23.0	21.5
Activation energy of viscous flow ($KJ\ mol^{-1}$)	19.4 [104]	18.0 [104]

The energy of activation for the quenching process can be assumed not to depend on mass transport, since the energy of activation for viscous flow in n-propanol is lower than that for n-butanol, but the observed values of E for the quenching process are higher in n-propanol than in n-butanol. It is therefore reasonable to suggest that the observed E refers to a step in the formation of the mixed dimer.

That energy transfer is observed in benzene solution to each of $Co(AA)_2$, $VO(AA)_2$ and $Mn(AA)_2$ is probably an indication that the monomer exchange rate in oligomers of each of these complexes is much faster than that observed in $Ln(AA)_3.3H_2O$ dimers, where no energy transfer is observed. $Co(AA)_2$ shows a low k value ($0.002 \times 10^6\ mol^{-1} dm^3 s^{-1}$) in benzene. On mixing benzene solutions

of $Tb(AA)_3.3H_2O$ and each of $Co(AA)_2$, $Mn(AA)_2$ and $VO(AA)_2$, only in the case of $Co(AA)_2$ is a slow decrease in the Tb^{3+} $^5D_4$ phosphorescence yield observed (see Chapter 5). This indicates that although some dynamic quenching is observed, the exchange rate of monomer in $Co(AA)_2$ oligomers and any CoTb mixed dimers is slow compared with those of $Mn(AA)_2$ and $VO(AA)_2$.

In pyridine, each of $Co(AA)_2$, $Mn(AA)_2$ and $VO(AA)_2$ are monomeric, and the cobalt and vanadyl complexes exhibit energy transfer. The mechanism of this quenching process is probably similar to that exhibited by $Cr(AA)_3$, $Mn(AA)_3$ and $Co(AA)_3$, described in section (iii) of this chapter. The $Mn(AA)_2$ complex exhibits no significant quenching in pyridine solution. Experiments using $MnCl_2.H_2O$ as the quencher indicate that no measureable transfer of energy from the Tb^{3+} $^5D_4$ level occurs to the "bare" Mn^{2+} ion.

(vii) Summary

The mechanism of energy transfer from $Tb(AA)_3.3H_2O$ to transition metal acetylacetonates in solution has been found to depend on the behaviour of the quencher complex in the given solvent. There are three groups of quenching complexes,

(i) tris-acetylacetonates; $Mn(AA)_3$, $Cr(AA)_3$, and $Co(AA)_3$ which are all octahedral and monomeric in solution,

(ii) bis-acetylacetones; $Cu(AA)_2$ and $Pd(AA)_2$ which are both monomeric in solution

(iii) bis-acetylacetonates which tend to oligomerise in non- and weakly-polar, and are monomeric in strongly coordinating

solvents such as pyridine. In this group are $Ni(AA)_2$, $Co(AA)_2$, $VO(AA)_2$ and $Mn(AA)_2$.

Two distinct mechanisms of quenching have been observed. The first occurs with the monomeric tris- and the monomeric square-planar bis-acetylacetonates. This involves a collisional deactivation of the Tb^{3+} $^5D_4$ level, and the bimolecular rate constant, k, for this process is at least three orders lower than the diffusion rate, and is independent of temperature. It is proposed that this energy transfer mechanism involves the formation of a collisional complex, $(TbQ)^*$, the activation energy for this process being zero, or near zero. The energy transfer step can then only occur when the donor and acceptor ions attain a specific orientation to each other, thereby explaining the low k value.

The second mechanism of energy transfer is exhibited by those acetylacetonates which tend to oligomerise in non-polar solvents. It is proposed that this process involves the formation of mixed dimers or oligomers between the Tb^{3+} and quencher complexes, the Tb^{3+} $^5D_4$ excited level being deactivated very rapidly in the mixed oligomers. For this dynamic quenching process to be observed, the exchange rate of monomers between the parent complexes must be faster than the rate of decay of the Tb^{3+} $^5D_4$ level. This type of behaviour is exhibited by $VO(AA)_2$, $Mn(AA)_2$ and $Co(AA)_2$. $Ni(AA)_2$ does not dynamically quench the Tb^{3+} complex in weakly coordinating solvents. This is probably due to the $(NiAA)_n$ oligomers being particularly stable, and therefore the monomer exchange rate is relatively slow.

Chapter 5

Oligomeric acetylacetonate complexes containing Tb^{3+} and Ni^{2+} or Co^{2+} ions

(i) Introduction

In Chapter 4, the self-association of certain transition metal acetylacetonates in non-polar solvent solutions was discussed[89]. The intermolecular energy transfer process from $Tb(AA)_3.3H_2O$ to $Co(AA)_2$, $VO(AA)_2$ and $Mn(AA)_2$ was interpreted as being dependent on the formation of mixed dimers, viz $(TbM)^*$. $Ni(AA)_2$ was also proposed to form mixed dimers or oligomers with $Tb(AA)_3.3H_2O$. The $Co(AA)_2$ and $Ni(AA)_2$ complexes have been reported to form relatively stable oligomers in non-polar solvents[89]. This chapter describes the investigations into possible formation of mixed oligomeric acetylacetonate complexes containing Tb^{3+} and Co^{2+} or Ni^{2+} ions. The terbium acetylacetonate complex was used because of the possible diagnostic value of the Tb^{3+} phosphorescence.

(ii) Results and Discussion

Vapour pressure osmometric measurements of $Tb(AA)_3.3H_2O$ in benzene solution at 301K gave a value of $\bar{n} = 1.98 \pm 0.15$ [80], where $\bar{n}$ = the average number of monomers per solute molecule. The result suggests that, within experimental error, the terbium complex exists entirely as a dimer in benzene solution. Similar measurements of the anhydrous cobalt complex, $Co(AA)_2$, gave a mean value of $\bar{n} = 3.66$ over the concentration range 0.007 to 0.05 mol dm^{-3} (see Table 5, 1). These values are higher than those reported by Cotton

and Soderberg[98] who used an isopiestic method at ca 298K, but are close to values these workers obtained cryoscopically in benzene solution. The values of $\bar{n}$ are consistent with the presence of considerable concentrations of tetramers or higher oligomers in this solvent.

Molecular weight measurements were also made in a series of equimolar mixtures of the cobalt and terbium acetylacetonates in benzene solution, and the results are shown in Table 5,1. These values may be compared with those obtained for the individual complexes.

Table 5,1:- Molecular Weight Measurements of $Tb(AA)_3.3H_2O$ and $Co(AA)_2$ in benzene solutions at 310K

CONCENTRATION		TOTAL	
$Co(AA)_2$ mol dm^{-3}	$Tb(AA)_3.3H_2O$ mol dm^{-3}	mol dm^{-3}	$\bar{n}$ (a)
-	0.0100	0.0100	1.98 ± 0.15 [80]
0.0073	-	0.0073	3.57 ± 0.25
0.0103	-	0.1003	3.62 ± 0.25
0.0498	-	0.0498	3.80 ± 0.25
0.0070	0.0070	0.0140	2.24 ± 0.15
0.0080	0.0080	0.0160	2.05 ± 0.15
0.0100	0.0100	0.0200	2.24 ± 0.15

0.01M solutions of $Tb(AA)_3.3H_2O$ and $Co(AA)_2$ gave $\bar{n} = 1.98$ and 3.62 respectively, whereas a mixed solution which 0.1 mol dm^{-3} with respect to each complex gave $\bar{n} = 2.24$. The latter value is

significantly lower than the value of $\bar{n} = 2.80$, ie. $(1.98 + 3.62)/2$, expected if the degree of association of each complex is unaffected by the presence of the other. This behaviour is reflected in the $\bar{n}$ values in solutions where each complex is 0.0007 mol dm^{-3} and 0.008 mol dm^{-3}. These results indicate that the two complexes interact in solution and that species may exist in the mixed solutions which are not present in either of the individual solutions. They do not, however, give any specific information abou the possible value of such species.

The absorption spectrum between 410 and 710 nm of a 0.005 mol dm^{-3} solution of $Co(AA)_2$ in dry benzene is shown in Figure 5,1. This absorption is due to d-d transitions in Co^{2+} ions and is therefore absent in the terbium complex. The spectral profile is markedly changed on addition of the terbium complex (Fig. 5,1), indicating that the environment of the Co^{2+} ions is changed. Since the terbium complex is a trihydrate, there exists the possibility that the water molecules may coordinate to the Co^{2+} ions, causing dissociation of the cobalt oligomers to give species such as $Co(AA)_2.2H_2O$. Such a process would be analogous to the effect of added pyridine on the cobalt oligomers reported by Fackler[100]. The absorption spectrum of $Co(AA)_2.2H_2O$ in benzene solution is shown in Figure 5,1, and it is apparent that the additional water molecules in this case do not have as marked an effect on the spectral profile as does the added $Tb(AA)_3.3H_2O$ complex. It may therefore be concluded that the water molecules alone are unlikely to be responsible for the marked change in profile on addition of $Tb(AA)_3.3H_2O$.

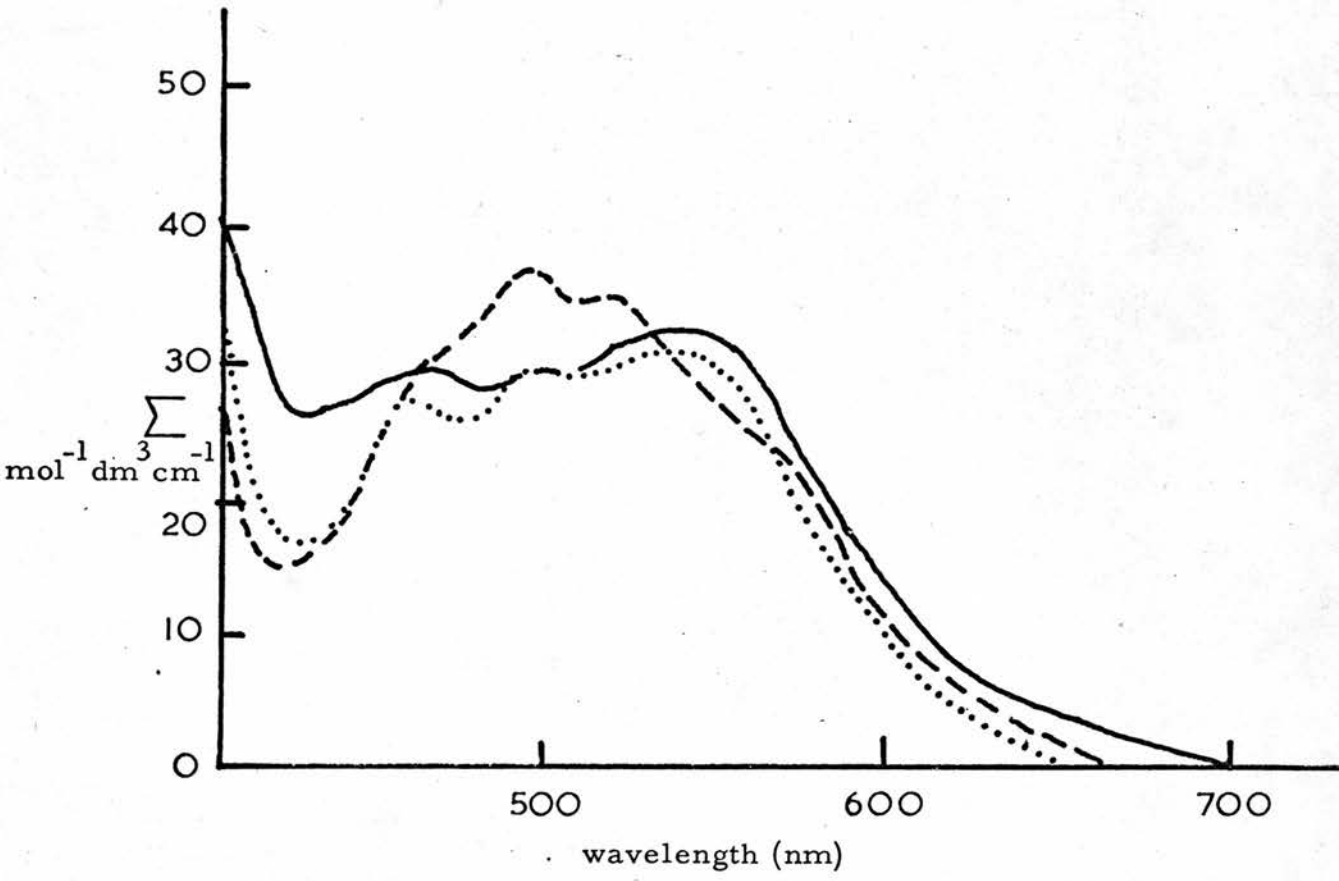

Figure 5, 1: Absorption spectra of

(a) 0.005 mol dm^3 $Co(AA)_2$ (————————)

(b) 0.005 mol dm^3 $Co(AA)_2.2H_2O$ (· · · · · · · · · · · · ·)

(c) 0.005 mol dm^3 $Co(AA)_2$ + 0.005 mol dm^3

$Tb(AA)_3.3H_2O$ (----------)

in benzene solution at 293K

To obtain further information, the phosphorescence of the Tb^{3+} ion was investigated in mixed solutions. The principal emitting level of the Tb^{3+} ion is the $^5D_4$, and in benzene solutions this level has an exponential lifetime of 900 μs $\pm$ 15 μs. The most intense emission is caused by the $^5D_4 \longrightarrow {}^7F_5$ transition at ca 545 nm. It was observed that after mixing benzene solutions of $Co(AA)_2$ and $Tb(AA)_3.3H_2O$ the Tb^{3+} ion phosphorescence yield, Φ, decreased slowly and eventually reached a steady value. An example of this type of behaviour is shown in Figure 5.2 The Tb^{3+} emission spectral profile remains unchanged, and τ decreases by no more than 3% during this change in Φ. This indicates that the only emitting species in the mixed solution is the terbium complex dimer. The decrease in Φ may thus be correlated with a decrease in the terbium complex dimer concentration, leading to an equilibrium where, under the conditions used to obtain the data in Figure 5,2, the dimer concentration has decreased to ca 20% of its original value. There is therefore, at equilibrium, a considerable proportion of Tb^{3+} ions in a complex form in which the Tb^{3+} ions do not phosphoresce. This behaviour may be explained by proposing that a slow reaction between the terbium and cobalt complex species produces dimers or higher oligomeric species containing both Co^{2+} and Tb^{3+} ions, ie. mixed metal complexes. The relative proximity of the Co^{2+} and Tb^{3+} ions in such species could allow a rapid energy transfer between excited Tb^{3+} ions and acceptor levels in the Co^{2+} ion which would result in zero or near zero phosphorescence from the Tb^{3+} ion. This interpretation is supported by the observation that the addition of pyridine to an equilibriated mixture of the two complexes results in

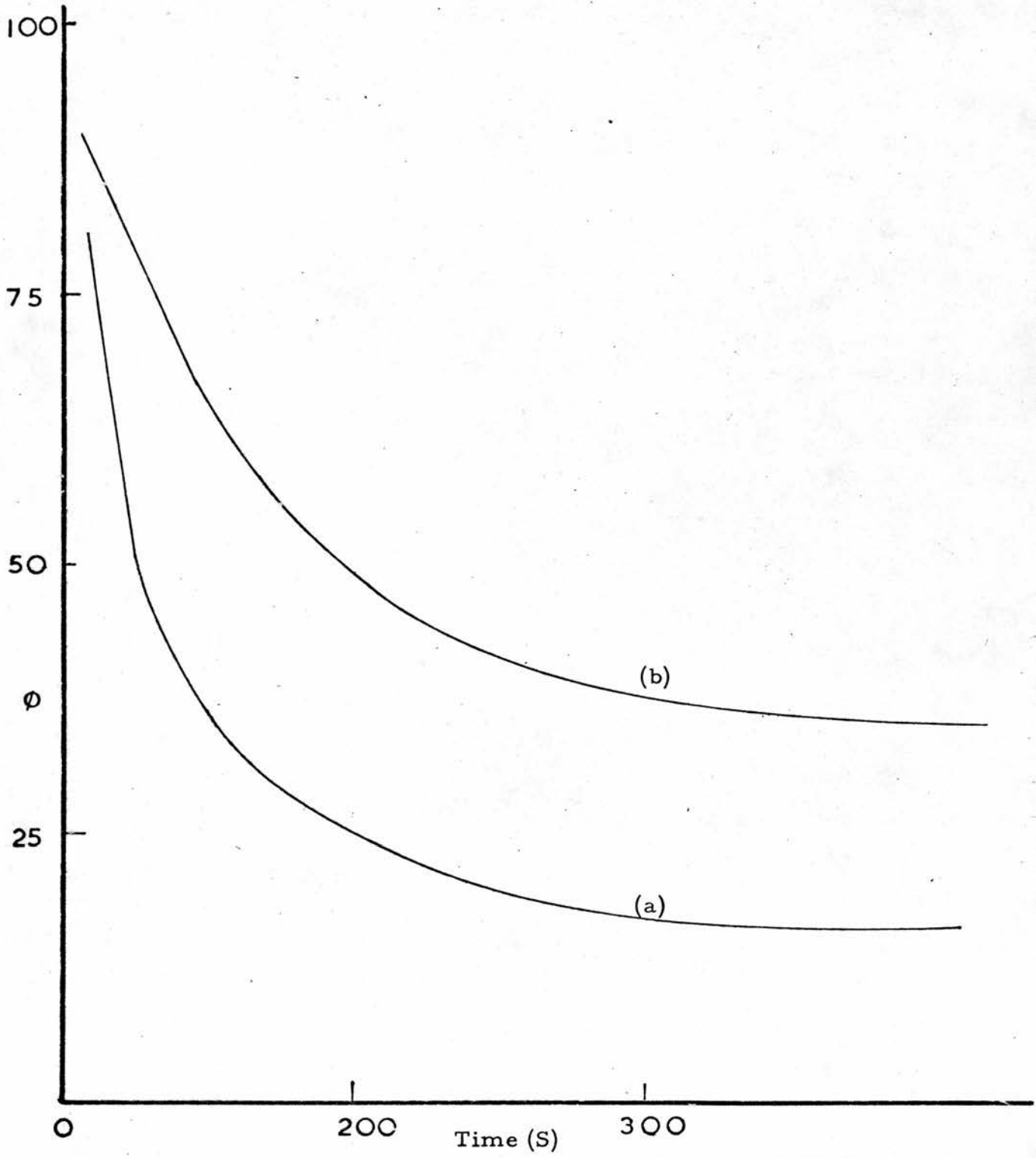

Figure 5,2: The decrease in the Tb^{3+} ion phosphorescence yield, Ø, (arbitrary units) after mixing equal volumes of 0.0025 mol dm^{-3} $Tb(AA)_3.3H_2O$ and (a) 0.0025 mol dm^{-3} $Co(AA)_2$ and (b) 0.0025 mol dm^{-3} $Ni(AA)_2$ in benzene solution at 293K

an immediate increase in Φ, consistent with the strongly coordinating pyridine molecules breaking down the oligomeric species to form monomeric cobalt and terbium complexes. A similar type of behaviour has been found[80] to occur on mixing benzene solutions of terbium and europium acetylacetonates, and in this case the slow decrease in Φ was accompanied by an increase in the phosphorescence yield of the Eu^{3+} ion. Since the europium acetylacetonate does not phosphoresce in the absence of the terbium complex (see Chapter 6), this observation gave direct evidence of a $Tb^{3+} \rightsquigarrow Eu^{3+}$ energy transfer step occurring in the mixed dimer $TbEu(AA)_6.6H_2O$.

The values of $\bar{n}$ obtained in the mixed cobalt and terbium acetylacetonate complexes (see Table 5, 1) suggest that a mixed dimer such as $CoTb(AA)_5.3H_2O$ may be formed. Although the values of $\bar{n}$ and the decrease in Φ are consistent with the presence of an equilibrium of type:-

$$Co(AA)_2 + Tb(AA)_3.3H_2O \rightleftharpoons CoTb(AA)_5.3H_2O,$$

the errors in the various $\bar{n}$ values are too high to firmly establish the occurrence of this specific equilibrium.

Similar investigations have been made using anhydrous $Ni(AA)_2$ instead of $Co(AA)_2$. A decrease in Tb^{3+} phosphorescence occurs after mixing benzene solutions of $Ni(AA)_2$ and $Tb(AA)_3.3H_2O$ similar to that found with $Co(AA)_2$ (Figure 5, 2). The $^3A_{2g} \longrightarrow {}^3T_{1g}$ absorptions of the Ni^{2+} ion in $Ni(AA)_2$, $Ni(AA)_2.2H_2O$ and $Ni(AA)_2$ plus an equimolar concentration of $Tb(AA)_3.3H_2O$ are shown in Figure 5, 3. As in the corresponding cobalt case, the marked change in the absorption

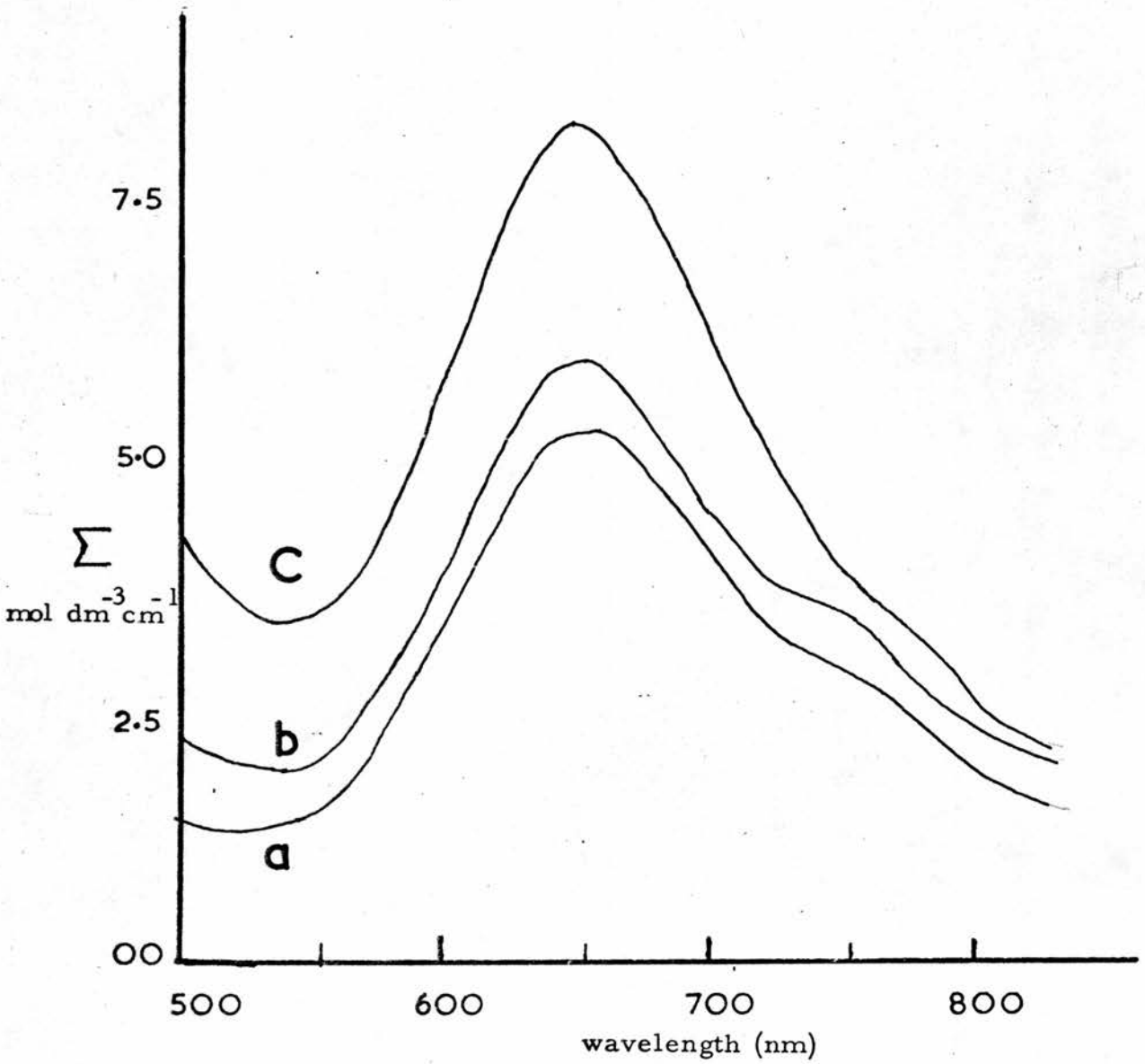

Figure 5, 3: Absorption spectra of

(a) 0.01 mol dm^{-3} $Ni(AA)_2$

(b) 0.01 mol dm^{-3} $Ni(AA)_2.2H_2O$ and

(c) 0.01 mol dm^{-3} $Ni(AA)_2$ and 0.01M $Tb(AA)_3.3H_2O$

in benzene solution at 293K

spectrum on the addition of the terbium complex is not primarily due to the water molecules coordinating to the transition metal ion. Molecular weight measurements equivalent to those carried out with $Co(AA)_2$ were made, and are reported in Table 5,2. The resultant $\bar{n}$ calues are consistent with the formation of mixed metal oligomers in solution, although in contrast to the results obtained with $Co(AA)_2$, they suggest that associations to form trimers, tetramers or higher oligomers occurs. There is also an indication that the nature of the oligomers formed in solution is concentration dependent, and it is therefore unlikely that any particular species has a marked energetic advantage.

Neither the terbium acetylacetonate nor the anhydrous cobalt and nickel acetylacetonates is particularly soluble in benzene, the solubility limit at room temperature being of the order of 0.015 mol dm^{-3}. Solutions containing both the lanthanide acetylacetonate and either the cobalt or the nickel acetylacetonate can however be prepared at much higher concentrations than is possible with any of the complexes above. It has been possible to isolate crystals from such solutions with analyses corresponding to $CoTb(AA)_5.3H_2O$ and $NiTb(AA)_5.3H_2O$. This was achieved by dissolving the $Tb(AA)_3.3H_2O$ and the required transition metal acetylacetonate in the minimum necessary volume of warm benzene. A small volume of petroleum ether (100-120°) was added and the solution was allowed to stand. After several hours crystals were filtered from the solution and air dried. This procedure was followed for 1:1 and 2:1 molar ratios of transition metal complex to lanthanide complex,

Table 5, 2:- Molecular Weight Measurements of $Tb(AA)_3.3H_2O$ and $Ni(AA)_2$ in benzene solution at 310K

CONCENTRATION (mol dm^{-3})			
$Ni(AA)_2$	$Tb(AA)_3.3H_2O$	TOTAL	$\bar{n}$
(a)			
0.0083	-	0.0083	2.77 ± 0.20
0.0105	-	0.0105	2.71 ± 0.20
0.0482	-	0.0482	2.89 ± 0.20
(b) 1:1 Ni:Tb molar ratio			
0.0070	0.0070	0.0140	2.76 ± 0.20
0.0080	0.0080	0.0160	2.91 ± 0.20
0.0100	0.0100	0.0200	2.99 ± 0.20
(c) 1:2 Ni:Tb molar ratio			
0.0025	0.0050	0.0075	3.31 ± 0.25
0.0033	0.0066	0.0100	3.65 ± 0.25
0.0050	0.0100	0.0150	4.08 ± 0.30
(d) 2:1 Ni:Tb molar ratio			
0.0050	0.0025	0.0075	3.56 ± 0.25
0.0066	0.0033	0.0100	3.69 ± 0.25
0.0100	0.0050	0.0150	3.72 ± 0.25

and analytical data for the isolated crystals are shown in Table 5, 3.

Microscopic examination of these crystals shows them to be homogeneous and of different crystalline form from either of the two parent complexes in the case of both Ni^{2+} and Co^{2+}. No Tb^{3+} phosphorescence is detectable under ultraviolet irradiation of the

crystals which is consistent with an efficient excited Tb^{3+} ion to transition metal transfer step.

Table 5, 3:- Analytical data for crystals isolated from mixed benzene solutions of $Tb(AA)_3.3H_2O$ and $Ni(AA)_2$ or $Co(AA)_2$–

Initial Molar Ratio	Calculated for $MTb(AA)_5.3H_2O$*		FOUND		M.pt.
	%C	%H	%C	%H	°C
1:1 Co/Tb	39.13	5.39	39.07	6.01	132-134
2:1 Co/Tb	39.13	5.39	39.32	5.81	128-130
1:1 Ni/Tb	39.14	5.39	39.24	5.30	120-121
2:1 Ni/Tb	39.14	5.39	39.31	5.43	119-120

* where M=Co or Ni as appropriate

Pyridine solutions of the crystals do, however, emit the characteristic Tb^{3+} phosphorescence on irradiation, indicating breakdown into the individual solvated metal complexes.

The results suggest that mixtures of terbium acetylacetonate and cobalt (or nickel) acetylacetonate in benzene solution preferentially form mixed metal oligomeric complexes. The oligomerisation of cobalt and nickel acetylacetonates in non-polar solvents may be rationalised in terms of their preference for a 6-coordinate octahedral stereochemistry. They may still achieve 6-coordination in a mixed metal complex by showing oxygen atoms of the terbium complex ligands A possible dimeric arrangement is shown in Figure 5,4(a) and a mixed trimer in Figure 5,4(b), where in both cases the transition metal ion is 6-coordinate. These two specific and speculative examples serve to illustrate the possibility that these and higher oligomeric

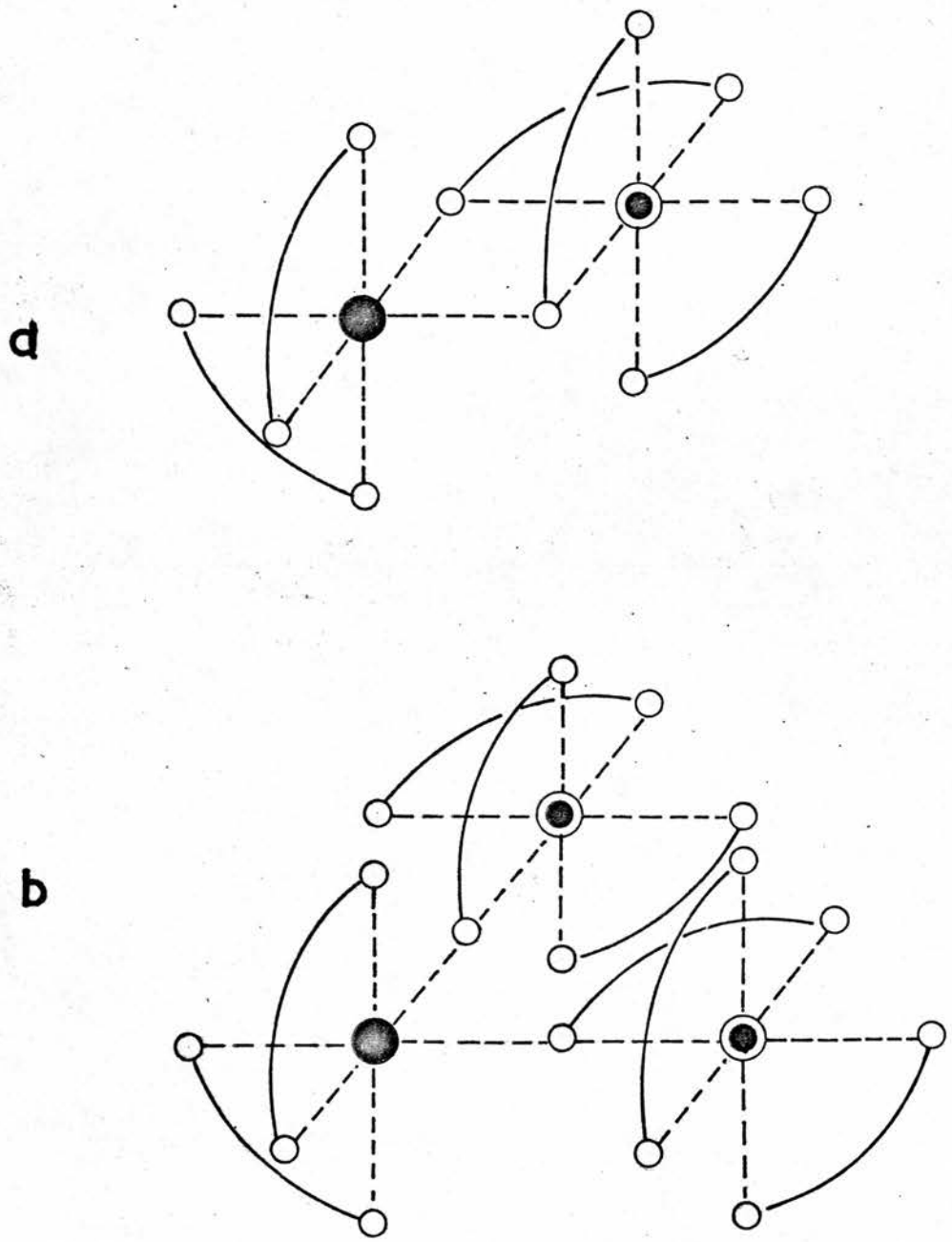

Figure 5, 4: Example of possible stereochemistries of (a) a mixed metal dimer and (b) a mixed metal trimer where ● = Co^{++} or Ni^{++}, ⊙ = Ln^{3+} and O = oxygen atoms of the acetylacetonate ligand. A large number of isomeric arrangements may be drawn. The water molecules are not shown.

complexes can be accommodated in a scheme where, as the spectral results indicate, the transition metal ion is 6-coordinate. It is not clear why the formation of mixed metal oligomers should be apparently energetically favourable with respect to single self-association of the individual complexes, but it may be connected with the disparate ionic radii of the lanthanide and transition metal ions, leading to an advantageous sterochemical arrangement for the bridging bonds. It may be significant that the intensities of the d-d absorptions increased in both the cobalt and nickel complexes on addition of the terbium complex, which would be consistent with a decrease in the centrosymmetry of the Ni^{2+} and Co^{2+} ions.

This evidence supports the hypothesis put forward in Chapter 4, that $Co(AA)_2$ and $Ni(AA)_2$ form mixed dimers with $Tb(AA)_3.3H_2O$ in solution.

Chapter 6

Charge Transfer Excited State in $Eu(AA)_3.3H_2O$

Introduction

Most of the work reported in this thesis is concerned with acetylacetonate complexes of various metal ions. $Tb(AA)_3.3H_2O$ has been used widely, often because of the Tb^{3+} phosphorescence observed when the complex is irradiated in the ligand absorption band. From consideration of the energy levels of the acetylacetonate ligand and Eu^{3+} and Tb^{3+} ions (see Figure 6, 1), Eu^{3+} might be expected to phosphoresce in $Eu(AA)_3.3H_2O$ on irradiation in the (AA) absorption band, as does the Tb^{3+} ion. In the solid state, no Eu^{3+} phosphorescence is observed, and Dawson et al have estimated the quantum efficiency, ϕ_{Eu} of Eu^{3+} emission in methanol solution to be less than 0.002 [75] on irradiating the ligand. In contrast, the analogous terbium complex quantum efficiency is 0.19 [75]. The ϕ_{Eu} is very low indeed, and this chapter reports an investigation into this anomalous behaviour.

Results and Discussion

On irradiating $Eu(AA)_3.3H_2O$ in the ligand absorption band, the quantum efficiency for Eu^{3+} ion phosphorescence, ϕ_{Eu}, may be expressed as

$$\phi_{Eu} = \phi_{1s}\phi_{Tm}\phi_c\phi_{^5D_o},$$

where ϕ_{1s} is the intersystem crossing efficiency of ligand singlet to ligand triplet, ϕ_{Tm} the ligand triplet to Eu^{3+} acceptor level transfer

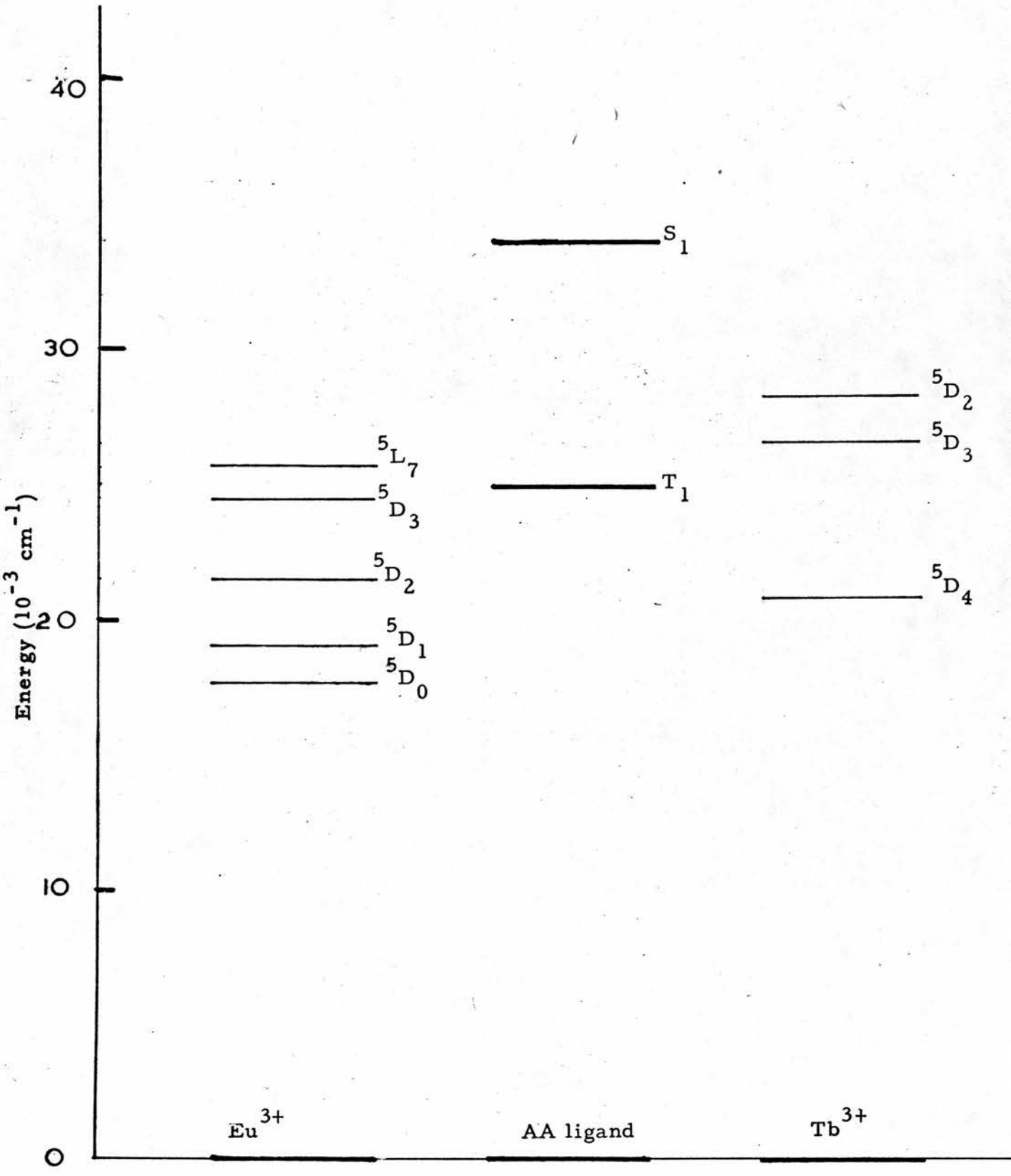

Figure 6,1: energy levels of Tb^{3+}, Eu^{3+} and the acetylacetonate ligand

efficiency, ϕ_c the efficiency of the cascade process from the Eu^{3+} acceptor level to the $^5D_0$ emitting level, and $\phi_{^5D_0}$ is the radiative efficiency of the $^5D_0$ level. From published data[75], in methanol solution $\phi_{^5D_0} = 0.18$ and $\phi_c(^5L_7 \rightsquigarrow {}^5D_0)=0.06$, $\phi_c(^5D_2 \rightsquigarrow {}^5D_0)=0.33$. Therefore if one assumes that the cascade process involves the $^5L_7$ level and $\phi_{Eu} < 0.002$ the product $\phi_{ls}\phi_{Tm}$ cannot exceed 0.2. The real value of $\phi_{ls}\phi_{Tm}$ is probably considerably lower than 0.2 since the value for ϕ_{Eu} of 0.002[75] is merely the upper limit representing the sensitivity of the quantum yield measurements. It may be concluded that the intersystem crossing and/or the ligand triplet, T, to Eu^{3+} transfer are much less efficient in the europium complex than in the corresponding terbium acetylacetonates.

The energies of the acetylacetonate π - and non-bonding orbitals would not be expected to be particularly sensitive to the nature of the lanthanide ion. This is confirmed by the absorption spectra of $Ln(AA)_3.3H_2O$ compounds in dry n-butanol solution. The absorption maxima and extinction coefficient of these complexes are shown in Table 6,1.

The absorption maxima at 290 ± 3 nm are assigned to the lowest energy $S_{\pi\pi^*} \longleftarrow S_0$ transition, and the unsolved shoulder at ca 305 nm to the weaker $S_{n\pi^*} \longleftarrow S_0$ symmetry forbidden transition (see Figure 6,2). The spectra are similar to that of $Al(AA)_3$ in ethanol solution in which the $S_{\pi\pi^*} \longrightarrow S_{n\pi^*}$ energy difference has been estimated at ca 2000 cm^{-1}. The maximum of the O-O band in the corrected ligand phosphorescence spectrum of $Gd(AA)_3.3H_2O$ in frozen ethanol solution at 77K at 397 nm establishes the energy of the lowest ligand

Table 6, 1:- Acetylacetonate absorption maxima, λ_{max}, and molar extinction coefficients, Σ_{max}, of $Ln(AA)_3.3H_2O$ in dry n-butanol solution at 293K

Ln	λ_{max} (nm)	log Σ_{max}
Pr	291.5	4.53
Nd	291.5	4.58
Sm	291	4.59
Eu	289	4.57
Gd	289.5	4.57
Tb	289.5	4.55
Dy	289	4.62
Ho	288	4.59
Er	288	4.64
Yb	287	4.56

triplet, which is a $T_{\pi\pi^*}$ state[105]. This is in reasonable agreement with previously reported values[76,77], and the energy is unlikely to vary significantly with a change in Ln^{3+}. There is no evidence to suggest that any Ln^{3+} dependent variation in $S_{\pi\pi^*}$, $S_{n\pi^*}$, $T_{\pi\pi^*}$ is directly responsible for the anomalous behaviour of the europium complex.

Closer examination of the absorption spectrum of the europium acetylacetonate shows a low frequency absorption edge of relatively low intensity which extends into the visible region (Σ_{360}=205 mol dm^{-3} cm^{-1} Σ_{415}=10 mol dm^{-3} cm^{-1}). In the other lanthanide complexes examined, with the exceptions of Ho and Er which have relatively strong f-f absorptions above 360 nm, the molar extinction coefficients are

$<$ 15 mol dm^{-3} cm^{-1} at wavelengths above 360 nm. The additional band in the case of the $Eu(AA)_3.3H_2O$ complex is not resolved from the steep absorption edge of the ligand $\pi - \pi^*$ and $n-\pi^*$ absorption (see Figure 6, 2) but comparison with the other lanthanide spectra indicates that λ_{max} is ca 320 nm with $\Sigma_{max} > 500$ mol dm^{-3} cm^{-1} ie. at lower energy than the $S_{n\pi^*}$. The absorption spectrum of $Eu(DPM)_3$[106] [DPM=$(Bu^tCOCHCOBu^t)^-$] has been examined, and a long wavelength absorption has also been found (Σ_{350}=560 mol dm^{-3} cm^{-1} Σ_{400}=15 mol dm^{-3} cm^{-1}) which is absent in the corresponding $Tb(DPM)_3$ (Σ_{350}=30 mol dm^{-3} cm^{-1}). $Eu(DPM)_3$ has, like the acetylacetonate Eu complex, a very low ϕ_{Eu} in the solid state and in solution, whereas $Tb(DPM)_3$ shows a relatively high ϕ_{Tb}. It is proposed that the additional absorption band in the europium complexes is due to ligand to metal charge transfer. Its occurrence at low energy in the Eu^{3+} cases is supported by the low reduction potential (Eu^{3+}/Eu^{2+} aq = -0.35V)[107] in comparison with the other tripositive lanthanide ions.

Barnes[108] has reported charge-transfer(CT) absorption in complexes of Eu^{3+} with NCS^- (345 nm), Br^- (320 nm) and Cl^- (276 nm) in ethanol solution. The europium complex CT bands lie 3-5000 cm^{-1} lower in energy than the corresponding complexes of Yb^{3+}, the next most readily reduced lanthanide tripositive ion (Yb^{3+}/Yb^{2+} aq = 1.15V)[107]. Similar long wavelength absorption bands to those of $Eu(AA)_3.3H_2O$ and Eu(DPM) have been observed in Eu^{3+} complexes of a series of substituted benzoic acids, and have been attributed to CT transitions[109]. Absorption at ca 245 nm in various

Figure 6, 2: Absorption spectra of

(a) $Eu(AA)_3 . 3H_2O$

(b) $Gd(AA)_3 . 3H_2O$

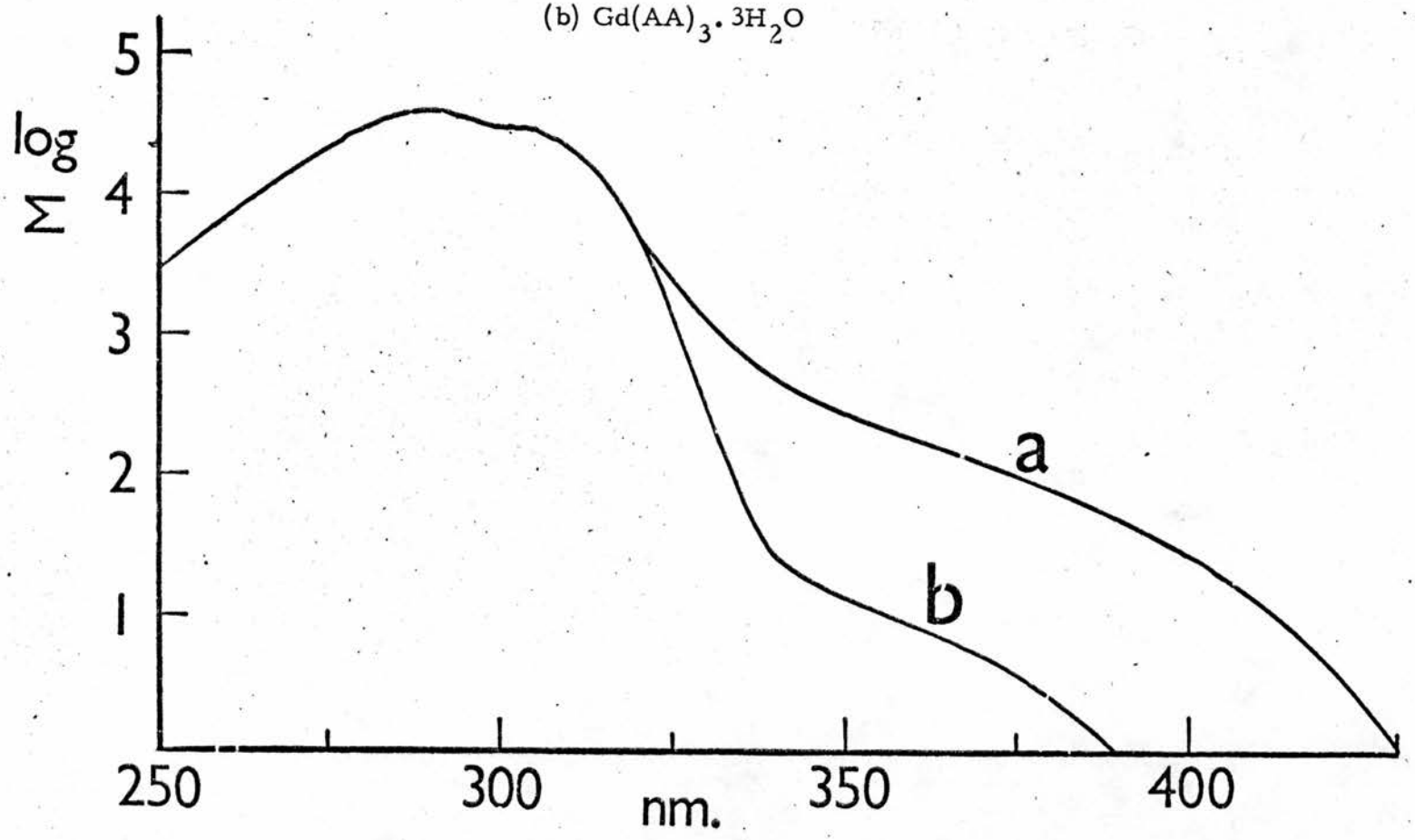

$Cu(\beta\text{-diketoenolate})_2$ complexes has been assigned[110] as ligand to metal ion CT involving a non-bonding ligand electron. The greater covalency of the Cu^{2+}-ligand bonding may be largely responsible for the apparent inverted order (Cu^{2+}/Cu^{+} aq = +0.153V)[111] of the Cu^{2+} and Eu^{3+} CT transitions.

The very low ϕ_{Eu} of the acetylacetonate and dipivaloylmethane complexes may be associated with the presence of the low energy CT band. It is significant that many europium tris(β-diketoenolates) including, for example $Eu(HFAA)_3.2H_2O$ and $Eu(BTFA)_3.2H_2O$[112] [HFAA=$(CF_3COCHCOCF_3)^-$, BTFA=$(CF_3COCHCOPh)^-$] exhibit very efficient intramolecular energy transfer. In these particular cases the lower ligand singlet levels lie at lower energy than the AA complexes (see Figure 6,3) and the corresponding CT transition presumably occurs above the $S_{n\pi^*}$ and perhaps also above the $S_{\pi\pi^*}$ state. In both the AA and DPM complexes of europium, it is proposed that an $S_{\pi\pi^*} \rightsquigarrow S_{n\pi^*} \rightsquigarrow$ CT exceeds the normal intersystem crossing rate, thus vastly reducing the ligand triplet yield. An alternative explanation that the $S_{n\pi^*}$ intersystem crossing to a CT triplet state, which undergoes rapid deactivation to the ground state, is less satisfactory in that it does not necessitate CT(singlet)$\rightsquigarrow S_{n\pi^*}$, and might therefore be expected to reduce ϕ_{Eu} in a wider range of europium complexes than is observed. Haas et al[113] have observed fluorescence in aqueous solutions of Eu^{3+} following excitation in the CT band from both the CT band and an excited state of Eu^{2+}. No corresponding fluorescence has been observed in the europium acetylacetonate solutions.

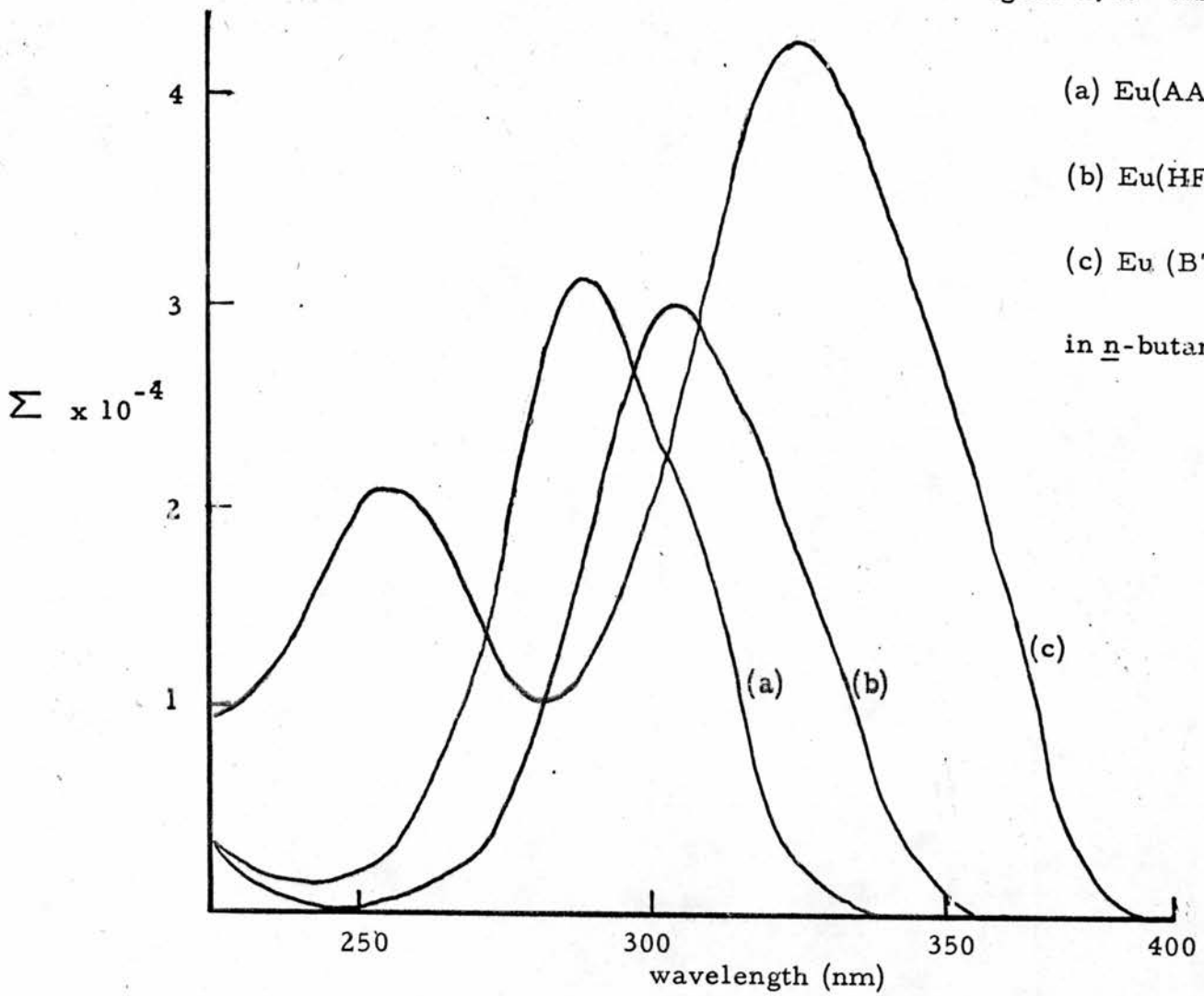

Figure 6, 3: Absorption spectra of

(a) $Eu(AA)_3 . 3H_2O$

(b) $Eu(HFAA)_3 . 2H_2O$

(c) $Eu(BTFA)_3 . 2H_2O$

in n-butanol solution

Investigations into the effect of adding KBr and KNCS to ethanolic solutions of hydrated $Eu(BTFA)_3$ and Eu(HFAA) have been reported in a previous paper[114]. The phosphorescence yield, ϕ_{Eu} was unaffected by KBr in either solution. ϕ_{Eu} was also unaffected by KNCS in $Eu(BTFA)_3$, but KNCS quenched Eu^{3+} phosphorescence in $Eu(HFAA)_3$.

The CT absorption of $Eu(NCS)^{2+}$ and $Eu(Br)^{2+}$ species[108] and the singlet levels of HFAA and BTFA (see Figure 6, 3) indicate that the CT level due to the added salt will lie below the singlet $S_{n\pi^*}$ only in the case of $Eu(HFAA)_3$ in the presence of NCS^-. The quenching of Eu^{3+} phosphorescence in $Eu(HFAA)_3$ by the addition of NCS^- ions may therefore be interpreted as intramolecular energy transfer from the $S_{n\pi^*}$ level to the CT band in mixed complexes such as $Eu[(HFAA)_n(NCS)_m]^{3-m-n}$, with subsequent non-radiative deactivation of the CT band. It is however possible that the NCS^- ion is quenching an excited Eu^{3+} level, for example the $^5D_1$ or $^5D_2$.

These experiments using KBr and KNCS as potential Eu^{3+} phosphorescence quenchers give further support to the proposal that the absorption band with λ_{max} at ca 320 nm in the $Eu(AA)_3.3H_2O$ spectrum is due to a charge-transfer transition.

Chapter 7

Temperature Dependence of the Tb^{3+} $^5D_4$ Lifetime in $Tb(AA)_3.3H_2O$ in Hydroxylic Solutions

Dawson et al[75,115,116] in a series of papers, investigated the temperature dependence of phosphorescent lifetimes of various lanthanide complexes in solution. They found that several terbium chelates showed a decrease of the Tb^{3+} $^5D_4$ lifetime with increasing temperature[75]. The temperature dependence was explained in terms of quenching of the emitting level via thermal excitation to the lowest triplet level of the ligand. This behaviour has also been observed in tris(dipivaloylmethanato)terbium(III) ($Tb(DPM)_3$) in the solid state[117].

If temperature dependence of the Tb^{3+} $^5D_4$ lifetime is the result of thermal excitation from the emitting level to the lowest ligand triplet level, then the energy difference between these levels, E_{ET}, will obviously be of importance in determining the deactivation rate. A schematic diagram for the thermal deactivation to the lowest triplet from the Tb^{3+} $^5D_4$ level is given in Figure 7,1.

The rate constant for the process, k(T), should be related to E_{ET} by

$$k(T) = A \exp(-E_{ET}/RT) \qquad \text{——— 1,}$$

where A = pre-exponential term (s^{-1})
E_{ET} = activation energy (J mol^{-1})
R = gas constant (J $mol^{-1}K^{-1}$)
T = temperature in K.

If k(T) is the only temperature dependent process for the deactivation of the emitting level, relation (2) should also be obeyed.

Figure 7, 1:- Thermal deactivation of the Tb^{3+} $^5D_4$ level to the lowest ligand triplet

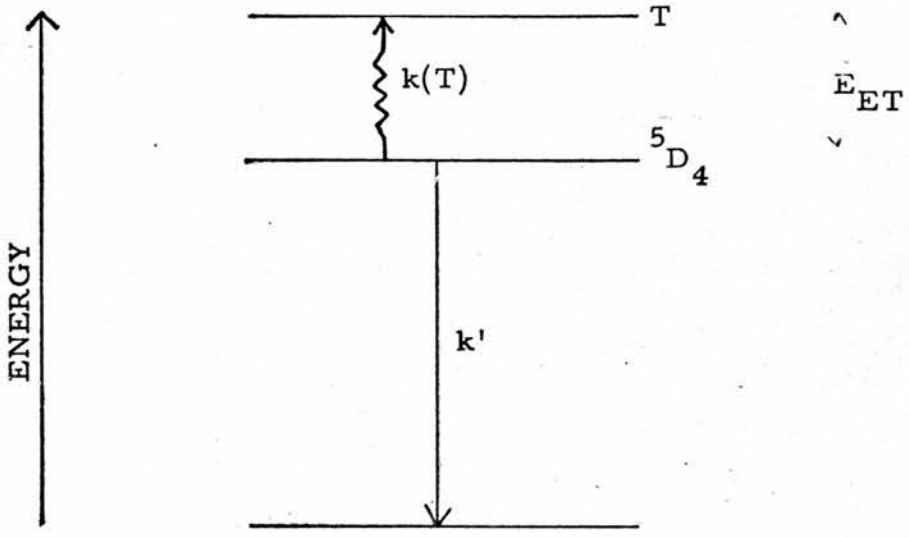

k' = temperature independent deactivation rate of the Tb^{3+} $^5D_4$ level

k(T) = temperature dependent back-donating rate of $^5D_4$ T

E_{ET} = energy difference between Tb^{3+} $^5D_4$ and triplet (T) levels.

$$k(T) = \frac{1}{\tau_T} - \frac{1}{\tau_m} = A \exp(E_{ET}/RT) \quad [75] \qquad \text{——— 2,}$$

where τ_T = phosphorescent lifetime at temperature T_K

τ_m = phosphorescent lifetime in the absence of temperature-dependent quenching process (ie. $\frac{1}{k'}$).

A plot of $\ln(\frac{1}{\tau_T} - \frac{1}{\tau_m})$ against $\frac{1}{T}$ should therefore be linear and allow a determination of the energy, E_{ET}, for the process. τ_m is estimated experimentally by using the lifetime at a low enough temperature where no significant thermal quenching is expected. Dawson et al[75] found that the experimentally determined values of E_{ET} for the terbium tris(trifluoroacetylacetonate) complex ($Tb(TFAA)_3$) in both methanol and toluene solutions were in reasonable agreement with

spectroscopically determined E_{ET} values. $Tb(AA)_3.3H_2O$, however, did not exhibit any thermal deactivation of the Tb^{3+} $^5D_4$ level in toluene solution up to 323K. This was consistent with the large E_{ET} value of ca 4500 cm^{-1} in this complex, which predicted $-\frac{E_{ET}}{RT}$ to be ca 10^{-10} at room temperature. If temperature dependent quenching is subject purely to thermal excitation from the emitting level to the lowest ligand triplet level, plots of $(\frac{1}{\tau} - \frac{1}{\tau_m})$ against $\frac{1}{T}$ for solutions of a certain complex in different solvents should yield the same gradient, and hence E_{ET} values, as was found in the case of $Tb(TFAA)_3$ [75]. In investigations described in Chapters 3 and 4, the quenching of the Tb^{3+} $^5D_4$ level in $Tb(AA)_3.3H_2O$ by other metal acetylacetonates in solution was investigated. Lifetimes, τ, of the Tb^{3+} $^5D_4$ level in the absence of quencher at various temperatures have also been determined, and in the cases of n-butanol and n-propanol a marked decrease in from 273K to 323K was observed. Further investigations into this behaviour are discussed below.

A solution of $Tb(AA)_3.3H_2O$ (2.5×10^{-3} mol dm^{-3}) in n-butanol was cooled to ca 190K, just above the freezing point of the solvent (183.5K) [118]. The solution was allowed to warm very slowly, and the lifetime of the Tb^{3+} $^5D_4$ level was determined at various temperatures. The results are shown in Table 7,1.

Figure 7,2 shows the plot of $\ln(\frac{1}{\tau} - \frac{1}{\tau_m})$ v. $\frac{1}{T}$ to be linear within experimental error over the temperature range shown. Using equation (2), one obtains an activation energy E=15.2 KJ mol^{-1}, ie. ca 1300 cm^{-1}, and an estimate of A, the pre-exponential term is ca 2.1×10^5 s^{-1}. The values of A and E are quite sensitive to the value taken for τ_m and it is estimated that the error limits for E and

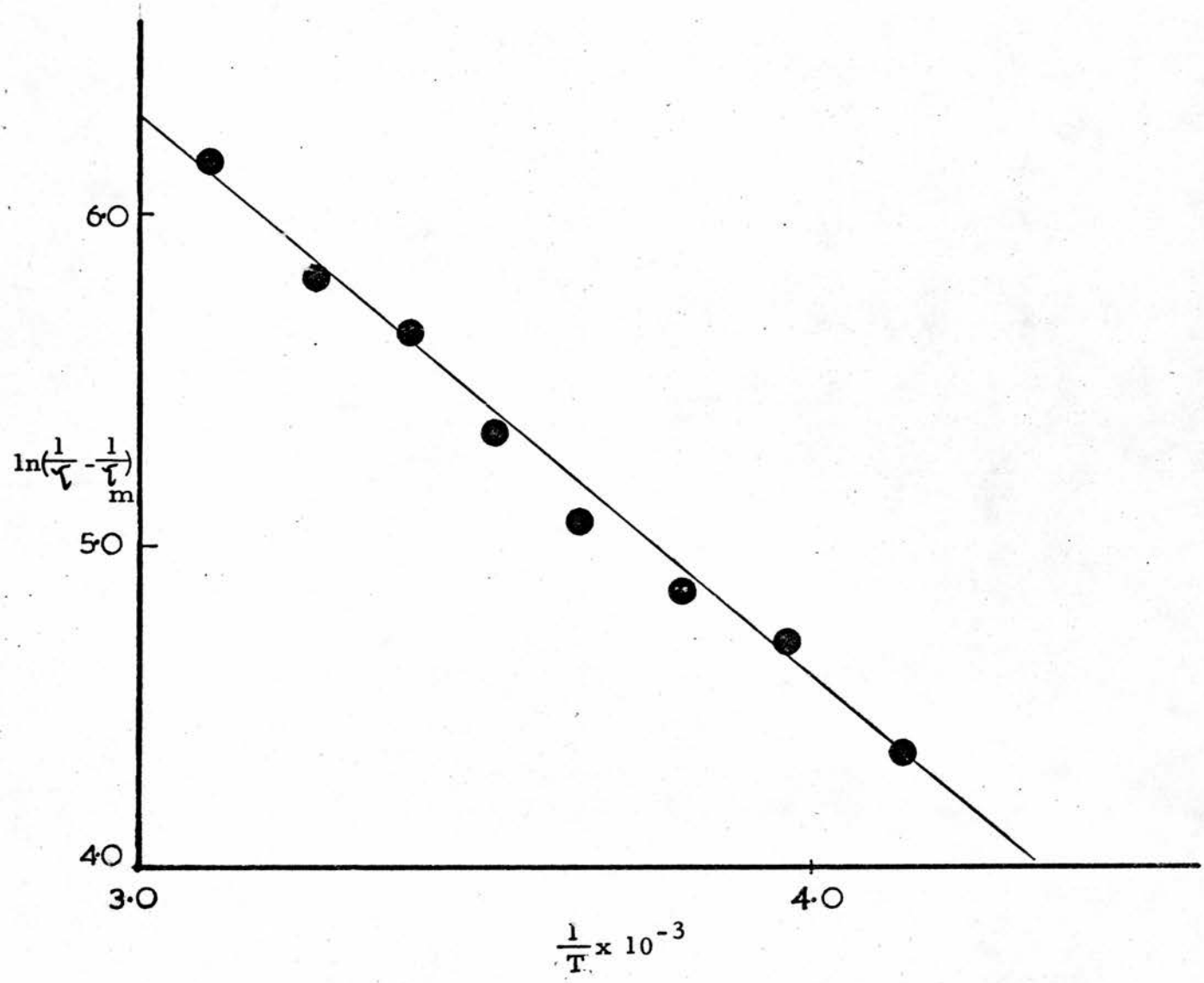

Figure 7, 2: plot of $\ln\left(\frac{1}{\tau} - \frac{1}{\tau_m}\right)$ versus $\frac{1}{T}$ for Tb^{3+} $^5D_4$ lifetimes in $Tb(AA)_3.3H_2O$) in n-butanol solution.

$\tau_m = 1010\ \mu s.$

A are $\pm$ 3 KJ mol^{-1} and $\pm$ 0.5 x 10^5 s^{-1}.

Table 7,1:- Lifetimes, τ of the Tb^{3+} $^5D_4$ level in $Tb(AA)_3.3H_2O$ in n-butanol solution at different temperatures

Temperature (K)	τ (μs)	$\ln(\frac{1}{\tau} - \frac{1}{\tau_m})$ (a)
190	1010	(b)
202	1005	(b)
214	1010	(b)
228	969	3.78
241	938	4.36
251	911	4.70
262	898	4.83
273	873	5.06
284	861	5.16
293	790	5.64
307	756	5.81
323	681	6.17

(a) The value of τ_m was taken as 1010 μs, the value to which τ tended at low temperature.

(b) These values were in the temperature region where no significant variation of τ with T was observed.

The experimentally determined activation energy, E, is therefore much smaller than the E_{ET} value for $Tb(AA)_3.3H_2O$, and the temperature dependence of τ cannot be explained by a thermal deactivation process to the ligand triplet. Further investigations were carried out in toluene and n-propanol solutions, and the results are given in Tables 7,2 and 7,3 respectively. The results in toluene

Table 7, 2:- Lifetime, τ, of the Tb^{3+} $^5D_4$ level in $Tb(AA)_3.3H_2O$ in 2.5×10^{-3} mol dm^{-3} toluene solution at different temperatures

Temperature, K	τ (ms)
202	907
214	904
235	920
249	921
263	915
271	910
282	912
292	908
304	907
314	895
327	903

solution are in complete agreement with those of Dawson et al[75], in that there is no significant variation of τ with temperature.

In n-propanol, a similar temperature dependence of τ to that which occurs in n-butanol is observed. The plot of $\ln(\frac{1}{\tau} - \frac{1}{\tau_m})$ v. $\frac{1}{T}$ is shown in Figure 7, 3, and the activation energy obtained from the gradient of the line is 14.2 kJ mol^{-1}, ie. 1200 cm^{-1}. The value of A is estimated at ca 2×10^5 s^{-1}.

No temperature dependence of τ is observed in toluene solution, showing that any such behaviour is a solvent-dependent property, cf. the work of Dawson et al[75]. The terbium complex in toluene solution will probably exist as relatively long-lived dimers, compared with the

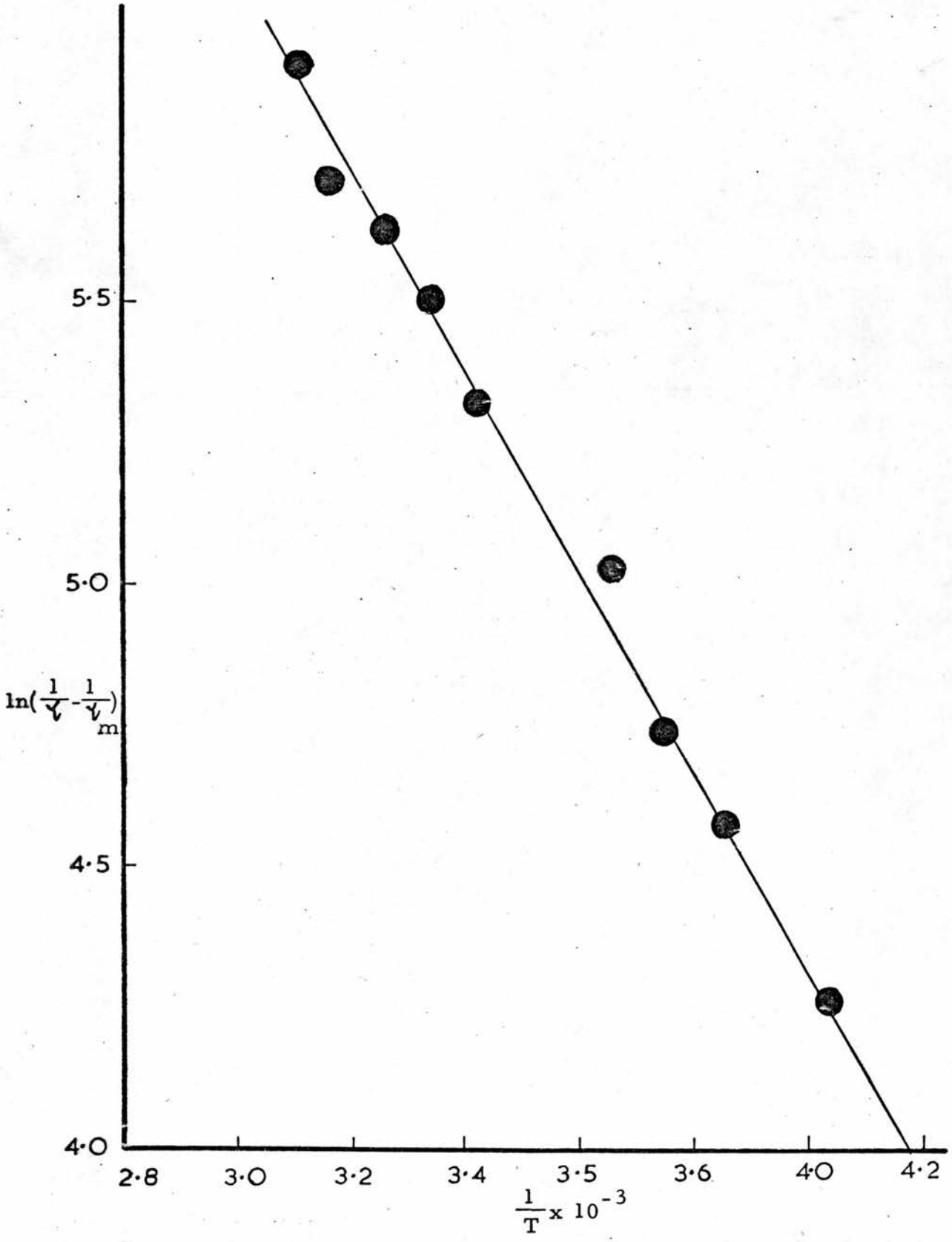

Figure 7, 3: plot of $\ln\left(\frac{1}{\tau} - \frac{1}{\tau_m}\right)$ versus $\frac{1}{T}$ for Tb^{3+} $^5D_4$ lifetimes in $Tb(AA)_3 . 3H_2O$ in n-propanol solution $\tau_m = 1000\,\mu s$.

Table 7, 3:- Lifetime of the $Tb^{3+}\ ^5D_4$ level in a 2.5 $\times 10^{-3}$ mol dm^{-3} n-propanol solution of $Tb(AA)_3 . 3H_2O$ at different temperatures[a]

Temperature, K	τ (ms)	$\ln(\frac{1}{\tau} - \frac{1}{\tau_m})$ [b]
190	1006	(c)
202	997	(c)
215	1001	(c)
226	1000	(c)
239	952	3.92
249	939	4.17
260	911	4.58
267	897	4.74
273	866	5.04
299	800	5.52
307	781	5.64
315	764	5.73
323	727	5.93
339	612	6.45

(a) Measurements were made from temperatures above the freezing point of n-propanol (146.5K)[118]

(b) τ_m was taken as 1000 ms

(c) These values of τ are in the region where no significant variation of τ with temperature occurs

$Tb^{3+}\ ^5D_4$ lifetime, but in hydroxylic solvents a monomer-dimer equilibrium will occur. The rate of monomer-dimer exchange in this equilibrium is faster than the rate of decay of the $Tb^{3+}\ ^5D_4$ level[80]. That temperature dependence of τ is observed in n-propanol and n-butanol, but not in toluene may be a function of this "monomer

exchange rate". It is proposed that temperature dependence of the lifetime of the $Tb^{3+}\ ^5D_4$ level in $Tb(AA)_3.3H_2O$ solutions will only be observed if a monomer-dimer exchange is faster than the rate of decay of the $Tb^{3+}\ ^5D_4$ level. The values obtained for E and A for n-propanol and n-butanol solutions are shown in Table 7,4.

Table 7,4:- Activation energies, E, and pre-exponential terms, A, for the temperature dependent deactivation of the $Tb^{3+}\ ^5D_4$ lifetime in $Tb(AA)_3.3H_2O$ in n-propanol and n-butanol solutions

SOLVENT	E (kJ mol^{-1})	A (s^{-1})
n-propanol	14.2 ± 3	$2.0 \pm 0.5 \times 10^5$
n-butanol	15.2 ± 3	$2.1 \pm 0.5 \times 10^5$

The values of A and E for the respective solvents are identical within experimental error, suggesting the actual temperature-dependent mechanism of deactivation of the $Tb^{3+}\ ^5D_4$ level in each case is the same, or very alike. The values of A are very low compared with those observed by Dawson et al[75]. Low values of A in reactions in solution often suggest that the observed reaction involves some kind of association[119]. It may be that the temperature-dependent deactivation mechanism depends on the formation of a dimer, ie.

$$Tb^* + Tb \rightleftharpoons (Tb_2)^* ,$$

with deactivation of the $Tb^{3+}\ ^5D_4$ level during this process.

Chapter 8

Energy Transfer from Uncomplexed Tb^{3+} Ions to Uncomplexed Transition Metal Ions in Solution

In chapters 3 and 4, energy transfer between $Tb(AA)_3.3H_2O$ and the acetylacetonate complexes of both lanthanide ions and transition elements has been discussed. In this chapter, the results of some investigations into the transfer of energy between uncomplexed Tb^{3+} and uncomplexed transition metal ions are given. The sulphate ion was used as the counter-ion.

The absorption spectrum of $Tb_2(SO_4)_3.8H_2O$ in water solution is shown in Figure 8,1. On irradiation at certain wavelengths with ultraviolet light, this solution exhibits phosphorescence characteristic of the Tb^{3+} ion. The excitation and emission spectra are shown in Figures 8,2 and 8,3 respectively. The absorption maxima coincide with maxima in the excitation maxima, and can in most cases be correlated with transitions from the Tb^{3+} $^7F_6$ ground state (see Table 8,1).

Phosphorescence lifetimes for the Tb^{3+} emissions at 490 nm, 547.5 nm and 586 nm were determined, and are given in Table 8,2. The emission at 621 nm ($^5D_4 \longrightarrow {}^7F_3$) was too weak to be detected on the lifetime apparatus.

The lifetime of the Tb^{3+} $^5D_4$ level was monitored in the presence of varying concentrations of transition metal sulphates in solution. The emission at 547.5 nm was studied, since it is the most intense band. All the solutions used in these experiments were in 1 mole dm^{-3}

Figure 8, 1: Absorption spectra of $Tb_2(SO_4)_3 . 8H_2O$ in 1 mol dm^{-3} H_2SO_4 solution

Tb^{3+} concentration = 1 x 10^{-1} mol dm^{-3}

1 cm path length cells

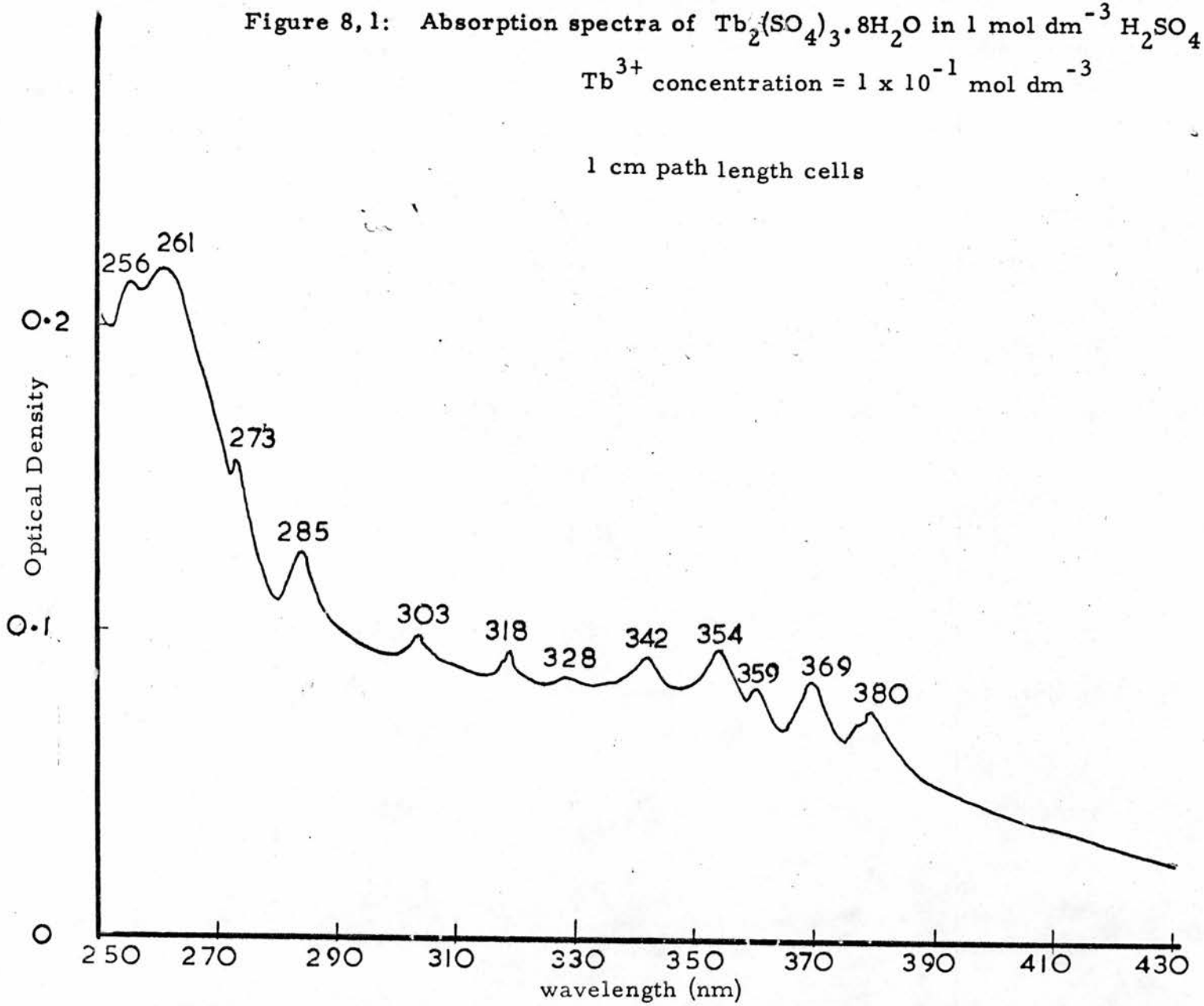

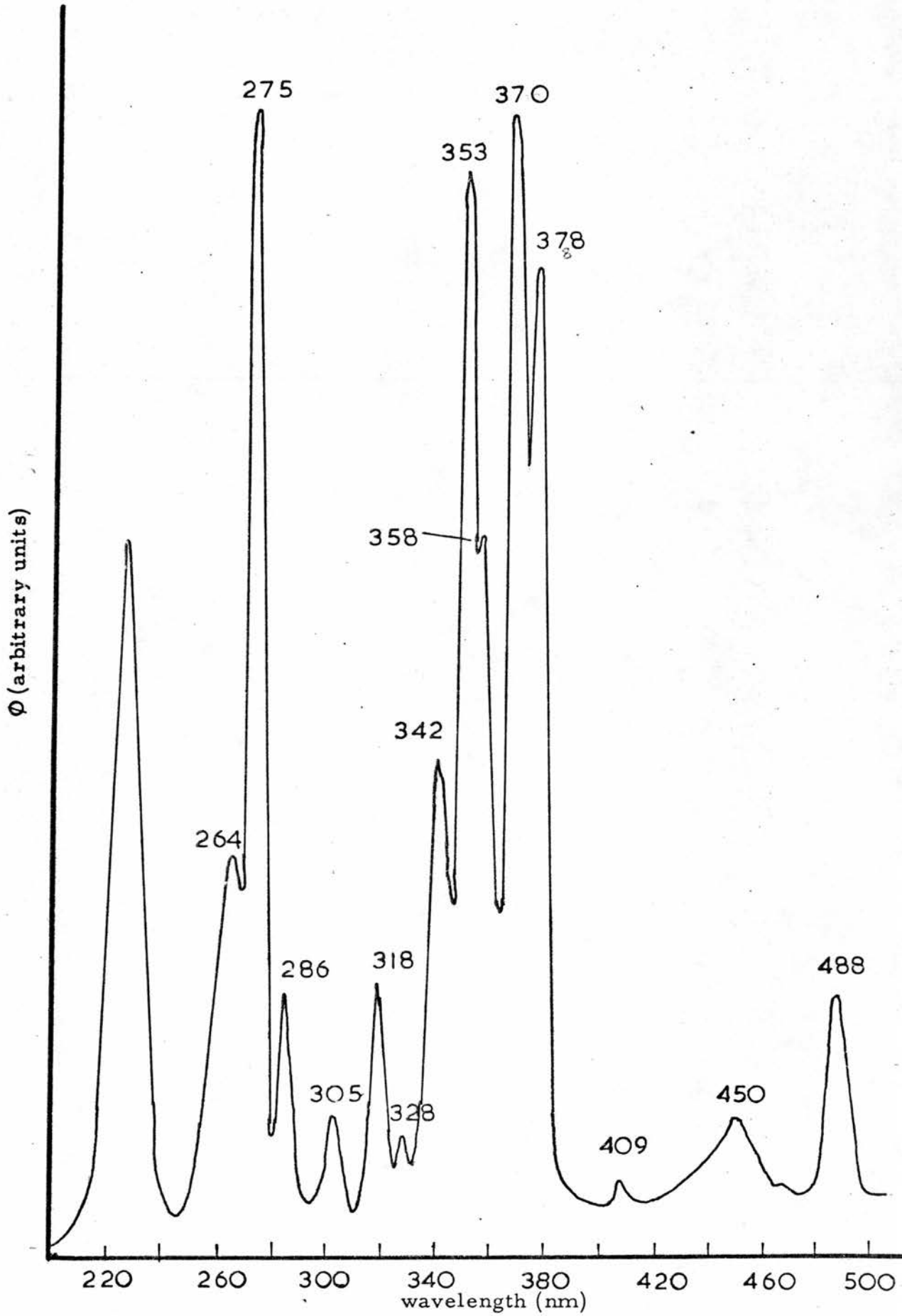

Figure 8,2: Uncorrected excitation spectrum of $Tb_2(SO_4)_3 . 8H_2O$ in 1 mol dm^{-3} H_2SO_4 solution.
Emission wavelength = 547.5 nm

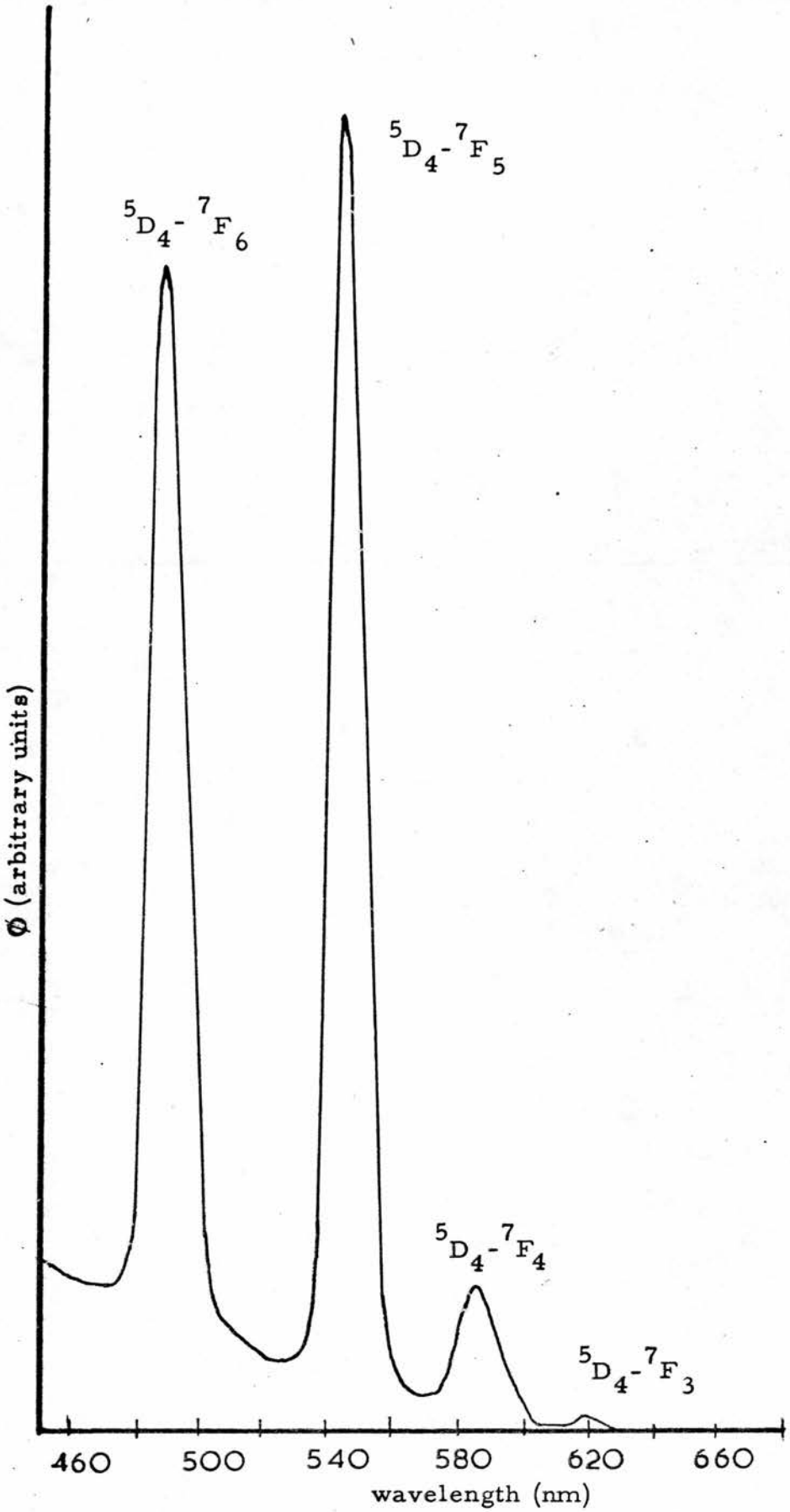

Figure 8, 3: Uncorrected emission spectrum of $Tb_2(SO_4)_3 . 8H_2O$ in 1 mol dm^{-3} H_2SO_4 solution. Excitation wavelength = 357 nm

Table 8, 1:- Absorption and excitation spectra maxima for $Tb_2(SO_4)_3.8H_2O$ in 1 mol dm^{-3} H_2SO_4 solution. Predicted transitions from the Tb^{3+} $^7F_6$ ground state are also given[(a)]. Emission at 547.5 nm was monitored in the determination of the excitation spectrum

Absorption Spectrum maxima (nm)	Excitation Spectrum maxima (nm)	Predicted Transitions from Tb^{3+} $^7F_6$ level (nm)
256		
261	264	
273	275	
285	286	286
303	305	303
318	318	318
328	328	
342	342	341
354	353	352 (b)
359	358	357
369	370	370
380	378	380 (c)
	409	
	450	
	488	490 (d)

(a) These values are calculated from data given in reference 120

(b) This corresponds to the $^7F_6 \longrightarrow {}^5D_2$ transition

(c) This corresponds to the $^7F_6 \longrightarrow {}^5D_3$ transition

(d) This corresponds to the $^7F_6 \longrightarrow {}^5D_4$ transition

Table 8, 2:- Phosphorescence lifetimes (μs) for Tb^{3+} ion emissions in $Tb_2(SO_4)_3.8H_2O$ in 1 mol dm^{-3} H_2SO_4 solution

Wavelength of emission (nm)	Transition	Phosphorescence lifetime (μs)
490	$^5D_4 \longrightarrow {}^7F_6$	508
547.5	$^5D_4 \longrightarrow {}^7F_5$	510
586	$^5D_4 \longrightarrow {}^7F_4$	509

sulphuric acid, and thus at constant ionic strength[43]. The Tb^{3+} ion concentration was kept constant at 5×10^{-2} mol dm^{-3}, and appropriate concentrations of the specific quenching metal sulphate were used. In all cases where the Tb^{3+} $^5D_4$ lifetime decreased with added quencher concentration, the Stern-Volmer relation was obeyed (see Chapter 1). Calculated bimolecular rate constants for the energy transfer process are given in Table 8, 3.

Table 8, 3:- Bimolecular rate constants, k, for energy transfer from the Tb^{3+} $^5D_4$ level[(a)] in $Tb_2(SO_4)_3.8H_2O$ to other metal sulphates in 1 mol dm^{-3} sulphuric acid

Quencher	k ($mol^{-1} dm^3 s^{-1}$)
$Cr_2(SO_4)_3.15H_2O$	2.91×10^6
$CoSO_4.nH_2O$	6.10×10^5
$VOSO_4.nH_2O$	2.19×10^5
$MnSO_4.nH_2O$	2.15×10^5
$NiSO_4.6H_2O$	3.04×10^4
$CuSO_4.5H_2O$	2.12×10^4
$ZnSO_4.7H_2O$	(b)

(a) Lifetime of the Tb^{3+} $^5D_4$ level in the absence of quencher is 510 μs
(b) The rate of transfer $< 5 \times 10^2$ $mol^{-1} dm^3 s^{-1}$

The absence of quenching by $ZnSO_4.7H_2O$ indicates that energy transfer occurs only in the quenching metal ion has energy levels below that of the emitting Tb^{3+} $^5D_4$ level (see Chapter 4).

Table 8,4 contains rate constants for intermolecular energy transfer from the Tb^{3+} ion in three different environments. It is very unlikely that any oligomeric units of $Tb(AA)_3.3H_2O$, or of the quenching acetylacetonates are present in pyridine solution due to the

Table 8,4:- Bimolecular rate constants, k, $dm^3 mol^{-1} s^{-3}$, for the quenching of the Tb^{3+} $^5D_4$ level in complexed and uncomplexed forms in pyridine and 1 mol dm^{-3} H_2SO_4 – at 293K

DONOR SOLVENT QUENCHER	$Tb(AA)_3.3H_2O$ pyridine k x 10^{-4} $dm^3 mol^{-1} s^{-1}$	$Tb_2(SO_4)_3.8H_2O$ 1 mol dm^{-3} H_2SO_4 k x 10^{-4} $dm^3 mol^{-1} s^{-1}$
Cr^{3+} (a)	670	291
Co^{2+} (a)	650	61
VO^{++} (a)	480	22
Mn^{++} (a)	0 (b)	22
Ni^{++} (a)	83	3
Cu^{++} (a)	470	2
Zn^{++} (a)	0 (b)	0 (b)
$Cr(AA)_3$	690	
$Co(AA)_2$	199	
$VO(AA)_2$	280	
$Mn(AA)_2$	0 (b)	
$Ni(AA)_2$	0 (b)	
$Cu(AA)_2$	210	
$Zn(AA)_2$	0 (b)	

(a) Counter ion is $SO_4^=$ in H_2SO_4 solution, and Cl^- in pyridine solution
(b) k 5×10^2 $mol^{-1} dm^3 s^{-1}$

strongly coordinating nature of the solvent. It can be seen that the observed intermolecular energy transfer rate in pyridine solution does depend (within a factor of $<$ ca. 3 in all cases except Ni^{++}) on whether the quencher is added as the acetylacetonate or as the metal salt. Since the added metal salt will equilibriate with the terbium acetylacetonate to some extent, the precise nature of the acceptor species in these cases is not known, but it is clear that the degree of complexation of the donor and acceptor ions has a significant effect on the observed energy transfer rate constants. The similarity in the rates for $CrCl_3.6H_2O$ and $Cr(AA)_3$ in pyridine solutions may result from the added Cr^{3+} ion being, at equilibrium, almost entirely in the form $Cr(AA)_3$ (all the other ions examined form less stable acetylacetonate complexes).

The importance of complexing is also shown, by comparison of the relative rates in 1 mol dm^{-3} H_2SO_4 and in pyridine solutions. In the sulphuric acid solutions, Cr^{3+} is ca. 5 times more effective as a quencher than any of the other ions. All the metal ions are expected to exist largely as hydrates under these conditions, ie. $M(H_2O)_n^{m+}$. The absolute rates are not comparable between these two solvents due to ionic strength effects[43].

REFERENCES

1 J.B. Birks, Photophysics of Aromatic Molecules, (Wiley, 1970)

2 A.J. Terenin, Acta Physiochim., 1943, 18, 210

3 G.N. Lewis and M. Kasha, J. Amer. Chem. Soc., 1945, 67, 994

4 G.N. Lewis and M. Kasha, J. Amer. Chem. Soc., 1944, 66, 2100

5 F.A. Cotton and G. Wilkinson, Advanced Inorganic Chemistry (Interscience, 1973)

6 N.E. Topp, Topics in Inorganic and General Chemistry, Vol. 4 (1965)

7 T. Moeller, Lanthanides and Actinides, ed. K.W. Bagnall (Butterworths, 1972)

8. S.P. Sinha, Complexes of the Rare Earths (Pergamon Press, 1966)

9 F.A. Hart and F.P. Laming, J. Inorg. Nucl. Chem., 1965, 27, 1605

10 S.P. Sinha, Spectrochim. Acta, 1964, 20, 879

11 A. Sonesson, Acta Chem. Scand., 1958, 12, 1937

12 A. Sonesson, Acta Chem. Scand., 1959, 13, 998

13. A. Sonesson, Acta Chem. Scand., 1959, 13, 1437

14 N.K. Davidenko, Russ. J. Inorg. Chem., 1962, 7, 1412

15 B.G. Wybome, Spectroscopic Properties of Rare Earths (Interscience, 1965)

16 D. Sutton, Electronic Spectra of Transition Metal Complexes (McGraw-Hill, 1968)

17 S.I. Weissman, J. Chem. Phys., 1942, 10, 214

18 R.E. Whan and G.A. Crosby, J. Mol. Spectr., 1962, 8, 315

19 G.A. Crosby, R.E. Whan and J.J. Freeman, J. Phys. Chem., 1962, 66, 2493

20 G.A. Crosby, R.E. Whan and R.M. Alive, J. Chem. Phys., 1961, 34, 743

21 J.J. Freeman, G.A. Crosby and K.E. Lawson, J. Mol. Spectr., 1964, 13, 399

22 M.L. Bhaumik and M.A. El Sayed, J. Chem. Phys., 1965, 42, 787

23 M.L. Bhaumik and M.A. El Sayed, Appl. Opt. Supplement, 1965, 2, 214

24 M. Kleinerman, J. Chem. Phys., 1969, 51, 2370

25 J.J. Freeman and G.A. Crosby, J. Phys. Chem., 1963, 67, 2717

26 W.R. Ware, in Creation and Detection of the Excited State, (Dekker, 1971)

27 G.E. Peterson, Trans. Metal Chem., Ser. Advan., 1966, 3, 202

28 A. Terenin and V.L. Ermolaev, Trans. Faraday Soc., 1956, 52, 1042

29 H.L.J. Backström and K. Sandros, Acta Chem. Scand., 1958, 12, 823

30 M.A. El Sayed and M.L. Bhaumik, J. Chem. Phys., 1963, 39, 2391

31 M.L. Bhaumik and M.A. El Sayed, J. Phys. Chem., 1965, 69, 275

32 N. Filipescu and G.W. Mushrush, J. Phys. Chem., 1968, 72, 3516

33 N. Filipescu and G.W. Mushrush, J. Phys. Chem., 1968, 72, 3522

34 F.L. Minn, G.W. Mushrush and N. Filipescu, J. Chem. Soc. (A), 1971, 63

35 G.W. Mushrush, F.L. Minn and N. Filipescu, J. Chem. Soc. (B), 1971, 427

36 P.K. Gallagher, A. Heller and E. Weissman, J. Chem. Phys., 1964, 41, 3921

37 J. Chrysochoos and A. Evers, Chem. Phys. Lett., 1973, 20, 174

38 B.M. Atipenko and V.L. Ermolaev, Opt. Spectr., 1959, 26, 415

39 B.M. Atipenko and V.L. Ermolaev, Opt. Spectr., 1970, 28, 504

40 B.M. Atipenko and V.L. Ermolaev, Opt. Spectr., 1970, 29, 47

41 B.M. Atipenko and V.L. Ermolaev, Opt. Spectr., 1971, 30, 39

42 B.M. Atipenko, I.M. Bataev, V.L. Ermolaev, E.I. Lyabimov and T.A. Privalova, Opt. Spectr., 1970, 29, 177

43 V. Balzani, L. Moggi, M.F. Manforin and F. Bolletta, Coord. Chem. Rev., 1975, 15, 321

44 P. Debye, Trans. Electrochem. Soc., 1942, 82, 265

45 Th. Fo'rster, Disc. Faraday Soc., 1959, 27, 71

46 D.L. Dexter, J. Chem. Phys., 1953, 21, 836

47 A.A. Lamola and N.J. Turro, Technique of Organic Chemistry, 14 (Interscience, 1969)

48 B. Smaller, E.C. Avery and J. R. Renko, J. Chem. Phys., 1965, 43, 922

49 G.T. Morgan and H.W. Moss, J. Chem. Soc., 1914, 105, 189

50 W.C. Fernelius and B.E. Bryant, Inorg. Synth., 5, 105 (1957)

51 J.K. Marsh, J. Chem. Soc., 1947, 1084

52 J.G. Stites, C.N. McCarty and L.L. Quill, J. Amer. Chem. Soc., 1948, 70, 3142

53 F.P. Dwyer and A.M. Sargeson, J. Amer. Chem. Soc., 1953, 75, 984

54 G.W. Pope, J.F. Steinbach and W.F. Wagner, J. Inorg. Nucl. Chem., 1961, 20, 304

55 M.F. Richardson, W.F. Wagner and D.E. Sands., Inorg. Chem., 1968, 7, 2495

56 R.C. Young, Inorg. Synth., 2, 25 (1946)

57 B.E. Bryant and W.C. Fernelius, Inorg. Synth., 5, 115 (1957)

58 W.C. Fernelius and J.E. Blanch, Inorg. Synth., 5, 130 (1957)

59 R.G. Charles, Inorg. Synth., 8, 183 (1963)

60 B. Emmert, H. Gottschneider and H. Stanger, Ber., 1936, 69, 1319

61 B.E. Bryant and W.C. Fernelius, Inorg. Synth., 5, 188 (1957)

62 J.B. Ellern and R.O. Ragsdale, Inorg. Synth., 11, 83 (1968)

63 R.G. Charles and M.A. Pawlikowski, J. Phys. Chem., 1958, 62, 440

64 T.M. Shepherd, J. Chem. Soc. Dalton, 1972, 813

65 G. Rudolph and M.C. Henry, Inorg. Chem., 1964, 3, 1317

66 G.A. Barbieri, as described in Chem. Abs., 1914, 8, no. 2988

67 R.G. Charles, Inorg. Synth., 6, 164 (1960)

68 F.A. Cotton and R.H. Holm, J. Amer. Chem. Soc., 1960, 82, 2979

69 D.D. Perrin, W.L.F. Armavego and D.R. Perrin, Purification of Laboratory Chemicals (Pergamon Press, 1966)

70 C.A. Parker, Photoluminescence of Solutions (Elsevier, 1968)

71 J.F. Ireland, Ph.D. Thesis, St. Andrews, 1972

72 R. Argauer and C.E. White, Fluorescence Analysis (Dekker, 1970)

73 T.M. Shepherd, Chem. and Ind., 1973, 332

74 T.D. Brown, Ph.D. Thesis, St. Andrews, 1973

75 W.R. Dawson, J.L. Kropp and M.W. Windsor, J. Chem. Phys., 1966, 45, 2410

76 J.S. Brinen, F. Halverson and J.R. Leto, J. Chem. Phys., 1965, 42, 4713

77 W.F. Sager, N. Filipescu and F.A. Serafin, J. Phys. Chem., 1965, 69, 1092

78 T.D. Brown and T.M. Shepherd, J. Chem. Soc. Dalton, 1973, 336

79 N. Filipescu, C.R. Hunt and N. McAvoy, J. Inorg. Nucl. Chem., 1966, 28, 1753

80 J.D. Neilson and T.M. Shepherd, J. Chem. Soc. Faraday, 1976, 72, 337

81 H. Montgomery and E.C. Lingafelter, Acta Cryst., 1963, 16, 748

82 D.P. Graddon and D.G. Weeden, Aust. J. Chem., 1963, 16, 980

83 E.A. Shugam and L.M. Shkol'nikova, Dokl. Akad. Nauk SSSR, 1960, 133, 811 (translation)

84 G.T. Morgan and H.D.K. Drew, J. Chem. Soc., 1921, 119, 1058

85 L.M. Shkol'nikova and E.A. Shugam, Kristall, 1960, 5, 32

86 A. Chakravorti and S. Basu, J. Chem. Phys., 1961, 65, 2194

87 B. Morosin and J.R. Brathovde, Acta Cryst., 1964, 17, 705

88 R.G. Pearson and D.A. Johnson, J. Amer. Chem. Soc., 1964, 86, 3983

89 D.P. Graddon, Coord. Chem. Rev., 1969, 4, 1

90 L. Dahl, Mol. Phys., 1962, 5, 169

91 C.K. Jørgensen, Acta Chem. Scand., 1955, 9, 1362

92 G.J. Bullen, Nature, 1956, 177, 537

93 G.J. Bullen, R. Mason and P.J. Pauling, Nature, 1961, 189, 291

94 G.J. Bullen, R. Mason and P.J. Pauling, Inorg. Chem., 1965, 4, 456

95 D.P. Graddon and E.C. Watton, Nature, 1961, 190, 906

96 F.A. Cotton and J.P. Fackler, Jr., J. Amer. Chem. Soc., 1961, 83, 2818

97 J.P. Fackler, Jr., and F.A. Cotton, J. Amer. Chem. Soc., 1961, 83, 3775

98 F.A. Cotton and R.H. Soderberg, J. Amer. Chem. Soc., 1962, 84, 872

99 D.P. Graddon, Nature, 1962, 195, 891

100 J.P. Fackler, Jr., Inorg. Chem., 1963, 2, 266

101 D.P. Graddon and G.M. Mockler, Aust. J. Chem., 1964, 17 1119

102 R.P. Dodge, D.H. Templeton and A. Zalkin, J. Chem. Phys., 1961, 35, 55

103 D. Hall, A.J. McKinnon and T.N. Waters, Acta Cryst., 1964, 17, 613

104 N. Martinus and C.A. Vincent, unpublished results

105 J.A. Kemlo and T.M. Shepherd, to be published

106 K.J. Eisentraut and R.E. Sievers, J. Amer. Chem. Soc., 1965, 87, 5254

107 L.J. Nugent, R.D. Baybarz, J.L. Burrell and J.L. Ryan, J. Phys. Chem., 1973, 77, 1528

108 J.C. Barnes, J. Chem. Soc., 1964, 3880

109 V.L. Ermolaev, N.A. Kazanskaya, A.A. Petrov and Yu.I. Kheruze, Opt. Spectr., 1970, 28, 113

110 J.P. Fackler, Jr., F.A. Cotton and D.W. Barnum, Inorg. Chem., 1963, 2, 97

111 W.M. Latimer, Oxidation Potentials, 2nd Ed., (Prentice-Hall, Englewood Cliffs, 1952)

112 R.G. Charles and E.P. Riedel, J. Inorg. Nucl. Chem., 1966, 28, 3005

113 Y. Haas, G. Stein and M. Tamkiewicz, J. Phys. Chem., 1970, 74, 2558

114 G.D.R. Napier, J.D. Neilson and T.M. Shepherd, Chem. Phys. Lett., 1975, 31, 328

115 W.R. Dawson and J.L. Kropp, J. Opt. Soc. Amer., 1965, 55, 822

116 J.L. Kropp and W.R. Dawson, J. Chem. Phys., 1966, 45, 2419

117 T.D. Brown and T.M. Shepherd, J. Chem. Soc. Dalton, 1972, 1616

118 Handbook of Chemistry and Physics, 52nd Edition (The Chemical Rubber Co., 1971)

119 W.J. Moore, Physical Chemistry (Longman's, 1968)

120 G.H. Dieke and H.M. Crosswhite, Appl. Opt., 1963, 2, 675